Molecular guidance of serotonin raphe neurons during development

Teng Teng

THESE DE DOCTORAT DE L'UNIVERSITE PIERRE ET MARIE CURIE

Spécialité NEUROSCIENCES

Ecole doctorale Cerveau Cognition Comportement

Présentée par Teng TENG

Pour obtenir le grade de

DOCTEUR DE L'UNIVERSITE PIERRE ET MARIE CURIE

Molecular guidance of serotonin raphe neurons during development

Soutenue le 23 septembre 2016 devant le jury compose de:

Dr Michael Reber	Rapporteur
Dr Christina Lillesaar	Rapporteur
Dr Salah EI Mestikawy	Examinateur
Dr Fekrije Selimi	Examinateur
Dr Afsaneh Gaillard	Examinateur
Dr Patricia Gaspar	Directeur de thèse

Acknowledgements

First of all, I would like to thank to Patricia Gapsar for being my supervisor and the teacher of enlightenment in neuroscience. Under her careful supervision, I become more and more interesting in neuroscience. She teaches me how to be a good researcher and a good anatomist. She makes me holding a unbreakable faith to keep on my way in science.

I would like to thank all my jury members for taking time to read and judge my thesis. And I would like to thank Jean-Antoine Girault for applying the opportunity to perform my project in the institute.

I would like to give my great thanks to all the members in Gaspar and Metin's team. With all of your help, I can enjoy the nice atmosphere on doing research in a foreign country. Thanks to Aude Muzerelle for your excellent logistics work that is the strongest guarantee making my projects going well. And thanks for your help on stereotaxic injection experiment, your amazing injections really improved my findings. Thanks to Mariano Soiza-Reilly, to discuss with you can always solve my doubts and many thanks to your proposals and ideas. Thanks to Sophie Scotto for giving me many suggestions on the study of olfactory bulb. Thanks Alexandra Rebsam who taught me the explants culture and helped a lot on axon guidance studies.

I would like to thank David Godefroy who used to work in the Plateforme Imagerie of Institut de la vision. With your help I can have perfect figures and 3D videos that supports my research. As well as Mythili Savariradjane and Theano Eirinopoulou who work in the Plateforme Imagerie of Institut du fer a Moulin, they also help me on imagining.

I would like to thank all the collaborators. Thanks to Fabrice Ango, with your help I learn more about the cell sorting. Thanks to Afsaneh Gaillard and Filippo Rijli for providing the precious animal models. Thanks to Michael Reber for providing the plasmids for ISH and IUE, these plasmids help me a lot on my studies.

At the end, I would like to thank my wife for supporting my daily life without any grumble. You are the source of strength that support me working hard!

Introduction

Abstract

In mice, serotonin (5-HT) midbrain neurons are born from embryonic day 10 to 12, and start extending axons, shortly after neurogenesis, both rostrally to the telencephalon and caudally to the brainstem. These projections are highly collateralized but with some degree of topographic organization. In the telencephalon, the pattern of 5-HT innervation arising from the dorsal (B7, B6) or the medial (B5-B8) nuclei differs. However, there are no systematic detailed developmental studies in mice, which are the most extensively used model, in particular for genetic studies. Such data are important to gather in order to analyze the effects of mouse mutations on defined molecular pathway of serotonin neurons. Moreover the guidance molecules that direct these 5-HT raphe neurons to different targets are not known. We performed several studies of 5-HT innervation aimed at detecting how the dorsal and median raphe nuclei are targeted to different forebrain regions during development.

We investigated the role of ephrinA-EphA signalling in selective targeting. Our results demonstrate that EphA5 mRNA is selectively expressed in distinct subpopulation of serotonin raphe neurons. Particularly, EphA5 exhibited the highest level in dorsal raphe serotonin neurons (B7). The results of in vitro explant cultures and in vivo electroporation analyses indicated that the ligands of EphA5 (ephrinA5 and ephrinA3) act as repellent factors for the serotonergic axon growth cones. Anterograde tracing in the ephrinA5 -/- mice showed mistargeting of dorsal raphe neurons projections, including the serotonergic projection. Particularly, our analysis of tracing studies shows that targeting of the dorsal and median raphe axons to different layers of the olfactory bulb is altered in the ephrinA5 KO. However we do not know at what developmental stage these alterations occur, in particular whether this reflects an alteration in the orientation of ascending fibre tracts, or whether this reflects late developmental maturation when raphe axons collateralize and branch in specific target regions.

We have taken advantage a new morphological method, which allows analysing immunocytochemical labelling in 3D. 5-HT immunolabeling, in whole brain serotonergic projection in 3D. Our findings show that serotonergic fibres projecting to olfactory bulb require a special timing to enter the target. The expression pattern of ephrinA5 suggests that ephrinA5 can be one of the factors that modulate this timing.

Overall, our results show for the first time the implication of a guidance molecule for the region-specific and time-specific targeting of serotonin raphe neurons and have implications for the anatomo-functional parsing of raphe cell groups.

Abbreviation list:

5-HT	5-hydroxytryptamine, serotonin
AAV	adeno-associated virus
Arc	arcuate nucleus
BLA	basolateral amygdala nucleus
BNST	bed nucleus of stria terminals
DR	dorsal raphe nucleus
DRD	dorsal raphe nucleus, dorsal part
DRV	dorsal raphe nucleus, ventral part
DRL	dorsal raphe nucleus, lateral part
EPL	external plexiform layer
GCL	granular cell layer
GL	glomerular cell layer
GPI	Glycosylphosphatidylinisotol
ML	mitral cell layer
MnR	median raphe nucleus
RMS	rostral migratory stream
SCN	superchiasmatic nucleus
SERT	serotonin transporter
VMH	ventromedial hypothalamic nucleus
VMHDM	ventromedial hypothalamic nucleus, dorsomedial part
VMHVL	ventromedial hypothalamic nucleus, ventrolateral part

Introduction

Part 1: Serotonin raphe neurons and topographic mapping of serotonergic projections

Serotonin (5-hydroxytryptamine, 5-HT) neurotransmission is implicated in a large number of physiological functions from the most elemental such as feeding, sleep, and biological rhythms, to more elaborate such as mood, and learning (Lucki, 1998; Fernandez and Gaspar, 2012). As a consequence, 5-HT dysfunction has been implicated in a large number of neurological and psychiatric disorders such as depression, anxiety, autism, and attention deficit disorder. Furthermore, 5- HT modulators are indispensable therapeutic tools in depression and anxiety disorder (Hussain, 2016).

1. History

Serotonin was initially isolated from beef serum extracts as an extract that produced peripheral vasoconstriction; because of this vasoconstriction function this substance was named serum vasoconstrictor, serotonin (a serum factor that affected blood vessel tonus) (Rapport et al., 1948). A year later, he identified the chemical composition of this extract as 5-hydroxytryptamine, 5-HT. At about the same time Vially and Erspamer had identified « enteramine » in the enterochromaffin cells of the gastrointestinal mucosa that was increasing gut motility. In 1952, enter amine was identified to be the same substance as serotonin (Erspamer and Asero, 1952). Shortly after that, serotonin was detected for the first time in the mammalian CNS by biochemical analyses of brain tissue extracts initially in dogs. (Amin et al., 1954) Their study indicated that the central nervous system of mammals as well as certain ganglia and peripheral nerves of invertebrates contain detectable quantities of serotonin and that some of the richest areas containing serotonin were in the diencephalon and midbrain. Further studies extended this analysis to a wide range of species from mammals, to birds, reptiles and fish (Correale, 1956). The first visualization of serotonin neurons was achieved with fluorescence histochemistry methods that were based on the endogenous yellow fluorescence of indoleamines when these are fixed with aldehydes. The studies of Kjelle Fuxe and Annita G_Dahlstrom in rat in 1964 described for the first time the localization and the distribution of the neurons containing serotonin in the brain stem, as the B1-B9 cell groups; that were named as such to oppose them to the A1-A15 catecholamine-containing neurons.(Dahlstroem and Fuxe, 1964)

The studies of Dahlström and Fuxe attracted the interest of neuroscientists to the structure of the “raphe” nuclei in the brainstem. Raphe nuclei are an anatomical term for brain nuclei located in the midline of the hindbrain. Raphe nuclei were in particular described by Santiago Ramon y Cajal using the Golgi method. (Figure1) The silver chromate-impregnation method was in these early days the most important method to describe the cellular composition and organization of the nervous system, Ramon y Cajal studied the brains of newborn rabbit and kitten; he designated the raphe nuclei as “intermediate or unpaired nucleus” and “median subaqueductal nucleus of the raphe” which approximates the location of the rostral raphe group. He also mentioned that, in the magnocellular central nucleus of the raphe, a “thin cellular trail extends ventrally penetrating between both longitudinal fascicles”. This description resembles the localization of the interfascicular DRN and, possibly, rostral parts of the MRN. Cajal also observed that the DRN contained four types of neurons, which he described as being voluminous, fusiform, triangular and stellate. (Ramón Cajal, 1906)

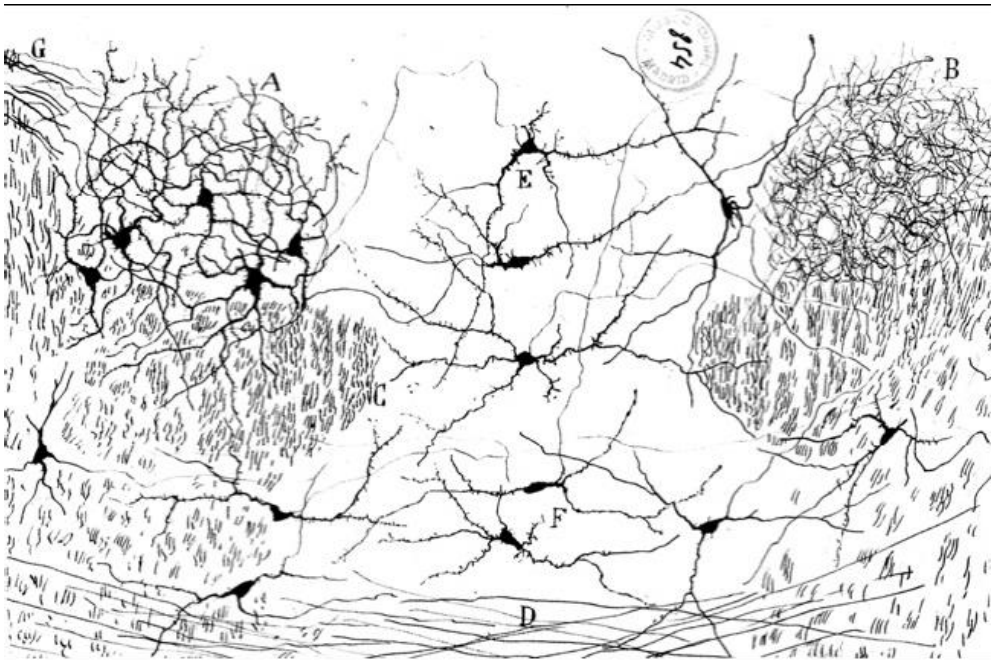

Figure1. Cajal's drawing of a transverse section through the caudal region of the superior colliculus of a few-days-old kitten. A, cells of the trochlear nerve nucleus; B, collaterals within the same nucleus; C, medial longitudinal fasciculus; D, fibers of the superior cerebellar peduncles; E, cells of the “subaqueductal nucleus of the raphe”, which probably resembles the DRN. F, ventral cells of the raphe; G, radicular fibers of the trochlear nerve. Image source: the annotated and edited translation of Cajal's “Texture of the Nervous System of Man and the Vertebrates” by Pedro Pasik and Tauba Pasik (Ramón Cajal, 1906), used by permission.

In the early sixties, Elizabeth Taber described the detailed anatomical structure of raphe in the cat brain stem. She described the raphe nucleus as two linear nuclei (nucleus linearis intermedius and

nucleus linearis rostralis), which are approximately the location of rostral raphe group and caudal group, and subdivided these nuclei into 8 groups (Taber et al., 1960). Later on, as mentioned above, this was described more precisely by Dahlström and Fuxe in 1964. They used the formaldehyde-induced fluorescence (FIF) method to study the rat raphe nuclei; this technique had been developed by Falck & Torp, (1962) to visualize monoamines and soon became the most popular tool for visualizing serotonergic neurons. Based on this technique, the morphology and the organization of the raphe nuclei neurons were described in many different species, such as cat (Taber et al., 1960), human (Braak, 1970; Nobin and Bjorklund, 1973; Hornung and Fritschy, 1988), frog (Parent, 1973), rabbit (Felten and Cummings, 1979) and rat (Steinbusch and Nieuwenhuys, 1981) and fish (Pierre et al., 1992). The total number of raphe serotonin neurons differs between species, for instance, in rodents the population of serotonin raphe neurons was estimated to be 17000 (Ishimura et al., 1988), 20000 in rats (Jacobs and Azmitia, 1992), in cat this number increased to 60000 (Jacobs and Azmitia, 1992) and in human approximate 300 000 (Baker et al., 1991). The serotonin raphe neurons are well organized and topographically distributed along the caudal to rostral axis of the hindbrain as different raphe subnuclei. Indeed, Dahlstrom and Fuxe identified 9 serotonin subgroups in the rat hindbrain, from B1caudally to B9. (Dahlstroem and Fuxe, 1964) These cell groups compose 2 main clusters: a rostral raphe group comprising the B9-B4 groups and the caudal raphe group that comprise the B3-B1 cell groups. The rostral raphe group is the largest cluster of serotonin neurons; it contains approximately 70% of the total serotonin population. This rostral cluster also corresponds to defined cytoarchitectonic entities that are named as follows: caudal linear nucleus (CLi) corresponding to the rostral B7, the supralemniscal cell group, that corresponds to the B9 group, the dorsal raphe nuclei which corresponds to the B7-B6 groups and the median raphe nuclei, which corresponds to the B5-B8 cell groups. The caudal raphe clusters comprises the raphe obscurus, the raphe pallidus and the raphe magnus. (Steinbusch and Nieuwenhuys, 1981; Jacobs and Azmitia, 1992; Michelsen et al., 2007; Hale and Lowry, 2011)

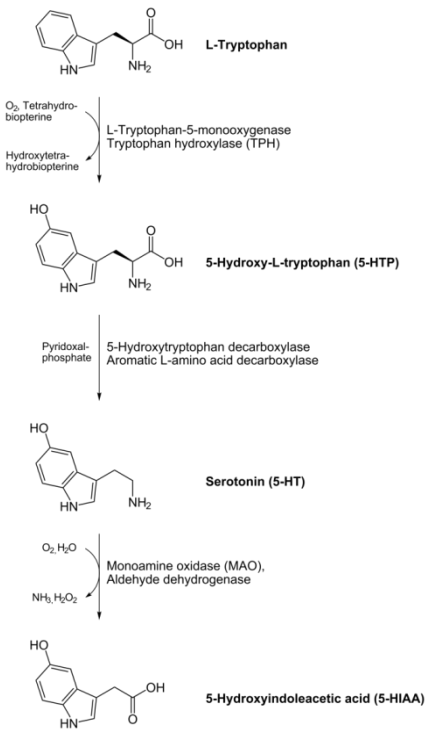

Figure2. The synthesis and metabolism of serotonin. (From NEUROtiker)

2. Biochemistry of serotonin system

Serotonin neurons share a common neurochemical phenotype. The biosynthetic pathway for serotonin includes

tryptophan hydroxylase (TPH), the key enzymes for producing serotonin from amino acid, tryptophan (Grahame-Smith, 1964; Sato et al., 1967) and decarboxylase of aromatic l-amino acids. TPH carries out the first step and is the rate-limiting enzyme in 5-HT biosynthesis. Moreover, it is the only specific enzyme in serotonin metabolism. In contrast, the decarboxylase of l-aromatic amino acids is a widespread non-specific enzyme.

Once 5-HT is produced it is concentrated into synaptic vesicles by the vesicular monoamine transporter, VMAT2, which is required for calcium dependent vesicular release. Once released 5-HT is rapidly cleared away from the extracellular space by the serotonin transporter SERT (Scl6a3) either to be recycled or to be degraded. In addition to the high affinity transporter 5-HT uptake is removed by high affinity amine transporters, OCT3.

After reuptake, 5-HT is degraded essentially by 2 enzymes: monoamine oxidase-A which has the highest affinity for 5-HT, and MAOB which has a lower affinity for 5-HT (Levitt et al., 1982); (Figure2).

TPH

The enzyme TPH belongs to a small family of structurally and functionally related aromatic aminoacid hydroxylases that utilize tetrahydropterins as cofactor. In eukaryotes, these enzymes are composed of a homologous catalytic domain with a highly conserved C-terminal tetramerization regions and sequence-specific N-terminal regulatory domains are attached (Fitzpatrick, 1999). About 15 years ago, the first TPH gene in rat, mouse and human (Darmon et al., 1988; Boularand et al., 1990; Stoll et al., 1990) was described and, most of this time, this gene has been thought to be the only TPH gene in the genome. Later, evidence accumulated indicating different biochemical properties of the TPH enzymes depending on the analyzed tissue. However, efforts undertaken to identify another TPH gene isoforms were unsuccessful until Diego Walther with colleagues generated a TPH knockout mice (Walther and Bader, 2003). They found that these mice lacked 5-HT in the blood, in the periphery tissues and in the pineal gland. However, there was only a minor 5-HT decrease in the brain structures. These surprising results, suggested the existence of another gene not affected by the gene targeting. This lead Diego Walther and colleagues to discover a second TPH gene in the genome of mice, rats and humans, called Tph2. It has been shown that Tph2 is predominantly expressed in the brainstem and located on human chromosome 12 and mouse chromosome 10 (Walther and Bader, 2003; Walther et al., 2003). TPH1 and TPH2 enzymes are

highly homologous proteins exhibiting 71% of amino acid identity in humans; however, the N-terminals containing the regulatory domain are quite different. (Walther and Bader, 2003)

MAO

MAO catalyzes oxidative deamination of monoaminergic neurotransmitters, 5-HT, noradrenaline and dopamine. There are two forms of MAO (A and B) that are involved in 5-HT metabolism. MAO A and MAO B enzymes are encoded by different genes (Bach AW, 1988) localized on the X-chromosome (Lan et al., 1989; Sims et al., 1989). MAO A has a higher affinity to 5-HT than MAO B and is considered as the principal enzyme of 5-HT degradation.

Co-neurotransmission

There is evidence that serotonin can be associated with other neurotransmitters. This was first discovered for neuropeptides. Substance-P was found in the Nucleus Raphe Magnus (Chan-Palay, 1981; Magoul et al., 1986; Halliday et al., 1988; Arvidsson et al., 1994). Glutamate, an excitatory neurotransmitter, is also co-localized with serotonin and substance-P in raphe neurons (Nicolas et al., 1992). Other peptides described within the serotonergic neurons are calretinin (Acsady et al., 1993), galanin (Arvidsson et al., 1991), enkephalin (Millhorn et al., 1989; Henry and Manaker, 1998), N-acetyl-aspartyl-glutamate (Forloni et al., 1987), neuropeptide-Y (Halliday et al., 1988; Krukoff et al., 1992), angiotensin II (Krukoff et al., 1992), and thyrotropin releasing hormone (Ulfhake et al., 1987; Sharif, 1989; Arvidsson et al., 1994). It has been suggested that serotonin is localized to the small clear vesicles and peptides are concentrated in the dense core vesicles (Pelletier and Laflamme, 1977; Johansson et al., 1980; Van Bockstaele and Chan, 1997). There is evidence for the co-localization of peptides and serotonin in the dense core vesicles (Pelletier et al., 1981). It would be interesting to know if glutamate exists within both the small and dense core vesicles with serotonin.

3. Serotonin neuroanatomy - Anatomical organization of the raphe nuclei and serotonergic raphe neurons

Serotonin neuroanatomy is difficult for the neuroscientists to concretize, since its decentralized structure and complex cell morphological constitution. The serotonergic raphe nucleus forms an inhomogeneous reticular group of neurons. This reticular group is located approximately from the spinal cord caudally to the interpeduncular nucleus rostrally. (Jacobs and Azmitia, 1992) The distribution of the serotonin raphe neurons is irregular, for instance, in the dorsal raphe (DR) and

caudal linear nucleus (CLi), the nuclear boundaries of the serotonin neurons shows the classical assignation, whereas the serotonin neurons in the lateral wing (LW) and B9 group are scattered in unconventional locations. (Detail describe see followed part)

3.1 Serotonin neurons morphology

Histochemical studies of the raphe nucleus showed that the neurons, that contain the serotonin have different morphologies, overall, 4 types were identified, large, small, multipolar and fusiform

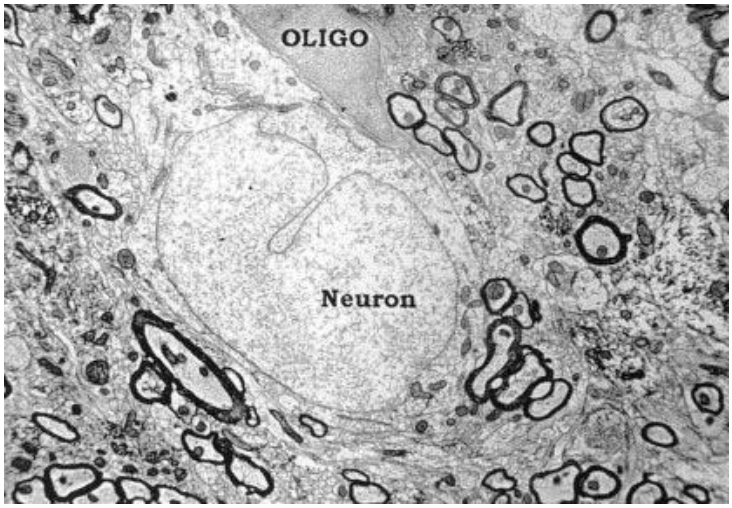

Figure3. An electron microscopic photograph taken of the Dorsal Raphe Nucleus of the adult rat. (Azmitia, 1999)

perikarya. In electron microscopic studies, the nucleus is seen as being invoginated and the cytoplasm has a well-defined Golgi apparatus and abundant microcanuculi.

Moreover, electron microscopic analysis showed that serotonin terminals contained 2 types of vesicles: small clear vesicles and large dense core vesicles (Leger and Descarries, 1978; Wiklund et al., 1981; Johnson and Yee, 1995)

Serotonin raphe neurons have different morphologies, this determined the variability of their size, generally, and the diameter of serotonin neurons is varies from 15 to 60 um. However this can also depend on the hormonal status of the animal: in adrenalectomized animals, lacking circulating adrenal glucocorticoids, the serotonergic neurons in all the raphe groups appear small with thin processes extending from the soma (Whitaker-Azmitia et al., 1993). If dexamethasone are added to the drinking water, the size of the soma and the processes increases, within an approximately 80%

increase within 24–72 hours in the volume of the tryptophan hydroxylase immunoreactive neurons (Azmitia, 1999).

3.2 Serotonin dendrites and axons morphology

Cajal (1911) described the serotonergic neurons as large neurons with extensive but untraceable axonal projections. He indicated that they were equipped with "several divergent and strongly spiny dendrites". Using 3H-proline as a marker, at least five separate tracts were found ascending from the superior group of raphe nuclei (Azmitia and Segal, 1978). Some serotonergic fibers are myelinated, whereas others are unmyelinated, and a variety of fiber diameters can exist within many brain regions (Kohler et al., 1980; Cropper et al., 1984). Some serotonergic neurons form synapses while others engage in non-synaptic interactions (Azmitia and Segal, 1978; Herve et al., 1987; Hornung et al., 1990).

Some researchers described morphological differences between the serotonergic fibers, and divided serotonin neurons into two groups depending on fiber morphology. One fiber type, which is thick, relatively straight and non-varicose, was described as originating from the Median Raphe Nucleus while the other, formed by thin, highly branched and varicose fibers was described as arising from the Dorsal Raphe Nucleus (Kosofsky and Molliver, 1987; Hornung et al., 1990). However, this is controversial, as other researchers reported that the morphology of the fibers may depend on the target region innervated (Azmitia and Segal, 1978). For instance one study showed that the origin morphology of fibers was changed after they arrived the target. In another study it was shown that serotonergic projection tract from raphe to lateral ventricles, the fibers are initially thick, straight, and non-varicose at the first postnatal week in the rat. However, the same fibers become thin, highly branched, and varicose by the third postnatal week (Dinopoulos and Dori, 1995).

3.3 Anatomical organization of the raphe nuclei

To understand function in the central nervous system it is a good idea to start from the anatomy studies which can let you have a spatial overview. Neurons in different region are not scattered or randomly, distributed, they have a very precise cytoarchitectonic organization that corresponds to their developmental origin, and to their particular connectivity patterns that are informative of function. The composition /organization of the different raphe nuclei are listed below. (Figure 4)

Dorsal raphe nucleus (DR) c = B7+ B6

The DR is considered as the one of the most important nucleus in the raphe complex since it contains the largest population of serotonergic neurons and is the focus of the vast majority of the serotonin research. The DR is located in the caudal midbrain and rostral pons, in a part of the brainstem called the tegmentum, just below the cerebral aqueduct. The DR has been further subdivided into several components based of the spatial location and density of cells.as the rostral extension, rostral, dorsal, ventral, ventrolateral, interfascicular, and caudal parts. There are four morphological cell types of neurons located in the DR: round, ovoid, fusiform and triangular (Steinbusch and Nieuwenhuys, 1981; Baker et al., 1991). However these cell morphologies have not been related to any functional characteristics. On the other hand, as will be discussed later there are neurochemical and connectivity differences among the DR subdivisions.

The following DR subdivisions are considered:

DR-Caudal linear nucleus (CLi)

The caudal linear nucleus is located in the midbrain just dorsal to the decussating fibers of the superior cerebellar peduncle and merges caudally and dorsally with the DR; it can be considered as the rostral extension of DR. There are two main types of neurons in the CLi: serotonergic neurons and dopaminergic neurons that are intermixed (Steinbusch and Nieuwenhuys, 1981). The morphology of the serotonergic neurons in the CLi is small and spherical with fewer dendrites that are oriented along the rostral-caudal axis (Tork, 1990). The morphology of dopaminergic neurons is small and fusiform which are extends caudally into the ventromedial portion of the rostral DR (Wiklund et al., 1981; Minami et al., 1999). Serotonin neurons in the CLi are considered as the smallest population in the raphe complex, in cats, the CLi contains 2,000 serotonergic neurons, approximately one tenth the number of total DR nucleus (Wiklund et al., 1981).

DR, Rostral part (DRr)

The rostral part of dorsal raphe located on the cerebral aqueduct – CLi axis dorsal-ventrally. Caudally, the rostral DR is bordered by the DRD and the DRV. The specificity of neurons in the rostral DR is like the CLi included both serotonergic neurons and dopaminergic neurons (Descarries et al., 1986; Stratford and Wirtshafter, 1990).

DR, dorsal part (DRD)

The DRD is bordered dorsally by the cerebral aqueduct, ventrally by the DRV, and laterally by the DRVL/VLPAG. The central midline region of the DRD contains the medium size, fusiform or bipolar cells which could be characterized as glutamatergic neurons, serotonergic neurons and GABAergic neurons. The distribution of serotonergic neurons can be grouped into two clusters, which are referred to as the DRD "core" and "shell" depends on the dense or scattered distributed serotonergic neurons respectively (Abrams et al., 2005; Clark et al., 2007; Hioki et al., 2010).

DR ventral part (DRV)

The DRV is bordered dorsally by the DRD, more precisely, a border of glutamatergic neurons which between DRD and DRV, ventrally and laterally by the dorsal tegmental nucleus. The DRV contains small, round serotonin neurons but also a population of glutamatergic neurons that are labeled by Vglut3. (Fremeau et al., 2002) (Gras et al., 2002; Schafer et al., 2002; Takamori et al., 2002) Serotonergic neurons in the DRV are densely packed, and as a consequence, this region shows the highest expression of Tph2, SERT and some 5-HT receptors mRNA raphe complex (Clark et al., 2006).

DR ventrolateral part (DRVL)

The DRVL group also called the lateral wings of raphe. Serotonergic neurons in this region are notable for their large size, relative to other subpopulations of serotonergic neurons, and their multipolar morphology, which is easily discernable with immunostaining for serotonin or tryptophan hydroxylase. The lateral wings do not include the glutamatergic neurons anymore but a large amount of GABAergic neurons (Jolas and Aghajanian, 1997; Day et al., 2004), which appear to play a role in local inhibitory control of serotonergic neurons within the dorsal raphe nucleus (Jolas and Aghajanian, 1997).

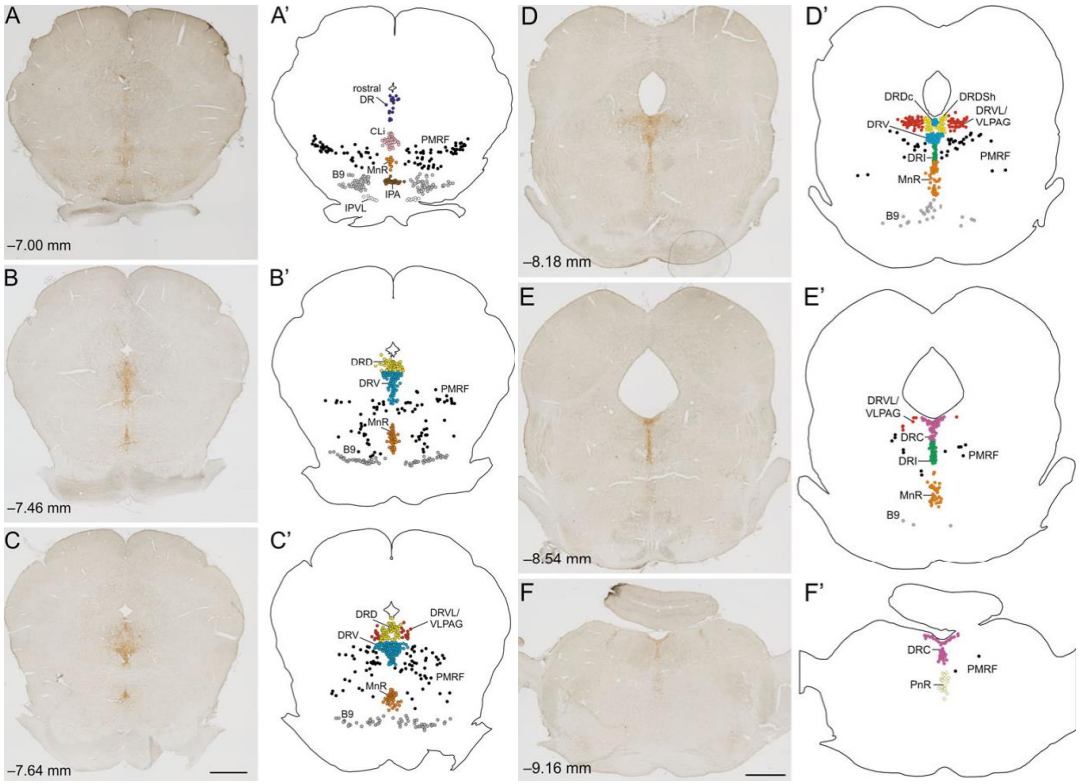

Median raphe nucleus (MnR)

The MnR is a midline structure ventral to the DR. The MnR and the DR have different developmental origins. Serotonergic neurons in the DR derive entirely from rhombomere 1 of the developing mouse brain, whereas serotonergic neurons of the MnR derive predominantly from rhombomere1, 2 and 3. (Jensen et al., 2008; Bang et al., 2012).

The B9 serotonergic cell group/supralemniscal serotonergic cell group (B9)

B9 serotonergic neurons extend throughout the rostral and mid-pons and are located within and dorsal to the medial lemniscus. Although it has received considerably less attention than other midbrain and pontine serotonergic cell groups, it contains a substantial number of serotonergic neurons (estimated to be 4,571 cells in the rat brain, roughly equivalent to the number in the MnR (Vertes and Crane, 1997). Substantial numbers of B9 serotonergic neurons also have been described in primates, including humans (Azmitia and Gannon, 1986). Steinbusch (1984) described a high

concentration of serotonergic neurons dorsal to the medial lemniscus and ventral to the nucleus rubber, particularly its lateral parts. A few cells were located in the nucleus rubber itself.

3.4 Serotonin raphe neurons axonal projections: from past to the present

There is hardly no region in the central nervous system that does not receive 5-HT innervation; all this innervation derives from the brain stem raphe nucleus, which are in relatively low numbers compared to the vast amount of neurons that they innervate. This indicates a high degree of collateralization; however anatomical evidence has also shown that there is also a fair amount of topographic organization of the serotonin projections arising from the raphe.

Cajal recognized that the fibers emerging from the raphe nuclei tended to "concentrate into ascending and descending dorsoventral bundles". However, he was not able to determine how far the fibers continued, because these fibers were not labeled with the Golgi method. The first specific description of raphe nucleus axonal projections was described by Dahlstrom and Fuxe using Formaldehyde induced Fluorescence (FIF) which could visualize the monoamines, this allowed the first description of the distribution pattern of serotonin projections. However, this technique has a big weakness which is the rapid fading of fluorescence (Dahlstroem and Fuxe, 1964). Later in the 70s to 80s, two crucial techniques were developed for serotonin projection histological analysis: specific antibody for immunohistochemistry analysis and anterograde/retrograde tracing. The first specific antibody against serotonin was developed and used by Steinbusch (Steinbusch and Nieuwenhuys, 1981); this allowed a much more precise and detailed analysis of the serotonin axon terminals in different targets. At the same time period axon tracing methods made tremendous progress. Horseradish peroxidase (HRP) was found to be very efficient for tracing fiber pathway as a retrograde tracer and was used for studying serotonin projection since 1975. (Miller et al., 1975) In parallel, anterograde tracing methods were developed such as the autoradiographic detection of [3H]-serotonin uptake and [3H]-labeled reserpine that were used for anterograde tracing analysis of serotonin system. (Calas et al., 1974; Richards, 1979) More precise anterograde tracing were developed such as Biolytic, which allowed a fine cellular of anterogradely labeled dorsal and medial raphe neurons, identifying their full axon projections (Vertes, 1991; Vertes et al., 1999). However these tracing methods are not selective of a defined cell type, thus identification of the serotonin projections relied on a combination of fluorescent retrograde tracers (fast blue, fluoroglo) with immunocytochemistry. More recently, genetic tools are available for selective serotonin tracing as there are many transgenic mouse lines expressing the "Cre" recombinase under the control of specific promoters. For instance, in serotonin system the common promoters are: Pet1, Sert and Tph2

Based on the improvement of tracing methodology; the initial map of raphe serotonin neuron has been extended and refined over the years; Initially serotonin pathways were described as emerging from two cluster bases on the specificity of projection targets- a rostral group (B5-B9) which mainly projects to the forebrain targets whereas the caudal group (B1-B4) mainly project to the brainstem and spinal cord. Serotonin neurons from the rostral group are the essential neurons that release serotonin into the forebrain targets and furthermore play the key role in the modulation of CNS functions. And this is also why researchers who study the serotonin system are more interested in rostral raphe neurons. The rostral raphe group contains the majority or most the population of serotonin neurons and innervated the whole forebrain, it's not difficult to imagine the complexity of their ascending pathways.

In the beginning of 21st century, neuroanatomists initially clarify the different pathway from rostral raphe which were described characteristic as followed: (a) the dorsal raphe forebrain bundle tract, travelling within the ventrolateral part of the medial forebrain bundle to the basal ganglia, amygdala and piriform cortex; (b) the medial raphe forebrain bundle tract, travelling within the ventromedial part of the medial forebrain bundle to the prefrontal cortex, cingulate cortex, medial septum and hippocampus. Four additional fiber tracts are located outside the medial forebrain bundle; (c) dorsal raphe cortical tract, travelling ventrolateral to the medial longitudinal fasciculus to the caudate putamen and parieto-temporal cortex; (d) dorsal raphe periventricular tract, travelling immediately below the midbrain aqueduct to the periventricular thalamus and hypothalamus; (e) dorsal raphe arcuate tract, travelling through the ventrolateral edge of the midbrain to the ventrolateral geniculate body nuclei and the suprachiasmatic nuclei; (f) raphe medial tract, travelling from the dorsal and median raphe nuclei ventrally between the fasciculi retroflexus to the interpeduncular nucleus and midline mammillary nuclei.

All these pathways can be simplified into three pathways: dorsal ascending pathway, median ascending pathway and ventral ascending pathway.

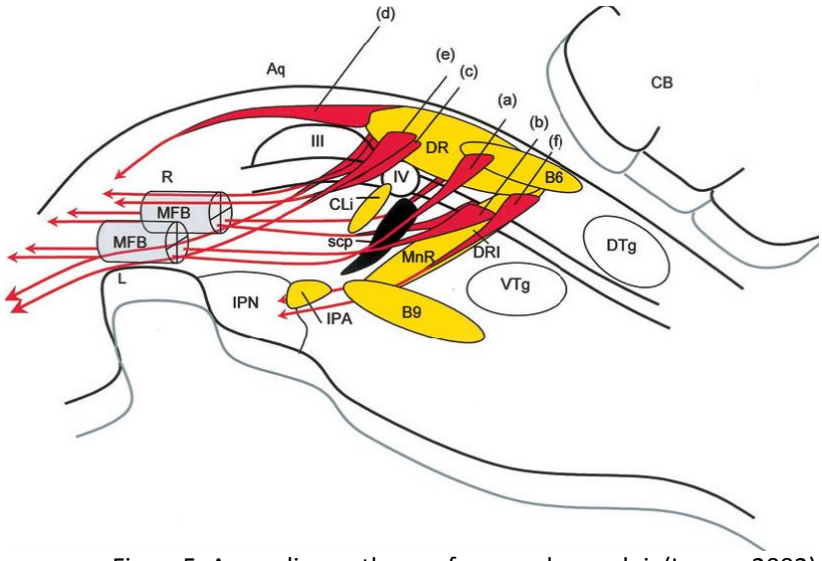

Figure5. Ascending pathways from raphe nuclei. (Lowry, 2002)

Dorsal ascending pathway

The dorsal ascending pathway rises from the medial and rostral DRN and innervates the striatum and globus pallidus (GP). The striatum is the most important target for DRN innervation and one of the first to be extensively studied. The earliest anatomical indications for DRN projections to caudate-putamen (CP) of the dorsal striatum (Anden, 1965) were subsequently supported by lesion studies, which showed a drop in striatal tryptophan hydroxylase (TPH) activity (Geyer et al., 1976) as well as a decrease in [3H]5-HT uptake (Kellar et al., 1977) after DRN lesions. Approximately a third of all serotonergic DRN neurons project to the CP. This is, however, region-specific: in a cluster in the dorsomedial DRN, 80–90% of serotonergic neurons were found to project to the CP (Steinbusch and Nieuwenhuys, 1981). Twenty percent of DRN neurons that project to the CP are non-serotonergic. Nucleus accumbens of the ventral striatum, and particularly its core, are also extensively innervated by DRN fibers (Van Bockstaele and Pickel, 1993; Van Bockstaele and Chan, 1997; Brown and Molliver, 2000). DRN efferent target the striatum at caudal to midlevels (Vertes, 1991). Approximately half of the neurons are located in the rostral third of the DRN, fewer in the middle third and very few in the caudal third (Steinbusch and Nieuwenhuys, 1981; Waselus et al., 2006). Pallidal afferents from the DRN have been demonstrated by tracing studies (DeVito et al., 1980; Vertes, 1991). The innervation of the GP is mainly serotonergic, as confirmed by micro-dialysis studies in the rat (McQuade and Sharp, 1997)

Medial ascending pathway

The main target of the medial ascending pathway is the substantia nigra (SN). The projections seem to arise from the rostral DRN (Miller et al., 1975; Imai et al., 1986a) and they target the pars compact division in particular (Fibiger and Miller, 1977; Bobillier et al., 1976). However, a study using the retrograde tracer PHA-L failed to demonstrate DRN innervation of the pars reticulate (Vertes, 1991). To a lesser extent, the pathway also innervates the CP. Some of the fibers branch, and target both the SN and CP (van der Kooy and Hattori, 1980; Imai et al., 1986a). Thus, single DRN neurons exert control over both the SN and the CP.

Ventral ascending pathway

Via the ventral ascending pathway, the DRN innervates many areas. The bilateral pathway ascends ventrolateral and then turns rostral to enter the medial forebrain bundle. The pathway also contains fibres from other raphe nuclei, especially median raphe. The main targets are thalamic and hypothalamic nuclei, habenula, septum, amygdala, cortex, the olfactory bulb, interpeduncular nucleus and geniculate body.

Indeed 5-HT neurons are generally intermingled with larger populations of non 5-HT neurons in each raphe subnuclei. An example of this is the DR cell group, which contains the highest proportion of 5-HT producing neurons, and yet comprises twice as much non-5-HT neurons (Descarries et al., 1982). So in order to identify 5-HT projections from the raphe relied on tracing techniques coupled to the histochemical revelation of 5-HT or combined with lesions. However, although these studies allowed to describe the projections of the raphe cell groups, many limitations effect the reliability of the studies, such as the variability of the injection site, variability of the uptake by passing fibres, the background from histochemical methods and the difference of the morphology after labelled by specific antibodies. Moreover, most of the studies generally focused on a particular target brain region or at most on a combination of few targets (van der Kooy and Hattori, 1980; Kohler et al., 1982; Kohler and Steinbusch, 1982; Waterhouse et al., 1986; Jones and Cuello, 1989; Van Bockstaele and Pickel, 1993; Vasudeva et al., 2011). Summarizing these studies is difficult because they relied on different experimental protocols and different animal models.

This is why, nowadays, neuroanatomists prefer to use genetic tools to study connectivity. Recent genetic studies defined the rhombomeric origin of the different raphe nuclei (Jensen et al., 2008) and provided a useful description of the 5-HT axon projections arising from the different

rhombomeres (Bang et al., 2012). In these studies, they performed multi genetic tools, which cross different recombinase marks promoted Cre recombinase to detect the connectivity relationships characterizing three serotonergic neuron subpopulations. These subpopulations were characterized by developmental gene expression associated with different rhombomeric (r) segments of the embryonic hindbrain. Subpopulation of serotonin neurons from r1 was derived from the combined expression of Pet1 (as a serotonin marker) and En1 as a marker of rhombomeric origin (r1). Likewise, r2 serotonergic neurons were characterized by the combined expression of Pet1 and Hoxa2 (as a marker of r2), while Egr2 was used for identifying the serotonin neurons from r3 and r5. The mature serotonin neurons of these three subgroups are located in the dorsal raphe (DR), median raphe (MR), B9 group and the rostral portion of raphe magnus (RMg) (Jensen et al., 2008). The same intersectional and subtractive genetic approach was used to visualize and selectively map the axon projections associated with each of these three different subpopulations of serotonin neurons. The multi genetic approach of Jensen is a set of Cre recombinase transgenic – En1::cre, Rse2::cre or Egr2::cre – each separately partnered with an ePet1::Flpe transgene, based on that they develop the approach which is with the indicator allele RC::FrePe to selectively identify the intersection neurons with enhanced green fluorescent protein (eGFP) expression. With this approach they separately mapped target brain regions served by each of these three subpopulations. Additionally, they examined how each of these eGFP-containing subgroups of serotonin neurons provided recurrent innervation to the remaining serotonin neurons that lacked eGFP, as a means to explore potential inter-system feedback inhibition. This could greatly enhance the dynamic and differential changes in extracellular serotonin concentrations across brain regions.

Their results suggest that rhombomeric origin is a contributor to organizing not only the location of serotonin cell bodies (Jensen et al., 2008), but also the organization of their projections, and thus genetic and developmental process may provide key insights into resolving aspects of the functional heterogeneity within the serotonin system. However, these approaches do not allow a specific delimitation of the topographic organization of raphe neurons originating from the same rhombomere.

In 2016, Muzerelle et al used conditional tracing methods (AAV, lox-stop-lox-GFP) in mice expressing the Cre-recombinase in 5-HT raphe neurons to obtain a selective anterograde tracing of these neurons. Using this method, they labeled small groups of 5-HT neurons within the different raphe sub-nuclei allowing a comprehensive mapping of their terminal axon fields in the brain. With these studies they provided a description of the main projecting areas of 5-HT axons arising from

different raphe sub-nuclei as well as a systematic semi-quantitative analysis of correlations between the origin of 5-HT axons (raphe sub-nuclei) and their targeted brain regions(Muzerelle et al., 2016).

DR projections (B7)

As I described above, dorsal raphe contain the biggest population of serotonin neurons and spatially divided into several subregions. Aude et al. showed that even in these sub-regions, the targets are different from each serotonin neurons.

Dorsal component of the dorsal raphe, DRD (B7d)

Ascending projections from the DRD were detected as ventrally and bilaterally towards the mlf, then serotonin fibers are spreading laterally to innervate the substantia nigra pars compacta (SNC) and ventral tegmental area (VTA). The most abundant terminal innervation was localized in the hypothalamus, followed by the lateral geniculate nuclei of the thalamus, SNC and parts of the basal ganglia, namely the nucleus accumbens, and caudal parts of the caudate-putamen and pallidum. These projections were mainly but not exclusively ipsilateral.

In the brainstem, DRD axons terminal innervation was dense in the superior colliculus and the periaqueductal gray (PAG). More ventrally it was essentially concentrated in the superior Oliver complex, 7N, and dorsal and ventral cochlear nuclei (DC, VC)

Ventral component of dorsal raphe, DRV (B7v)

Amygdala was strongly innervated by DRV serotonin fibers, where a strong accumulation of axon varicosities was observed with a particularly dense distribution in the central and basolateral components of the amygdala. A somewhat similar dense innervation was visible within the extended amygdala, such as the bed nucleus of the stria terminalis (BST). In contrast, despite the presence of ascending fiber tracts in the medial septum, no terminal innervation was visible in the lateral septal (LS) nuclei.

A dense innervation also reached the cerebral cortex, with a particular concentration in its rostral and ventrolateral parts including the orbital cortex and olfactory-related brain areas, in particular the piriform cortex, the anterior olfactory nuclei (AON) and the mitral and granular layers of the olfactory bulb. In the medial prefrontal cortex, varicose fibers were visible mainly in the infralimbic cortex, whereas the dorsal part and the cingulate cortex were more sparingly innervated.

In the thalamus, innervation was essentially concentrated in the midline thalamic nuclei. The habenula was only moderately innervated, with terminal fibers mainly in the lateral habenula (LHb). Strikingly, and contrasting with the heavy ascending fiber tract in the mfb, the hypothalamic nuclei received hardly no innervation. Similarly the hippocampus contained only few fibers that were essentially localized in the stratum lacunosum-moleculare of both the dorsal and ventral hippocampus. However, hardly any innervation was noted in the dentate gyrus. In the mesencephalon, innervation was particularly conspicuous in the substantia nigra pars reticulata with moderate innervation of the ventral periaqueductal gray (PAG) and the superior colliculus.

Lateral wings of the dorsal raphe, LW (B7l)

Ascending 5-HT innervation to the forebrain in this case was essentially concentrated in the thalamus, predominating in its more lateral components throughout its rostrocaudal extent. Bilaterally in the parasubthalamic nucleus and the LHb. Projections were also visible in the hypothalamus mainly in the ipsilateral mammillary/supramammillary components, and in the lateral hypothalamic cell groups. In the brainstem, terminal axons were essentially found in the superior and inferior colliculi, in the cochlear, motor trigeminal, and facial nerve nuclei.

Dorsal raphe caudal part, DRc (B6)

The common projections in these cases were projections to the dorsal and ventral hippocampus, the septal nuclei, and the preoptic cell groups. Projections to the amygdala were limited to the medial amygdala nuclei. Only few projections were found in the brainstem. Interestingly, however, in all the cases in which the B6 5-HT neurons were targeted, there was a substantial innervation of the subventricular 5-HT terminal network as well as in the SVZ.

Median raphe (B8)

Ascending projections from B8 collected in the most medial part of the mfb and

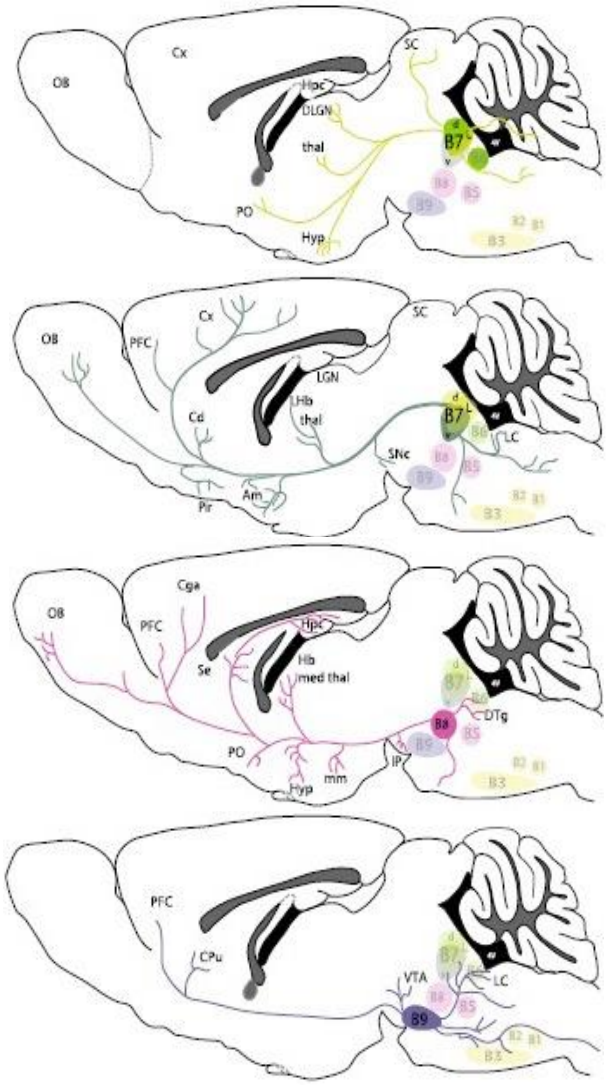

Figure6. A summary scheme of the principal targets of the main B5–B9 subgroups in sagittal brain diagrams. (Muzrelle et al. 2016)

provided a bilateral terminal innervation to a number of midline brain structures from the mesencephalon to the forebrain. Innervation was particularly dense in the interpeduncular nucleus, mammillary nuclei and in their lateral parts, and in anterior hypothalamic areas, including the preoptic area. Very dense terminal axons were noted in the suprachiasmatic nucleus. In the dorsal thalamus, the B8 5-HT innervation was particularly concentrated in the paraventricular thalamic nuclei (PV), whereas moderate innervation was visible in the reuniens and in midline non-specific thalamic nuclei, as well as in the medial habenula cell groups. More rostral, B8 axons provided a very dense innervation to both the medial and lateral septal nuclei. The B8 group provided a massive innervation to all components of the septum and hippocampus. A distinctive terminal-like innervation was also noted all along the subgranular cell zone (SGZ) of the dentate gyrus (DG), where adult neurogenesis is found. In the cerebral cortex, B8 innervation was generally scattered and essentially concentrated in the dorsomedial components of the cortex: in the medial prefrontal cortex, the

anterior cingulate and in the primary motor cortex. In contrast, in the olfactory bulb, a strong and selective B8 axon projection was found in the periglomerular cell layer In addition, few fibers were detected in the rostral migratory stream (RMS), at the OB. In the brainstem, the most remarkable concentration of 5-HT-labeled axons was found in the dorsolateral tegmental nucleus (DTg) also known as the tegmental nucleus of Gudden. This dense 5-HT innervation was visible in the mesopontine tegmental nuclei and the anterior tegmental nucleus (ATg), which are components of the DTg.

Supralemniscal (B9)

Ascending projections from the B9 were relatively sparse, in comparison with the DR and MR groups: they occupied a medial and dorsal position in the mfb providing terminal innervation essentially to parts of the septum and basal ganglia. Terminal-like innervation was observed in the medial septum, and fine terminal innervation of variable abundance according to cases was noted in the caudate-putamen, nucleus accumbens and pallidum. Sparse innervation was also noted in the cerebral cortex and hippocampus, but with no systematic distribution. In the hypothalamus, axon terminal innervation was mainly targeting the anterior and preoptic cell groups and the supramammillary area. Thalamic innervation was scarce and oriented toward midline structures. In the midbrain, terminal-like fibers were visible in the SNC and the VTA. Moreover B9 5-HT axons were the presence of descending projections towards the hindbrain.

Base on those studies of serotonin projections mapping, one can conclude that different subgroups of serotonin raphe neurons have their specific target and similar to other brain circuits, a combination of axon guidance molecules both attractive and repulsive is involved, to guide 5-HT raphe neuron axons to their proper brain targets.

3.5 Afferent connections to the raphe

In addition to sending broad projections to many brain areas, the raphe receives connectivity from many functional regions in the forebrain and brainstem. The following areas have been reported to provide innervation to the raphe nucleus: the medial prefrontal cortex, hypothalamus, hippocampus, habenula, dorsal tegmental nucleus and spinal cord. (Wang and Aghajanian, 1977; Behzadi et al., 1990; Hermann et al., 1997) These innervations determined that the serotonergic neurons itself can receive signals from both serotonin and non-serotonin axons. Moreover, many publications showed amount of neuropeptides could been detected in axonal terminals in the raphe

nucleus: serotonin (Dong and Shen, 1986); norepinephrine (Baraban and Aghajanian, 1981; Takagi et al., 1981; Dong and Shen, 1986; Lee et al., 1987); dopamine (Ferre et al., 1994); acetylcholine (Chen et al., 1992; Honda and Semba, 1994); GABA (Hayashi et al., 1997), substance-P (Magoul et al., 1986); CLIP/ACTH (Leger and Descarries, 1978); or neurotensin (Uhl et al., 1979) Serotonergic dendrites extend into the axonal bundles of the medial longitudinal fasciculus, medial lemniscus, trapezoid body, cerebral peduncles, the superior cerebellar peduncles and other fibre bundles which traverse the brainstem carrying both ascending and descending fibres (Azmitia and Segal, 1978). The spectrum of inputs from numerous anatomical sources having diverse chemical neurotransmitters and neuropeptides is not atypical for a large reticular neuron. But given the number of afferents and efferents of this single chemical system, it can transmit the varied signals to both neuronal and non-neuronal targets.

4. The development of serotonin neurons in raphe nuclei

During development, the serotonin neurons are divided into two groups based on their spatial difference as inferior group and superior group. The two groups of serotonin neurons have different migration patterns (Lidov and Molliver, 1982b; Wallace and Lauder, 1983), and within the superior group, there is evidence the 5-HT neurons form different subsets of cells. (Azmitia and Gannon, 1986)

In many studies, the neuroanatomical development and neuronal organization of 5-HT neurons has been analyzed in many different species, such as rats, primates and zebrafish (Steinbusch and Nieuwenhuys, 1981; Lidov and Molliver, 1982b; Wallace and Lauder, 1983; Azmitia and Gannon, 1986; Lauder, 1990; Lillesaar et al., 2007), and more recently in mice with genetic-based fate mapping (Jensen et al., 2008). Moreover, during embryogenesis, the hindbrain is transiently subdivided into several components called rhombomeres, which correspond to different subpopulations of serotonin neurons (Figure 7). Jensen et al. demonstrated that the raphe rostral group derive entirely from r1-r3, whereas the caudal from r5-r8. Among the rostral group, the DR nucleus (B7, B6) origioned from r1 whereas the median raphe nucleus (B8, B5) from entire r1-r3. (Jensen et al., 2008)

Mouse serotonin neurons are specified and appear initially in the ventral rhombencephalon during a brief period of neurogenesis, embryonic days 9.5–12. The initial contributing of the raphe nuclei is based on the ultimately cluster of newborn serotonin neurons in different disparate regions

of the midbrain, pons and medulla. The 5-HT neuron generation consists in several developmentally recognizable stages.

During the first stage, serotonergic progenitors in the ventral hindbrain are specified in a spatial organization along the dorsoventral and anterior-posterior axes, which are modulated by signaling molecules sonic hedgehog and fibroblast growth factors 4 and 8 respectively (Goridis and Rohrer, 2002; Vitalis et al., 2003; Cordes, 2005). The initial serotonin neurons are generated by progenitors from about E9.5 to E10.5 in rhombomere 1 (r1) co(Pattyn et al., 2003). Then a second wave of serotonin neurons are born about a day later in r2 and r3, as progenitors at these longitudinal levels initially generate visceromotor neurons (VMN) before becoming competent to generate serotonin neurons (Pattyn et al., 2003). Progenitor fate of caudal serotonin groups occurs with similar temporal characteristics in r5–r8, such that caudal serotonin neurons are born virtually simultaneously with those in the rostral domain. Interestingly, the synthesis of 5-HT in these newborn caudal serotonin neurons is delayed for 1–2 days (Lidov and Molliver, 1982a). Moreover, the serotonergic neurogenesis is never launched under normal circumstances in r4 (Pattyn et al., 2003).

During the second stage, progenitors do not exhibit serotonergic characteristic as yet. Serotonergic identity is then acquired through coordinated expression of serotonergic-type gene battery. The newborn serotonin neurons are phenotypically immature and have not been integrated into neural circuitry. Thus, beginning immediately after the birth of the 5-HT neurons and extending to at least the end of the third postnatal week, mouse 5-HT neurons undergo a series of complex maturation events (Lidov and Molliver, 1982b, a; Pattyn et al., 2003). These events include cell migration, dendric growth, expression of serotonin autoregulatory pathways, formation of highly collateralized axonal pathways and synaptogenesis.

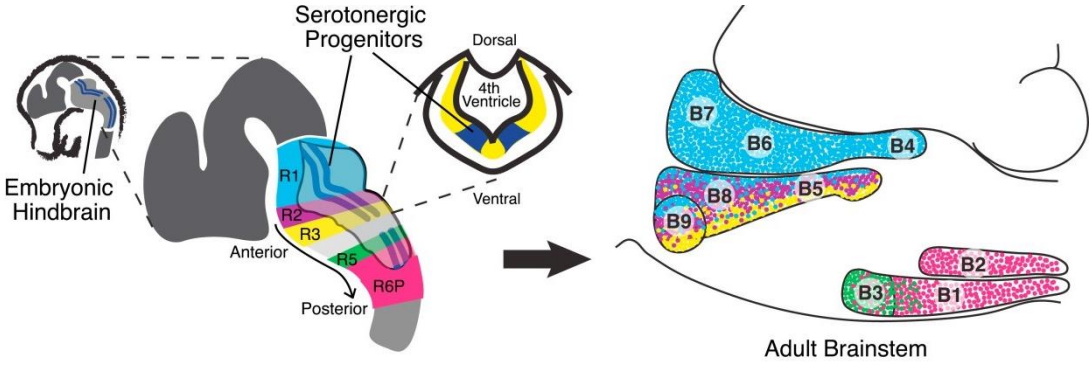

Figure7. Rhombomeric specify of serotonergic subpopulations (Okaty et al. 2015)

Development of serotonergic projections

Lidov and Molliver provided a detailed immunohistochemical study on the development of serotonergic projection in rat. (Lidov and Molliver, 1982b) In their study, the first time described the serotonin containing processes in the immature rodent CNS, but only ascendings were described but not descending. They described the ontogeny of the serotonergic axonal projections in three steps: At E13-E16, the initial axon elongation; E15-E19, the development of selective pathways; E19 to P21, the terminal field development.

Initially, serotonergic ascending axons are fasciculated and enter several well-defined fiber tracts starting from the medial forebrain bundle: specifically, the fasciculus retroflexus, stria medullaris, external capsule, fornix, and supracallosal stria. Depending on the different pathways, the serotonergic axons start to form the terminal arborizations in the thalamus, hypothalamus, basal and limbic forebrain, and cerebral cortex. In reaching the serotonergic terminal innervation targets, Lidov and Molliver observed that serotonergic fibers seem to be guided by some "pre-existing non-serotonergic tracts" which could be guidance cues. In particular, they described the terminal development in the cerebral cortex. From E19 to P21, the serotonergic fibers were starting and terminating the innervation in the cerebral cortex. Axons enter directly into the marginal and intermediate zones of the immature cortex, at the medial, frontal and lateral edges of the hemisphere, and subsequently spread tangentially to cover the hemispheres. Terminal ramifications then arise from the bilaminar axons and fill in the middle cortical layers.

During the first postnatal weeks the growth of serotonin axons across the forebrain appeared to be continuing. Interestingly, the development of terminal innervation is highly heterogeneous, occurring at different times and at different rates from region to region, which implies a possible role of chemical gradients produced in the targets to trigger the innervation.

These observations showed that serotonergic axons do not innervate immature, primarily proliferative neuronal populations and the formation of serotonin axon terminals is dependent on maturation of other elements in local neuronal circuitry. Evidences to surport this hypothesis are their findings of the delay in serotonin innervation of the suprachiasmatic nucleus, striatum, and middle cortical layers long after the axons have reached these structures.

Part 2: Molecular pathway of serotonin system and Eph family

1. From growth cone to axon guidance

Growing axons have a specialized structural differentiation at their tip known as the growth cone, which plays a crucial role in integrating the many signals that direct axons to their proper targets. The first detailed described of a growth cone was done by Cajal on spinal commissural axons, on three day old chick embryos. Morphologically, the growth cone is a fan-shaped structure with many long, thin spikes that radiate outward much like fingers on a glove. The prediction of Cajal that this might be a structure permitting the growing neuron to receive and integrate the variety of physico-chemical signals present along its pathway has now been validated by numerous cell biology experiments in vitro, but also with the improved visualizing techniques, in vivo. The signals that are sensed by the growth cones are produced by intermediate targets and the surrounding tissue and involve both chemical and biophysical cues. Such cues guide axons to their final target, where they establish synapses with one or more neurons (Mueller, 1999; Song and Poo, 1999). As predicted by Cajal, the growth cones are also highly motile structures. Video microscopic studies have shown that growth cones undergo continuous expansion and retraction before they reach their final targets. This was initially demonstrated in vitro on cell cultures (Harrison, 1959) and more recently in vivo (Tashiro et al., 2003).

We can explain the growth cone navigation system as driving. This system is similar to an experienced driver who can grasp different environmental changes, such as the traffic lights, street signs or bad road conditions in order to guarantee the right destination. Definitely, as the multiple environmental variables, the navigation system needs a series of molecules to form a signaling pathway in order to introduce spatial bias for steering the growth cone to the right targets.

To study the complex effects on the growth cone cytoskeletal machinery, recently, as interdisciplinary development, biophysical techniques became more and more popular to be used for cell biology assay. By performing the microfluidic devices has allowed the production of stable, precisely controlled gradients in various combinations of both diffusible and substrate-bound factors (Lang et al., 2008; Wang et al., 2008). These types of combined cues can more faithfully recapitulate the complexity of the in vivo environment, and thus, future experiments utilizing this method, in

combination with high-resolution cytoskeletal imaging, hold considerable potential for refining our understanding of the growth cone guidance mechanism.

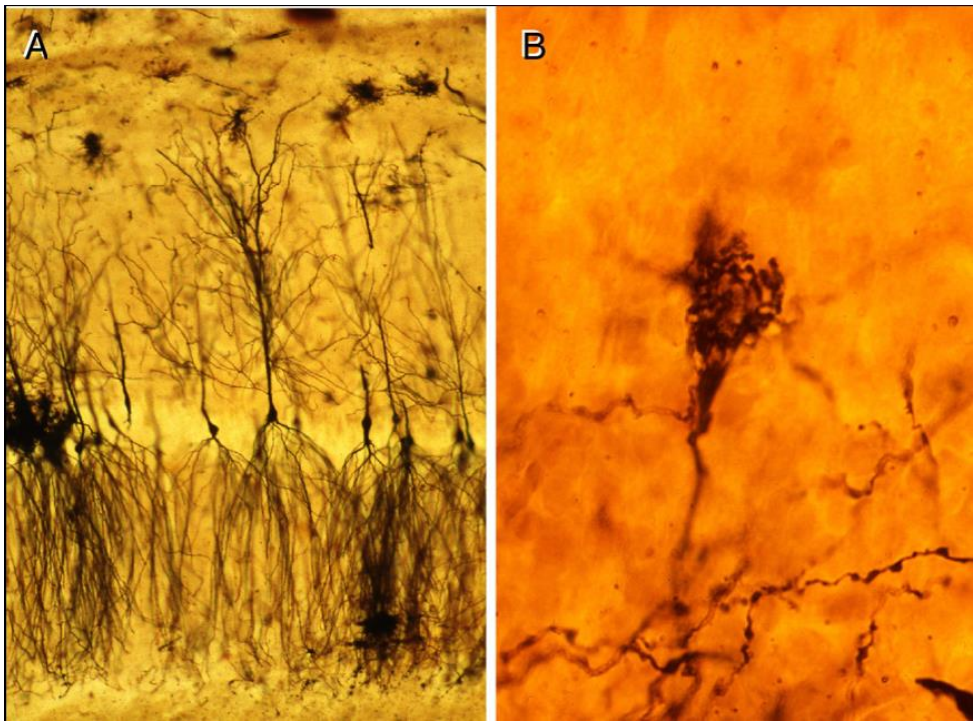

Figure1. Photomicrographs taken from some of Cajal's original preparations impregnated with the Golgi method. (A) Pyramidal cells in the Ammon horn of the adult rabbit (10×). (B) Pericellular nest formed around a Purkinje cell (empty) by a climbing fiber in the newborn kitten cerebellum (20×)

Besides the growth cone and axon themselves, the extracellular effectors that functionally steer extending neuronal processes are also important. There are probably both mechanical and chemical factors that orient the growing. However only molecular guidance cues will be discussed here. These can be subdivided into two types: long-range and short-range. Adhesion and guidance molecules are also important for the fasciculation of fibres into nerves and brain fascicles that connect one brain area to the other, such as the corpus callosum, or the corticospinal tract. Moreover, molecular signals can mediate interactions between axons and the substrates on which they extend. This is illustrated by the fact that some guidance molecules (such as entrain for instance) can be either chemo-attractive or chemo-repulsive, according to the substratum on which they are presented, which is thought to involve interactions of downstream signalling cascades. In particular,

intermediate or final targets provide information essential for selective guidance of distinct neuronal populations.

Main class of Molecular guidance cues

Molecular guidance cues play a key role in neuronal signalling to establish proper neuronal connectivity during CNS development and in adulthood. And the function of the guidance cue is critically on identifying the molecules and signalling events of neuronal guidance. Three experimental approaches over the past two decades have identified a wide variety of guidance molecules and their receptors: (1) pairing biochemistry and in vitro tissue culture assays to detect proteins with either attractive or repellent properties; (2) using forward genetics to identify mutations that affect axon trajectories in vivo; or (3) using genetic and tissue culture approaches to characterize the functions of molecules with distributions or molecular structures that make them attractive candidate guidance cues. (Kolodkin and Tessier-Lavigne, 2011) Using these different approaches, four major families of guidance cues with well-established roles in neuronal guidance have been identified: the Netrins, the Slits, the Semaphorins, and the Ephrins.

Other classes of molecules best known in different contexts are also now recognized to function as neuronal guidance cues; this includes certain morphogens and growth factors. For instance, cell-adhesion molecules (CAMs) of various classes have been implicated in neuronal guidance, and members of the immunoglobulin (Ig) and cadherin super-families play key roles in regulating distinct aspects of neuronal wiring. The identification and characterization of these cues and their receptors have led to several important generalizations about guidance mechanisms, including the existence of short- and long-range guidance cues, the multifunctional nature of several cues, and the evolutionary conservation of many guidance molecules and the roles they perform in neuronal guidance (Tessier-Lavigne and Goodman, 1996; Dickson, 2002). It is possible that additional classes of guidance cues remain to be discovered. However, the known guidance-cue families illustrate major principles of neuronal wiring mechanisms; it is likely that the combinatorial assembly of these signals ensure the precise encoding of specific neural targeting.

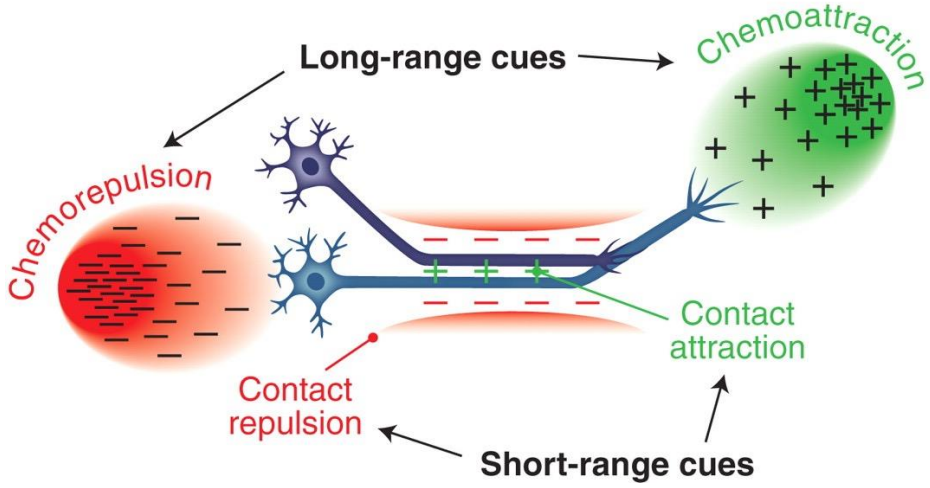

Figure2. The diversity of neuronal guidance mechanisms. Neuronal processes are guided by cues that can function at long and short distances to mediate either attractive or repulsive guidance. (Alex L. Kolodkin, 2011)

2. Molecular mechanism of serotonin raphe neuronal wiring.

As described in part 1, serotonin raphe neurons provide a massive and diffuse axonal projections to almost all the forebrain, brainstem and spinal cord. Moreover, as the studies of serotonin axonal projections become more complete and more detailed, the question that now arises is to identify the specific signals that allow this specific targeting.

Here I remind the three step of the development of serotonergic projections in rat, for helping to understand the relation of axon guidance in each period. First neurons migrate from their original site of production in the ventricles both ventrally and toward the midline. They initially form 2 bands on either side of the midline, and eventually fuse on the midline. The initial organization and orientation of serotonergic raphe neurons, can influence the spatial orientation of axon growth and the direction in which they grow; Secondly long-range guidance cue can guide serotonin axons grow along the main tracts toward their main targets; Finally . The short-rang effect, which is the terminal innervation of the specific targets of the axons. The molecular mechanisms of these steps during serotonin projection development were unknown until recent years- the genetic tools were developed, many genetic mouse lines were used to study these mechanisms.

Wnt—the anterior–posterior (A–P) organizer of serotonin axons in the hindbrain

The A–P projections of 5-HT neurons located in the hindbrain are established during midgestation and are essential for appropriate serotonergic circuit formation during subsequent developmental stages. Wnt family proteins are evolutionary conserved A–P guidance cues (Zou, 2006; Zou and Lyuksyutova, 2007). One of the Wnt signalling pathways, the planar cell polarity (PCP) pathway, is involved in tissue morphogenesis and directed cell migration (Wang and Nathans, 2007; Zallen, 2007; Goodrich, 2008; Simons and Mlodzik, 2008). Core PCP components include Frizzled, Flamingo (Celsrs in vertebrates), Van Gogh, Disheveled, Prickle, and Diego. Some of these factors were presented in serotonin neuron and axons at embryonic day 12, such as Frizzled3 (Fzd3), Celsr3, and Vangl2 (Fenstermaker et al., 2010). Interesting phenotypes were detected in the Frizzled3-/-, Celsr-/- and Vangl2-/- mice. At E12.5, ascending 5-HT neurons were detected with misprojections of R4 descending or lateral projection. In particular, the Frizzled3-/- and Vangl2-/- mice exhibit aberrant anteriorly projects 5-HT projections in the descending population and a marked reduction of proper descending axons. Additionally, the serotonin neuron cell body showed a different orientation in Frizzled3-/- and Vangl2-/- mice.

Slit—long projection pathways modulator of serotonin axon in the forebrain

Slit proteins have been implicated in axon guidance in both vertebrates and invertebrates. In mammals, the three Slit genes are expressed in, floor plate and roof plate of the spinal cord, and the septum area, hypothalamus, and hippocampus (Metin and Godement, 1996; Brose et al., 1999; Yuan et al., 1999). The expression patterns and in vitro observations suggest that Slit proteins are also likely to play important roles as repulsive guidance cues for multiple populations of migrating axons and cells, likely using Robo receptors for their functions as well (Brose et al., 1999; Hu, 1999; Nguyen Ba-Charvet et al., 1999; Piper et al., 2000; Ringstedt et al., 2000; Shu and Richards, 2001). A mammalian Slit protein was also independently identified as a positive regulator of branching and elongation of sensory axons.

Bagri et al. in 2002 studied on the long projection pathways of serotonin in forebrain in Slit1-/-, Slit2-/- and the double knockout mice. Their results indicated that in contrast to control mice serotonin fibers in the medial forebrain bundle of Slit2 mutants were displaced ventrally as they coursed through the diencephalon. In Slit1/Slit2 double mutants the medial forebrain bundle was commonly split in two components and numerous fibers descended ventrally into the hypothalamus,

approaching the midline a significant percentage abnormally crossed the midline in the basal telencephalon.

Pdcha— the forbrain terminal innervation effector of serotonergic neurons

The largest family in the cadherin superfamily is the clustered protocadherins, which are mainly expressed in neurons and localized to axons and synapses (Obata et al., 1995; Kohmura et al., 1998; Phillips et al., 2003; Junghans et al., 2008). Katori et al (Deneris and Wyler, 2012). In 2009, they detected a high level expression of pdcha in mouse raphe nuclei, particularly in rostral raphe. The maximum expression is from embryonic stage to the second postnatal week. Moreover, they analyse the serotonergic innervation in their forebrain targets of the pdcha-/- mice. In pdcha-/- mice, the abnormal distributed serotonergic fibers were detected in the hippocampus, substantia nigra and olfactory bulb at the endpoint of the third postnatal week in contrast to the wild type mice. Moreover, the globus pallidus and substantia nigra, in the mutants, exhibited as dense at the periphery of each region, but sparse in the center. In the stratum lacunosum-moleculare of the hippocampus, the mutants showed denser serotonergic innervation than in wild-type, and in the dentate gyrus of the hippocampus and the caudateputamen, the innervation was sparser. Their findings in the pdcha-/- mice indicated the pdcha is required for the terminal organization of serotonergic fibers.

Overall these studies have provided new clues on molecules that modulate serotonin raphe neurons outgrowth, and are starting to explain the different routes followed by axons from the rostral/caudal serotonin raphe neurons. However, we are still far from understanding what molecules guide the different subpopulation of serotonin neurons from the DR or MnR to their specific targets. A first step towards identification of these molecular cues is provided by gene expression screen in the raphe. A first screen was obtained by the team of Deneris and colleagues. Using the Pet1 promoter that is exclusively expressed in serotonin raphe neurons, they generated a transgenic mouse line, which expresses a fluorescent reporter (enhanced green fluorescent protein, eGFP) selectively in the serotonin neurons of the hindbrain. Using this transgenic mouse line, they sorted GFP+/GFP- neurons from microdissected raphe tissue of rostral and caudal hindbrain at embryonic day 12. Whole-genome screen was then done with microarrays comparing serotonin/non serotonin neurons, and rostral versus the caudal raphe cell groups. This first set of data identified hundreds of genes that are expressed specifically in serotonin neurons. Not surprisingly, in this gene list, axon guidance related genes were detected such as ephrins and Ephs, semaphorins and plexins, cadherins and protocadherins. A further analysis of the difference between rostral raphe and caudal raphe showed differential expression of several classes of molecules, suggesting that these factors could be

involved in the different targeting of the rostral and caudal serotonin cell groups. In a more recent study, the team of Susan Dymecki provided a detailed description of the differential genetic expression related to the subgroups difference. They used intersectional genetics combining a Pet1 driver to select for serotonin neurons and rhombomere specific drivers to identify the developmental origin of the serotonin neurons. With their animal models, serotonergic neurons arising from a given rhombomere (R)—R1, R2, R3, R5, or R6 and posterior could be distinguished in the fourth postnatal week, as a GFP-labeled 5HT neuron sublineage, and mRNA expression studies were performed both as population analysis and at the level of single cells. This provides a very valuable data set to compare gene expression patterns of serotonin neurons originating from different subgroup of serotonin neurons.

Based on these genome studies, we now have better evidence for selective expression of different guidance molecules in different subgroup of serotonin neurons. Based on the suspected role of different molecular guidance families, as described above, Eph receptors and their ligands were interesting candidates as potentially involved in the targeting of subpopulation of serotonin neurons since: i) they are one of the most prominent family of short-rang contact mediated guidance molecules; ii) According to the genome analyzing data, Ephs and their ligands showed a big difference between rostral-caudal (table 1) (Deneris and Wyler, 2012) and dorsal-medial (table 2) (Okaty et al., 2015) subnucleus.

Table 1

Deneris micro-array data (E12)			
Gene Symbol	Av R+C+	Av R+	Av C+
Epha3	894	371	1417
Epha4	836	1006	666
Epha5	1535	1974	1097
Epha7	631	669	593

Table 2

Dymecki RNA seq data (P21)				
Gene Symbol	R1(DR)pooled	R1(MnR)pooled	R2 pooled	R3 pooled
Epha2	0	0	2	0
Epha3	54	9	125	9
Epha4	4	248	1290	40
Epha5	634	676	4386	1272
Epha6	344	469	2110	388
Epha7	163	174	677	139
Epha8	16	48	140	24
Epha10	191	65	203	57

3. Eph receptors and their ligands ephrins

Receptor tyrosine kinases are key components in the transduction of certain extracellular signals across the cell membrane, as such they play critical roles in cell growth, differentiation, survival, and migration (van der Geer et al., 1994). These receptors regulate various aspects of embryonic development, such as tissue morphogenesis and formation of neuronal circuits.

The Eph family is the largest among all of the known receptor families, which includes at least 14 distinct members and can be considered as the largest subfamily among all of the receptor tyrosine kinases (RTKs). The Eph receptors are divided into two sub-families according to sequence homology: a A-subclass, which in mammals contains nine members (EphA1–EphA8 and EphA10), and a B-subclass with five members (EphB1–EphB4 and EphB6). EphAs and EphBs have a similar general structure: the extracellular domains of the Eph receptors are characterized by the presence of an IgG-like domain, a cysteine-rich region, and two fibronectin type III domains. (Zhou, 1998) However they differ in amino acid sequences and binding affinities to their ephrin ligands. (Egea and Klein, 2007)

Initial studies on the functional roles of Eph receptors were lacking the identifiable ligands. Foreseeably, after the isolation of at least eight distinct ligands, this provided a large progress of the studies of functional roles of the Eph receptors in many developmental processes and in adult life. Because of the large number of ligands and receptors in the Eph family, research in the field covered a large time span; this resulted in initial confusion in the nomenclature, as each different gene in the family was given a different name by independent investigators (Tuzi and Gullick, 1994). A unified nomenclature was proposed in 1997 to clarify the field (Eph Nomenclature Committee, 1997) and is at present the one currently utilized. In this nomenclature, the ligands are now named as ephrins, which is the abbreviation for Eph family receptor interacting proteins. The name is also related to the Greek word “ephoros,” meaning overseer or controller, which is implying a function in guidance. Similarly to Eph receptors, these ligands are also divided into two families: an A-subclass (ephrinA1–ephrinA5), which are tethered to the plasma membrane by a glycosylphosphatidylinositol (GPI) anchor, and the B-subclass (ephrinB1– ephrinB3) which have a transmembrane domain and an intracytoplasmic tail lacking endogenous catalytic activity. The receptors and ligands are numbered according to their date of initial publication (Eph Nomenclature Committee, 1997). There is an intra-class selectivity of the ligands for their receptors, as the A-type receptors typically will bind to

most A-type ligands; similarly, EphBs bind to most B-type ligands. A few exceptions exist; in particular, EphA4 and EphB2 were found to bind to both ephrinAs and ephrinBs

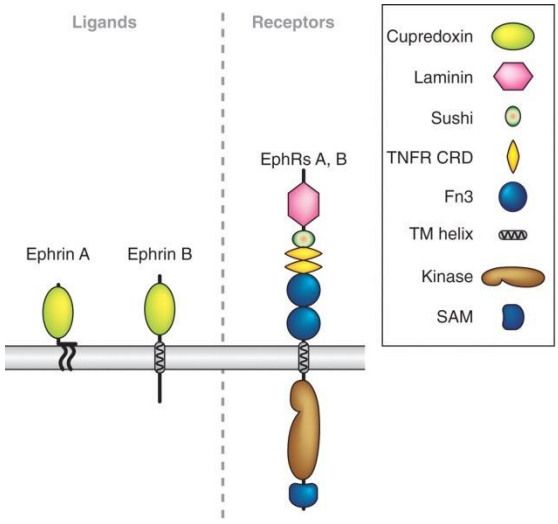

Figure4. Ephrins and their Eph receptors. The key defines distinct molecular domains found in these proteins. (Alex L. Kolodkin, 2011)

Althrough Eph-receptos belong to the subfamily of tyrosine kinases receptors, they have several unique features which distinguish them from other RTKs. 1). Ephs require the cell to cell interaction or communication which limits the action of this system to short-range distances, since the ligands require membrane attachment, whereas all other RTKs bind to soluble ligands; 2) Eph–ephrin signaling requires higher order clusters for signaling (Vearing and Lackmann, 2005), whereas receptor dimers are sufficient to activate the classical RTK; 3) Ephrins can act both as ligands and as receptors with their own signaling potential. Following ephrin binding to its receptor, besides the stimulating signaling cascades within the Eph-bearing cell, ephrins can induce the signals within the ephrin-bearing cell. Both signaling events can happen simultaneously, and the relative contributions of Eph forward and ephrin reverse signaling is variable, depending on cell to cell communication. 4) Ephs and ephrins, are both membrane-bound, and have an extracellular domain that can interact in‘cis’ when Ephs and Ephrins are co-localized in the same cell. Signaling events activated by Eph forward and ephrin reverse signaling are characterized, and seem to be different from classical RTK signaling. Classical RTKs signaling largely involves Ras–MAPK (mitogen-activated protein kinase) and phosphatidylinositol (PtdIns) 3-kinase (PI3K)–Akt pathways (Eswarakumar et al., 2005). In

contrast, Ephs -signaling is generally limited to the activation of Ras–MAPK and PI3K–Akt pathways and, instead, recruit phosphotyrosine-binding adaptor proteins to activate Rho GTPases and remodel the actin cytoskeleton (Noren and Pasquale, 2004). EphrinB reverse signaling also activates Rho GTPases and uses phosphotyrosine-independent docking mechanisms. (Klein, 2004)

4. Eph/ephrin signalling mechanisms

The expression of Eph and ephrin genes has been described in many different species, such as mouse, rat, zebrafish and chick (Boyd and Lackmann, 2001). These genes are widely expressed during development, in contrast with the vascular endothelium and specialized epithelia where Eph and ephrin are rarely expressed, expression is maximal in the central nervous system. To avoid the excursive ligand–receptor interactions, both spatial and temporal regulations of expression are important. The presence of multiple family members in the same place and time is nevertheless observed and may account for the lack of strong phenotypes in most single-molecule knockouts. Since Eph–ephrin interactions induce repulsive bi-directional signals, ligands and receptors are often expressed in adjacent but non-overlapping cell groups, thus defining and maintaining developmental tissue boundaries, an example being the formation of hindbrain rhombomeres (Boyd and Lackmann, 2001). In a similar way, ephrinB2 and EphB3 are expressed in developing arteries and veins, respectively, thus preventing the intermixing of these two cell types (Dodelet and Pasquale, 2000)

As I mentioned, Eph/ephrin signaling involves formation of higher order Eph/ephrin clusters (Himanen et al., 2010; Seiradake et al., 2010). Generally, the fist connection between Ephs and ephrins from different cells (called in ‘trans’), because of the spatial limitation, can guide the Ephs and ephrins forming the heterotetramers (two Ephs and two ephrins) at the connection site. However, the functional forward and reverse signaling demand a large signally cluster formed by the aggregation of Ephs and their ligands. To carry out this, Eph clusters can incorporate additional Eph receptors in an ephrinin-dependent fashion by lateral recruitment.

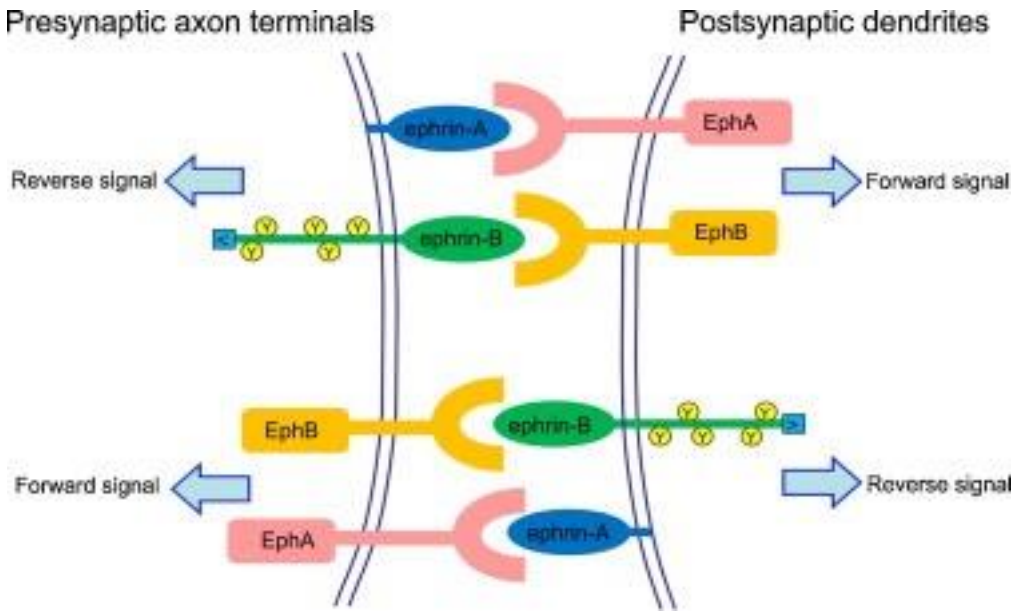

Figure 5. Bidirectional signals mediated by Eph/ephrin in both presynaptic axon terminals and postsynaptic dendrites. Eph receptors are divided into two separate subfamilies, termed EphA and EphB. (Xu et al., 2012)

Forward signaling

In recent years, many researchers studied the Eph-ephrin signaling pathways in a variety of different model organisms and cellular systems (Pasquale, 2008; Jorgensen et al., 2009; Bashaw and Klein, 2010; Bush and Soriano, 2012; Hruska and Dalva, 2012; Miao and Wang, 2012). Here I will discuss only results obtained in the mouse model. Eph forward signaling involves activation of a tyrosine kinase activity and down-stream tyrosine phosphorylation of intracellular effector proteins. These signaling pathways in turn modulate the activity of molecules of the small Rho family GTPases such as Rac1, Cdc42 and RhoA, thus modulating cytoskeletal dynamics. For instance, mice lacking EphA4 2-chimerin showed a rabbit-like hopping gait (Beg et al., 2007; Iwasato et al., 2007; Wegmeyer et al., 2007). This is because interaction between EphA4 and the RacGAP 2-chimerin is important for axon repulsion in the spinal circuits that control locomotion. Coincidentally, the SH2-adaptor proteins Nck1 and Nck2/Grb4 have been implicated in the same pathway (Fawcett et al., 2007). Furthermore, it has been shown that the Vav family of RhoGEFs directly interacts with EphA4 and EphB2, and promotes EphA endocytosis, which leads to growth cone collapse. (Murai and Pasquale, 2005).

Another family of RhoGEFs, the Ephexins, have been found to bind to Eph receptors. Ephexins are activated by tyrosine phosphorylation upon ephori binding and activates RhoA. Ephexin 1-mediated RhoA activation had similar effects as Vav (Sahin et al., 2005). However, ephexin activity can be inhibited by EphB signaling. One example is the EphB-mediated tyrosine phosphorylation that can inhibit synapse formation induced by ephexin 5. Additionally EphB can subsequently be involved in the degradation of ephexin 5 (Margolis et al., 2010). Other signaling pathways have been found outside the brain; In the intestine, EphB2-dependent migration of progenitor cells involves PI-3 kinase activity, while proliferation is promoted by Abl kinase and cyclin D (Pitulescu and Adams, 2010).

Reverse signaling

In contrast to the Eph forward signaling, less is known about ephrin reverse signaling. Recent studies indicated that ephrinAs reverse signaling, involves the Ret tyrosine kinase receptor; in motor axons this interactions promotes axon attraction (Bonanomi et al., 2012); similarly the interaction between ephrinA and the TrkB neurotrophin receptor promotes axon branching and synaptogenesis (Marler et al., 2008). On the other hand, ephrin B reverse signaling typically involves tyrosine phosphorylation of its intracellular domain and recruitment of PDZ domain-containing proteins (Xu and Henkemeyer, 2012). In the absence of ephrin B proteins, stimulated VEGF receptors are retained in the plasma membrane and fail to signal properly, leading to reduced endothelial sprouting. Activation of B-class ephrin signaling in neurons induces phosphorylation of Dab1 (possibly by activation of Src family kinases), the major effector of the reelin pathway (Doeppner et al., 2011). Loss of ephrin B3 proteins causes neuronal migration defects similar to the realer mouse.

Cis versus trans interactions

So far, I have summarized the condition where Eph and ephrin are expressed in opposing cells. However, in a majority of regions of the developing mouse brain, Ephs and ephrins are co-localized in the same cell. This condition raised the question of whether Ephs can interact with ephrins in cis and whether cis interactions change the responsiveness to ephrins presented in trans? Do Ephs and ephrins share the same membrane microdomains (Gauthier and Robbins, 2003) and downstream signaling molecules, or are they isolated into different microdomains and have unique signaling outputs?

To answer these questions, we should start from the very basic behavior of the axonal connection patterns in the central and peripheral nervous system, this means the organization into topographic maps in which the spatial order of neurons is mapped smoothly onto their axon terminals in the targets. The visual system has offered an ideal system to study axonal topographic mapping, as this organization is very well-known. In the visual system, the spatial order of neurons in the retina is transferred to higher visual centers of the brain, the superior colliculus and the lateral geniculate nucleus. Ephs and ephrins are well-accepted molecular cues involved in this retinotopic mapping (Lemke and Reber, 2005; McLaughlin and O'Leary, 2005; Flanagan, 2006). In the target region of retinal axons, a high expression of ephrinAs was detected, and these ephrinAs acted as a repulsive guidance cues, which can interact with their receptors EphAs in trans (Flanagan, 2006). Furthermore, researchers found that the EphAs functions are also modulated by the co-expressing ephrinA5. They found that in axons co-expressing EphAs and ephrinAs, EphA responsiveness is down regulated. This can be explained by EphA-ephrinAs interaction in cis. The consequence is that axons with higher ephrinA and EphA ratios are less responsive to the repulsive effect of ephrinAs in the target tissue (Hornberger et al., 1999; Yin et al., 2004). In further studies, two types of cis interactions were distinguished: interactions through the ligand binding domain (LBD) of Ephs (the normal cis interaction) and non-LBD-dependent interactions (Carvalho et al., 2006). Previous study showed that the LBD is necessary for the interaction between EphAs and ephrinAs in trans (Labrador et al., 1997). To detect the non-LBD-dependent interactions, researchers used an ephrinA5 mutant, which cannot bind to the LBD of EphAs. Comparing the native and mutated ephrinA5, they found that ephrinA5 mutants still interacted with EphAs through a non-LBD interface. Functionally, cis interactions reduced tyrosine phosphorylation levels of EphAs and the sensitivity of retinal axons towards ephrinA5 applied in trans. This suggested that cis interactions reduced the repulsive forward signaling and thereby, had a role in modulating retinotectal mapping. Such a mechanism could transform a uniform expression pattern of Ephs into a gradient of ‘active’ receptors (mediating stronger repulsive signals the less ephrinAs were co-expressed). How cis-interacting ephrins reduce Eph signaling is currently unknown. Ephrins might antagonize Eph receptor clustering by steric interference or they might sequester them into other membrane microdomains, preventing access to essential downstream signaling molecules.

5. EphA5 and ephrinA5 from past to present

EphA5 also named as REK7, Ehk-1 and Bsk was originally identified as a nervous-system-specific orphan tyrosine kinase receptor expressed at high levels in embryonic rat

brain and at lower levels in the adult brain, mainly in the cortex, hippocampus, and olfactory bulb (Maisonpierre et al., 1993; Zhou et al., 1994; Winslow et al., 1995).

Ephrin-A5, is the ligand for EphA5a; it is a GPI-linked cell-surface protein like the other ephrinA ligands. EphrinA5 was initially isolated from a human breast carcinoma cell line (Winslow et al., 1995) and it is expressed both in the nervous system and in a number of non-neuronal tissues.

In late 20th century, researchers found that cultured cell transfected with membrane-bound ephrin-A5, could activate the EphA5 receptors present on cortical neurons. On the other hand, the soluble ephrin-A5 could not (Winslow et al., 1995). Soon after, Meima et al tried to explain this phenomenon. They produced an ephrin-A5-IgG, which is a dimeric form of the molecule containing the extracellular domain of Ephrin-A5 but not the GPI-signal, this dimer fused to an IgG Fc-domain has comparable activity to membrane-bound Ephrin-A5. This indicates that Ephrins need to act as a complex, while the monomeric soluble ephrin-A5 failed to induce the receptor oligomerization (Meima et al., 1997b). Not surprisingly, a similar requirement for membrane attachment has been found for other members of the Eph-ligand family (Gale et al., 1996). However, soon after that, Meima et al. showed that dimerized soluble ligands are also unable to achieve receptor activation and therefore that additional crosslinking is required (Sakano et al., 1996; Meima et al., 1997a). The immunocytochemistry studies of embryonic cortical neurons with an anti-EphA5 antibody have suggested that heterogeneity exists in the population with respect to the level of EphA5 expression.

EphA5 expressing growth cones respond to Ephrin-A5-IgG with a collapse and retraction response, whereas growth cones with no EphA5 expression remain unresponsive. (Ingrid 1997) This indicated that EphA5 is the receptor mediating these effects. The fact is, as mentioned earlier, that Eph receptors and their ligand do not have strict selectivity and specificity in their binding properties (Brambilla and Klein, 1995; Gale et al., 1996). So it is interesting to know whether the other Eph receptors which can bind to ephrinA5 also present this effect. Embryonic cortical neurons have been shown to express at least two receptors besides EphA5, in particular; EphA3 (Hek) and EphA4 (Sek1) (Ingrid 1997).

Binding affinity measures showed that Ephrin-A5 activates EphA4 approximately 10-fold less efficiently than EphA5 or EphA3 (Gao et al., 1998), suggesting that its physiological effects are more likely to be mediated by the latter two receptors. In considering the interactions of cortical neurons with each other and with astrocytes, the situation is further complicated by the presence of multiple ligands. Astrocytes express both Ephrin-A3 (Ehk1L/Lerk3) and Ephrin-A5, while cortical neurons

express both Ephrin-A2 (Elf-1) and Ephrin-A3. Ephrin-A3 and EphrinA5 both induce the collapse of cortical growth cones. (Ingrid 1997) Receptor binding and activation experiments suggest that Ephrin-A5 and Ephrin-A3 are equally good at activating EphA5. On the other hand, Ephrin-A5 is much better than Ephrin-A3 at activating EphA3 (J.W.Winslow 1998). One possible interpretation of this paradoxical finding is that cortical axons express different amounts and different ratios of EphA5 and EphA3, and that both receptors contribute to growth cone collapse/guidance. The contributions of the different receptors might be additive until a certain threshold level is reached that activates a downstream signaling pathway. According to this hypothesis, Ephrin-A5 triggers a response in a large subset of cortical axons, because it can activate both receptors; Ephrin-A3 induces a response in a more limited subset (those that express sufficient levels of EphA5), because it can only effectively activate EphA5. Such a scheme would presumably allow for greater flexibility and a wider range of responses than could be achieved by using a single receptor-ligand interaction. With regard to fasciculation, the presence of Eph ligands such as Ephrin-A3 on cortical axons and on astrocytes poses an additional problem. It is possible that repulsive forces between axons (in this case, axons expressing sufficient levels of EphA5) are involved in modulating fasciculation and may contribute selectively to induce defasciculation.

5.1 The mechanism of EphA5 modulated growth cone collapse

The spatial organization and the morphology of the growth cones are modulated by the cytoskeleton. The actin filaments and microtubules which are the link between the guidance cues and the cytoskeleton, are not only related to the rearrangements of the cytoskeleton but also drive both neuritis elongation and steering in response to guidance cues (the extracellular environment) (Tanaka and Sabry, 1995). In growing axons, filamentous actin (F-actin) is concentrated at the leading edges of the growth cone (see part 2-1). Treatment with Ephrin-A5 induces a rapid rearward translocation of this F-actin away from the leading edges into the center of the growth cone. This happens within 5-10 min after the addition of Ephrin-A5, concurrent with retraction of the lamellipodia, and may be the driving force for growth cone collapse (Meima et al. 1997a).

Because these effects resemble those of cytochalasin D, a fungal toxin known to inhibit the polymerization of actin (Sampath and Pollard, 1991), it has been speculated that Ephrin-A5-induced growth cone collapse might be caused by a perturbation of actin polymerization. Measurement of the relative F-actin concentrations in cortical neurons revealed that prolonged treatment with Ephrin-A5 (longer than 60 min) leads to a net loss of F-actin from the cells, consistent with the hypothesis that Ephrin-A5 affects actin polymerization (Meima et al. 1997b). In contrast to its dramatic effects on

actin cytoskeleton, Ephrin-A5 does not appear to affect microtubules. Since a major role of EphA5 seems to be the regulation of axonal behavior with regard to axon fasciculation. EphA5 is expressed on both the axons and dendrites of cortical neurons.(Caceres et al., 1986; Dotti and Banker, 1987; Winslow et al., 1995) Double immunofluorescent staining with these antibodies together with an antibody against EphA5 has shown that EphA5 is present on the dendrites and on the axons of differentiated cortical neurons. These observations open up the possibility that, in addition to influencing the decisions that axons make, these molecules may also influence the patterning of dendritic arbors.

5.2 The role of EphA5-ephrinA5 interaction within the hypothalamus from glutamine system to aggressive behavior

EphA5-ephrinA5 interaction influence glutamine system

In recent years, researchers have focused on the functional role of EphA and ephrinA interactions in the glutamatergic system. This led to emergence of new ideas on the functional role of EphA-ephrinA interaction in synaptic maturation and synaptic plasticity.

EphA receptors were found to be localized in glutamatergic synapses in both the presynaptic (axon terminal), postsynaptic (dendritic spines) elements in neurons (Murai et al., 2003; Tremblay et al., 2007; Bouvier et al., 2008). EphA receptors were reported there to serve to regulate synaptic plasticity by acting as a binding partner for ephrins. Nestor et al. (Nestor et al., 2007) indicated that the interaction between EphA receptors and ephrinA influences the release of glutamate. Moreover, Filosa et al. (Filosa et al., 2009) found an upregulation of astroglial glutamate transporters in ephrinA3 and in EphA4 knockout mice, raising the possibility that EphA-ephrinA interactions may modulate glutamate/glutamine cycling and synaptic function.

Most recently, studies of Szepietowska et al. showed that EphA5-EphrinA5 interactions within the ventromedial hypothalamus (VMH) modulate local glutamine/glutamate balance in a hypoglycemia model. Their study indicated that similar activation of EphA5 receptors using VMH delivery of an exogenous ligand or local overexpression of ephrinA5 increases counter regulatory hormone responses to hypoglycemia. Conversely, local VMH knockdown of ephrinA5 gene expression suppressed counter regulatory hormone responses. Thus, EphA/ephrinA signaling within the islet and VMH could potentially act in concert in these two glucose-sensing centers to defend against hypoglycemia and contribute to defective counter regulation after intensive insulin treatment.

Previous studies have shown that glutamatergic neurotransmission in the VMH influences the magnitude of counter regulatory responses to hypoglycemia. Mice with impaired glutamatergic neurotransmission secondary to the loss the glutamate transporter, VGLUT2, selectively in SF1 VMH neurons exhibit a modest reduction in fasting glucose levels, marked suppression of glucagon secretion, and diminished catecholamine responses during insulin-induced hypoglycemia (Tong et al., 2007).

The study of Szepietowska et al., which is on a hypoglycemia mouse model, showed that targeted overexpression of ephrinA5 caused an increase in glucagon and epinephrine secretion that was maximal at the same time than an increase in glutamate levels occurred in VMH interstitial fluid during hypoglycemia. However, downregulation of ephrinA5 within the VMH produced a sustained reduction in glucagon and epinephrine release that occurred in conjunction with a profound and sustained decrease in the levels of glutamine in VMH interstitial fluid. These observations are consistent with the possibility that Eph5A/ephrin5A interaction influences glutamate neurotransmission. (Szepietowska et al., 2013)

EphA5 and ephrinA5 play a key role in aggressive behavior

To study the functional impacts of Eph and their ligands in neural circuit formation and consequences in behavior, the EphA and ephrinA5-/- mouse models have been analyzed extensively.

The ephrinA5-/- mouse line was first used to study the function of ephrinA in the topographic mapping of the visual system; this showed the key role of ephrinA5 in retinol topic making in the rostral to caudal organization of retinal axons arising from the temporal or nasal parts of the retina (see part2-5). More recently, Michal et al. studied the aggressive behavior in the ephrinA5-/- mice. They examined effects of its inactivation on male mouse aggression. In their studies, a series of behavioral test were performed with the male ephrinA5-/- mice. Found that the offensive aggression is severely reduced, however, this reduction of offensive aggression was not induced by the inability to attack the presence of the intruder, since the ephrin-A5−/−mice exhibited increased target biting and testosterone levels and general olfaction were normal. Moreover in the previous studies of the same team demonstrated that lacking of EphA5 also leads to the decrease in aggressive behavior in mice. (Sheleg et al., 2015) Interestingly, in previous studies of Ping Chao Mamiyaa et al. in 2008, similar data were detected in the EphA5-/- mice and moreover, they indicated that in the EphA5-/- mice brains, the serotonin level significantly reduced in the hypothalamus (Mamiya et al., 2008).

Results

Part 1：EphAs-EphrinAs signaling is required for the distinctive targeting of raphe 5-HT neurons in the telencephalon.

All serotonin (5-HT) innervation in the brain derives from the raphe nuclei in the hindbrain (the B1-B9 cell groups). These projections are highly collateralized but with some degree of topographic organization. In the telencephalon, the pattern of 5-HT innervation arising from the dorsal (B7, B6) or the medial (B5-B8) nuclei differs. However, the guidance molecules that direct these 5-HT raphe neurons to different targets are not known.

In the first, we investigated the role of ephrinA-EphA signaling in this selective targeting. In our results, we demonstrated that the EphA5 selectively expressed in distinct subpopulation of serotonin raphe neurons. Particularly, EphA5 exhibited the highest level in dorsal raphe serotonin neurons (B7). The results of in vitro explants culture and in vivo electroporation analysis indicated that the ligands of EphA5 (ephrinA5 and ephrinA3) act as a repellent factor to the serotonergic axonal growth cones.

Furthermore, the anterograde tracing analysis in the ephrinA5 -/- mice showed mistargeting of dorsal raphe neurons projections, which included the serotonergic projection.

Overall, our results shows for the first time the implication a guidance molecule for the region-specific targeting of serotonin raphe neurons and has implications for understanding the anatomofunctional parsing of the raphe cell groups.

EphrinA5 signaling is required for the distinctive targeting of raphe 5-HT neurons in the telencephalon.

Teng Teng [1, 2,3], Afsaneh Gaillard [4, 5], Aude Muzerelle[1, 2,3], Patricia Gaspar[1, 2,3]

Author affiliations:

1. Inserm UMR-S 839, 75005, Paris, France

2. Université Pierre et Marie Curie, Paris, France

3. Institut du Fer à Moulin, Paris, France

4. Inserm 1084, Poitiers, France

5. Université de Poitiers, France

Key index words: Dorsal raphe nuclei, Axon guidance, ephrinA, olfactory bulb, hypothalamus,

Manuscript information:

Number of pages: 26

Number of Figures: 7

Tables: 5

Number of words in abstract: 241

Number of words in Introduction: 537

Corresponding author:

Patricia Gaspar, INSERM U 839, 17 rue du Fer à Moulin, 75005, Paris, France

Tel: 331 45 87 61 28 Fax: 331 45 87 61 30

email: patricia.gaspar@inserm.fr

Acknowledgements: Sebastian Brot and Yohan Bertelle for animal breeding, the IFM imaging facility for useful advice, Michael Reber for helpful comments on the manuscript and for all the primers and EphrinA3 construct; Imane Moutkine for her help with molecular constructs.

Funding: Teng TENG was financed by the China Scholarship Council; Research was funded by the Fondation de la Recherche Médicale, Labex BioPsy, Inserm, and Université Pierre et Marie Curie. The team is part of the Ecole des Neurosciences de Paris training network;

Abstract (240 words)

Serotonin (5-HT) neurotransmission in the brain relies on a widespread axonal network originating from the hindbrain raphe nuclei. Raphe 5-HT projections are topographically organized: the caudal, dorsal (DR), and median raphe (MnR) nuclei have different brain targets and physiological functions. However, the guidance molecules involved in the selective targeting of raphe axons are unknown. Here, we show the implication of ephrinA signaling for organizing DR projections during development. EphA5 is selectively expressed in a subset of 5-HT neurons during embryonic and postnatal development. Highest co-expression of EphA5 and the 5-HT marker Tph2 was found in the medial DR while there was lower co-expression in the MnR, and caudal raphe nuclei. Accordingly, ephrinA induced a dose-dependent collapse response of the 5-HT growth cones cultured from rostral but not caudal raphe. Ectopic expression of ephrinA3 in the amygdala and piriform cortex repelled normal 5-HT raphe fiber ingrowth. Conversely, in eprhinA5 KO mice, anterograde tracing showed mispositioned DR axons in brain regions that are normally targeted only by the MnR. In particular, the overall density of 5-HT innervation was increased in the ventromedial hypothalamus, the suprachiasmatic nucleus and the outer layers of the olfactory bulb. All these brain areas have high expression of ephrinAs at the time of 5-HT fiber ingrowth. These results show for the first time the role of a guidance molecule for the region-specific targeting of raphe neurons and has implications to understand the functional parsing of central 5-HT neurons.

Keywords: Dorsal raphe nuclei, serotonin, Axon guidance, ephrinA, hypothalamus, olfactory bulb, primary culture

Significance statement: Our results demonstrate a new role of ephrinA signaling for the selective targeting of 5-HT raphe nuclei. The tyrosine kinase EphA5 is differentially expressed across 5-HT neurons from the different raphe nuclei, correlating with a different repulsive action of ephrinA on 5-HT axon growth. Ephrin-A5 loss of function causes a mis-targeting of dorsal raphe 5-HT axons, whereas over-expression of ephrin-A3 inhibits the ingrowth of 5-HT raphe axons in the amygdala and piriform cortex that are main targets of the dorsal raphe 5-HT neurons. Thus Eph-Ephrin signaling acts as a repulsive signal to differentially target 5-HT axons originating from different raphe nuclei.

Introduction

Serotonin (5-Hydroxytryptamine, 5-HT) neurotransmission is implicated in a large number of physiological functions raising the question of a division of labor among the different hindbrain nuclei that synthesize 5-HT (Calizo et al., 2011; Hale and Lowry, 2011; Kiyasova and Gaspar, 2011; Brust et al., 2014; Teissier et al., 2015). The 5-HT synthesizing neurons are distributed into several raphe nuclei in the hindbrain that have been parsed according to anatomical and physiological criteria. Different raphe nuclei target different brain regions and, consequently, have different functional roles. For instance the caudal 5-HT raphe nuclei (the B1-B3 cell groups) that are located in the medulla, project to brainstem and spinal cord and have been implicated in motor control and in neurovegetative functions (Schmidt and Jordan, 2000; Pflieger et al., 2002; Brust et al., 2014). Conversely, 5-HT neurons in the rostral raphe are located in the pons (the B5-B9 cell groups) and project to the telencephalon; these cell groups have been involved in diverse higher brain functions, such as mood, learning and different types of social behaviors, such as aggression or maternal behavior (Deakin and Graeff, 1991; Lucki, 1998; Fernandez and Gaspar, 2012). Further anatomo-functional distinctions can be made within the rostral 5-HT cluster where neurons of the dorsal raphe (DR =B6+B7) and the medial raphe (MnR= B5+B8) groups innervate different brain areas; and have consequently been implicated in different functions (Jacobs and Azmitia, 1992; Fernandez et al., 2015; Teissier et al., 2015). This organization suggests that specific axon guidance molecules orient the 5-HT neurons from different raphe nuclei to different targets, although the molecular mechanisms involved are largely unknown (Kiyasova and Gaspar, 2011).

Previous transcriptome profiling of developing 5-HT raphe neurons identified distinct expression profiles between the rostral pontine and the caudal medullary raphe cell groups (Wylie et al., 2010). Among these genes a list of axon guidance molecular candidates were available. We focused on the Eph receptors, several of which showed differential expression between the rostral and caudal raphe 5-HT neurons. Moreover the known properties of Ephs as short-range guidance factors make them attractive candidates for selective axon targeting. The Ephs are tyrosine kinase receptors activated by Ephrin ligands that comprise two main classes: class A Ephrins which are GPI-linked and interact at various degrees of selectivity with class A Eph receptors (EphA1-A10), and class B Ephrins which are transmembrane receptors interacting with class B Eph receptors (O'Leary and Wilkinson, 1999; Klein and Kania, 2014). EphrinA signaling has been involved in many functions, one of

the best known being it's role for establishing topographic maps (Prakash et al., 2000; Miko et al., 2007). Interestingly Eph-EphrinA have also been involved in the development of dopaminergic neurons based on expression studies and effects of EphrinA5 on axon growth and fasciculation (Deschamps et al., 2010;Prestoz et al., 2012).

In the present study we establish that the EphA5 receptor is selectively expressed in developing 5-HT raphe neurons of the rostral raphe cluster and that ephrinA5 exerts a repellent effect on 5-HT axon growth. We find that there is a differential EphA5 expression amongst the different 5-HT raphe neurons and that this explains several distinctive features of the DR 5-HT projections, in particular regarding the exquisite differential targeting of the DR and MR axons to specific laminae of the olfactory bulb and to specific hypothalamic neuronal sub-nuclei.

Material and methods

Animals

Gene expression analyses during development were performed on mice of the Swiss background (RjOrl:SWISS) purchased from a commercial breeder (Centre d'Elevage R. Janvier). E0.5 was defined as the plug date and P0 as the date of birth.

The Pet1-Cre::RCE-GFP mouse line was used for RT-qPCR analyses. ePet1-Cre mice (Scott et al., 2005) in which the serotonergic specific promoter of the Pet1 gene controls Cre expression were crossed to the RCE-GFP mouse line where enhanced green fluorescent protein is conditionally expressed under the Rosa-26 promoter (Sousa et al., 2009). Pet1-Cre::RCE-GFP mice were bred in our local facility and brains collected from P5, P15 and adult mice.

The ephrinA5-KO mouse line was a gift of the Frisen lab (Frisen et al., 1998) to Dr Afsaneh Gaillard and maintained on a C57Black6 background (Deschamps et al., 2009). Briefly, these mice have a PGK-neo cassette replacing the 5' acceptor splice site and the sequences encoding amino acid residues 42–129. The PCR primers for genotype are as follows: primer 1 (TCCAGCTGTGCAGTTCTCCAAAACA) and primer 2 (ATTCCAGAGGGGTGACTACCACATT) for wild-type sequences (397bp) and primers 1 and primer 3 (AGCCCAGAAAGCGAAGGAGCAAAGC) for mutant sequences (513bp).

All experiments were performed in compliance with the standard ethical guidelines (European Community Guidelines and French Agriculture and Forestry Ministry Guidelines for Handling Animals decree 87849). All efforts were made to reduce the number of animals used and their suffering.

Male and female mice were used indiscriminately in all experiments.

Histology

Section preparation Brains were collected at embryonic days 12(E12), E14, E16, E17, E18, at postnatal days 0(P0), P5, P10, P15 and from adult aged over 8 weeks.

Mice aged P5 or younger were anesthetized on ice. Mice older than P5 were anesthetized with pentobarbital, 25 mg/kg and xylazine, 5 mg/kg. Fixation was either with immersion (E14, E16) or perfusion (>E16) with 4% PFA (4% paraformaldehyde in 0.12 M phosphate buffer, pH 7.4). Dissected brains were post-fixed 2 hours (embryonic ages) or overnight (all postnatal ages) before cryoprotection in 10% sucrose and freezing in isopentane cooled with dry ice at -45° to -55°C. In some in situ hybridization (ISH) protocols no post-fixation was performed. Frozen brains were then cut with a cryostat to either coronal or sagittal 20µm thick sections and collected as series of 6. Sections were stored at -80°C before immunohistochemistry or in situ hybridization. Some brains were processed as floating sections and sectioned with a freezing microtome sectioning. In this case, the brains were cryoprotected in 30% sucrose and frozen directly on the platform of the cryotome at -40°C; serial 40um thick coronal sections were collected in 1X PBS with 0.01% sodium azide. Sections were stored at 4°C before immunohistochemistry or ISH processing

In situ hybridization was used to analyze EphARs and ephrinAs expression. Digoxigenin-labelled mRNA probes were transcribed from mouse EphA3, EphA4, EphA5, EphA7, ephrinA2, ephrinA3 and ephrinA5 cDNAs. Sense and antisense digest enzymes and polymerases of these probes are listed in Table 1. Sections were air-dried for at least two hours under a hood. Specific antisense RNA probes (0.1-1ug/ml) were mixed with hybridization buffer (50% formamide, 10% dextran sulfate, 1X Denhardt's, 5X SSC and 250 ug/ml tRNA) and incubated at 52°C, 58°C or 65°C for 10mins. 350ul of mixed hybridization buffer was added to each section, covered with a cover-slip, and incubated overnight at the same temperature. The sections were washed with PBS and PBS Triton 0.1% and incubated with anti-Digoxigenin (1/1000) 4° overnight. Sections were washed with 1X PBS and NTMT

(Tween 10%; Tris-HCL, pH 9.5, 1M; MgCl2, 1M; NaCl, 5M; H2O) buffer and incubated with NBT+BCIP or fast red (TR/Naphthol AS-MX Tablets, SIGMA F4523-50 SET) to reveal the reaction at 37°. Duration or the revelation (from 2 to 24 hours) was determined empirically according to the sensitivity of the probes and the concentration of the anti-Dig solution. The signal was checked with bright field and fluorescence microscopy and the sections were washed with 1X PBS. Sections were mounted in mowiol-Dabco (25 mg/ml) or processed with Immunohistochemistry.

Immunohistochemistry was performed either on alternate series of sections or in combination with ISH. Sections were washed in PBS, then in PGT (PBS with 0.2% gelatin and 0.25% Triton X-100) 4 X 15mins. Sections were incubated overnight at 4°C with the following primary antibodies: anti-Tph2 (mouse monoclonal, 1/1000, Sigma), anti-5-HT (rabbit polyclonal, 1/1000 Sigma), anti-SERT (rabbit polyclonal, 1/1000, Calbiochem). For fluorescence microscopy, sections were then incubated for 2 h at room temperature with the following secondary anti-body: donkey anti-rabbit 488 (1/200, Jackson), donkey anti-rabbit Cy3 (1/200, Jackson), donkey anti-mouse 488 (1/200, Jackson), donkey anti-mouse Cy3 (1/200, Jackson), or with the phalloidin 594 (1/40 Invitrogen). Then sections were rinsed in PB, mounted in mowiol-Dabco (25 mg/ml) and stored at +4°C.

RT-qPCR

Brains of Pet1-Cre RCE mice were collected at postnatal day 5, 15 and adult (6 weeks). Brains were kept in 1X PBS on ice and sectioned in the coronal plane with a tissue chopper to 300 um-thick sections. The dorsal and medial raphe nuclei were micro dissected under a fluorescent macroscope (Zeiss-MV10) and collected into 5ml tubes, which contained 2ml of cold 1X PBS, a cortical hemisphere was collected as a positive control. To obtain enough tissue for RNA isolation from the raphe, four cases were pooled together for each sample analyzed. Tissue was either directly processed for RNA isolation or fast frozen at -80°C.

RNA isolation from tissue was done with Trizol Reagent (Sigma). Samples were weighed (≤ 50mg) before homogenization, PBS was removed extensively and 1ml of trizol was added. Tissue was homogenized with a motor-driven tissue grinder until no visible pieces were left; the tip of the grinder was washed with 70% ethanol and milli-Q water between each tissue sample. Homogenates were transferred to 2ml eppendorf tubes with 0.2ml of chloroform and gently mixed for 15 seconds, and centrifuged 12000g, for 15mins at 4°C. The upper phase was collected and RNA was precipitated by mixing with isopropyl alcohol, 0.5ml, incubating at room temperature (5mins), centrifuged at 12000g for 10mins at 4°C. After removal of the

supernatant the RNA pellet was air-dried and dissolved in 100ul Milli-Q water and stored at -80°C.

Possible DNA contamination was cleared using DNase I (Thermo) and RT-PCR was done with the SuperScriptII kit (Invitrogen). Quantitative-PCR was performed with the Thermo SYBR Green Mix kit according to the manufacturers' instruction. Primers are listed in Table 2.

Raphe culture and collapse assay

E12 embryos were collected from Swiss timed-pregnant dams. Embryonic hindbrains were rapidly dissected as an 'open book' in ice cold 1X PBS. The rostral and caudal raphe were dissected separated based on fiducial marks. The dissected raphe was further cut into 200um explants with a tissue chopper or with a scalpel. Explants were placed onto polylysine/laminin-coated glass coverslips (Marlenfield, 0111540) in 4-well culture boxes (Nunclon, 176740) in DMEM F-12 medium to which BSA (1%), Peni/strep, Glutamine (200mM), and Glucose (50%) were added. Explants were cultured for 3 or 4 days at 37°C, in 5% CO2. For the collapse assay EphrinA5 (R&D System, 374-EA) was added at different concentrations (50mM, 250mM, 500mM) for 1hour. Explants were then quickly washed in PBS, fixed in buffered 4% PFA for 30mins, and washed extensively before 5-HT immunocytochemistry (anti-5-HT rabbit polyclonal, 1/1000 from Sigma) and phalloidin 594 (1/40 Invitrogen) staining.

Quantification of the collapse assay. Explants were imaged with a fluorescence microscope. Only round-shaped explants which contained 5-HT neurons were quantified, 5 explants and > 100 growth cones per condition were counted using a 63X/1.25 objective. The number of collapsed/non collapsed growth cones was counted for both 5-HT axons and non-5-HT axons, comparing the 5-HT immunostaining with the phalloidin staining. Counts were done on 5 different explants per condition from 3 independent experiments. These counts were used to calculate the mean ratio ± SEM per condition.

Anterograde Tracing

We used an adeno-associated virus (AAV1.CAG.tdtomato.WPRE.SV40 ref: AV-1-PV3365, Penn Vector) to express td-tomato fluorescence in the DR neurons and projections. A single injection (20ul of the virus non diluted) was done in the DR using a 10ul pulled glass capillaries. Dorsal raphe stereotaxic injections were performed as previously

described (Muzerelle et al., 2016). Adult ephrinA5 KO mice and littermate WT mice were anesthetized with ketamine (150 mg/kg) / xylazine (10 mg/kg). Animals were positioned on a foam board horizontally, the head was fixed and kept horizontal, and Bregma coordinates measured to calculate the position of the injection site and the angle of stereotaxic arm. To target the DR the following coordinates were used: antero-posterior: 0.5 to lamda; medio-lateral: 1; dorsoventral: 3.2. The animals were kept for 3 weeks and were perfused by 4% PFA. Brains were processed as described above, collecting serial 50um coronal sections throughout the brain.

In utero electroporation of EphrinA construct

GFP-ephrinA3 (kind gift of Dr. Michel Reber) was subcloned into the vector pCIG-Td-tomato and the pCIG-Td-tomato vector without the insert was used for the control condition. Both of the plasmids were purified by Qiagen EndoFree Plasmid Maxi kit. Stored at a final concentration of 2.5µg/µl.

To target gene expression in the amygdala, we followed a previously described in utero electroporation protocol (Remedios et al., 2004; Huang et al., 2014). The plasmids (1µg/µl) were mixed with 1% Fast Green (F7252, Sigma-Aldrich) and injected into one of the lateral ventricles of E12.5 embryos with 10ul glass-pulled micropipettes (5-000-1001-X10, Drummond; puller model 720, KOPF with a heat of 14,5 and solenoid 2). Then A P3 (3 mm diameter) electrode (LF650P3, BEX) was placed toward the caudal and ventral part of the telencephalon. Six electric pulses (30V, 50ms pulse length) with 950-ms intervals were applied using an electroporator (CUY21, BEX). After delivery, foster mothers delivering at the same time as the experimental subjects adopted the newborn pups. The electroporated pups were perfused at P5 and processed for immunocytochemistry as described above.

Image acquisition: For bright field microscopy, histological sections were imaged using a slide scanner (Nanozoomer 2.0-HT C9600, Hamamatsu, Japan) objective X20 or captured with a Cool SNAP camera mounted on a provis microscope (Olympus, France). For illustration purposes, images from the nanozoomer were exported in Tiff format using the NDP View2 software (Hamamatsu, Japan).

For fluorescence microscopy, images were acquired with a Leica DM 6000B system using a 40x/0.70 oil objective (tissue cultures), or acquired on a Leica SP5 confocal system (co-localization and fiber density analyses), equipped with an Argon laser (for the 488nm excitation), a Diode 561 nm and HeNe 633nm. Z-series stacks of confocal images were

acquired at 1024 x 1024 pixel resolution, with a pinhole set to one Airy unit and optimal settings for gain and offset. Characteristics of the images are described below for each procedure.

Image analyses

Co-localization: EphA5-Tph2 co-localization studies were done on P5 brains processed from 3 independent experiments. 20um-thick sections through the brainstem were collected as 6 series, one series wad processed for combined EphA5 HIS, Tph2 immunohistochemistry and DAPI and imaged with the confocal microscope. Sequential confocal images were acquired with a 40X/1.25 N.A Plan-apochromat at 3 different rostrocaudal levels through the raphe (Bregma -4.36mm, -4.60mm and -4.96). 5 confocal images spaced by 2um were taken over a 10 um depth. The wholes area containing TPH2+ neurons was acquired including the different subdivisions of the DR in the dorsal part (DRD), the ventral part (DRV) the lateral wings (DR-LW), and the caudal part (DR-C, B6). Acquisitions were done in the MnR in the B8 and B5 cell groups, and in the B9 cell groups. Confocal stacks were analyzed with image J. A 150um X 150um square mask was used for random selection of counting areas. Three random selections were positioned on each distinct 5-HT sub-nucleus. A cell counter plugin was used to count the Tph2 positive cells, EphA5 positive cells and the co-localized neurons.

Fiber density To quantify the anterograde tracing and the IUE data, fiber density were analyzed in two different ways. In the olfactory bulb and amygdala, confocal images were acquired at 4um intervals within an entire thickness of 20um. A maximum Z-projection of the image stacks was performed with image J. Then, a circular mask of 20um diameter was used for random sample selection. All labeled fibers that crossed the edge of the mask were counted with a cell counter to compute linear densities.

In the other brain target (VMH, SVZ, SCN and BNST), confocal images were copied to Image J with an 8-bit format. Subtraction of the background was done with a 20 pixels rollerball and a binary image was obtained after applying a fixed range of threshold for all the images. A circular mask of 100um diameter was used for random sample selection was to measure the area occupied by the fibers on the binary images as described in (Kiyasova et al., 2011).

Statistical analyses

All the statistical analyses applied were performed with GraphPad Prism6. One-way ANOVA was performed in the analyses of Q-PCR, co-localization and collapse assay. Tukey’s

multiple comparisons were performed to show the difference between any of the two samples within the group. Student t-test was performed for intergroup comparisons in the fiber density analyses. Unpaired t-test was used for comparison of independent samples and paired t-test was done for analyses comparing, ipsi and contralateral innervation in the same case. Data are expressed as Means +/- SEM, $P<0.05$ was considered as significant.

Results

Expression of EphA receptors in the raphe nuclei.

5-HT neurons of the hindbrain start extending axons by E12, and reach most of their forebrain targets between E15 and P0 while the development of a full terminal arborization extends over the first 2-3 weeks of postnatal life (Lidov and Molliver, 1982; Kiyasova and Gaspar, 2011).

We began by screening the expression of the EphA receptors at P5, a time when the DR and the MnR can be well individualized and are still actively growing. Q-PCR analyses were performed on micro-dissected DR. The areas containing 5-HT neurons were identified by using mice in which the GFP reporter was expressed selectively under the control of Pet1, a transcription factor selective of 5-HT neurons (Scott et al., 2005). Q-PCR analyses of the EphA3, A4, A5, A6, A7, and EphA8 mRNAs were performed and GAPDH was used as a housekeeping gene. This analysis showed that EphA4 and EphA5 are the main EphA receptors detectable in the dorsal raphe at P5, with lower expression of EphA3, EphA6, EphA7 and EphA8. (Figure 1A). To determine more precisely the cellular localization of the Eph genes, in situ hybridization (ISH) was performed on serial coronal sections through the raphe, using specific mRNA probes to EphA3, EphA4, EphA5 and EphA7 (Table 1). This showed that among the Ephs genes examined, only EphA5 was localized in the DR and the MnR; no expression was visible in the raphe magnus, obscurus and pallidus that correspond to the caudal B1-3 raphe cell groups in th medulla (Figure 1B). The other EphA genes, EphA3, EphA4 and EphA7 that were detected with QPCR, appeared to be essentially localized to nuclei that are in the close vicinity of the raphe, such as the dorsal lateral tegmental nuclei and superior olive, but not in the DR or the MnR (Figure 1B)

Overall, these results indicated a selective expression of EPhA5 in the developing rostral raphe nuclei (dorsal and medial raphe).

EphA5 expression is dynamically regulated during raphe development

To evaluate the possible developmental impact of EphA5 at different stages of raphe development, we analyzed its expression timeline. Serial sagittal (embryo) and coronal (postnatal and adult) sections were processed for EphA5 ISH at E14 (n= 4), P0 (n>5), P5 (n>5), P10 (n>5), P15 (n>5) and adult (n= 2). These experiments showed that EphA5 expression is detectable in the rostral raphe at E14 and that this expression is maintained at a high level over the first week following birth. Expression subsequently declines by P15 (Figure 1C) to adulthood where an only low level of expression is detectable (not shown). To obtain a quantitative evaluation of the time course of expression EphA5 mRNA was measured with Q-PCR on micodissected raphe at P5 (0.37±0.09, n=3), P15 (0.06±0.005, n=3) and in adult (0.09±0.02, n=3) (P5 vs. P15, P=0.0189; P5 vs. Adult, P=0.416; P15 vs. adult, P=0.787) brains, that showed a significant decrease between P5 and P15, consistent with the ISH result.

Serotonergic raphe nuclei differ in EphA5 expression pattern

Hindbrain raphe nuclei contain a heterogeneous neuronal population that includes in addition to 5-HT neurons, glutamate, GABAergic, and peptide-containing neurons. To determine whether EphA5 is expressed in the serotoninergic neurons we combined fluorescent EphA5 ISH and tryptophan hydroxylase (TPH2) immunocytochemistry on serial sections of E14 and P5 brains (Figure 2). At E14, EphA5 was broadly expressed in the alar plate of the isthmus and of rhombomeres 1-3 (R1-R3) in the area defined as the periventricular stratum of the mantle zone (Allen Brain Atlas, http://developingmouse.brain-map.org/static/atlas). At this embryonic stage 5-HT neurons have not yet achieved their full migration, making it difficult to distinguish the individual raphe cell groups other than the 2 main rostral and caudal clusters. The rostral hindbrain cluster comprises 5-HT neurons derived from the isthmus and from rhombomeres 1-3 while the caudal medullary cluster corresponds to rhombomeres 5-8 (Jensen et al., 2008; Alonso et al., 2013); Tph2+ neurons of the rostral hindbrain cluster overlapped with the EphA5 positive area in the alar plate (Figure 2A) and at higher magnifications a large number of EphA5-Tph2+ neurons were found in the dorsal region but not in the ventral part (Figure 2A’), that corresponds to respectively to the prospective DR and MnR. In the caudal cluster, Tph2+ raphe neurons which derived from rhombomeres 5-8 (Alonso et al., 2013) appeared to be entirely segregated from the EphA expressing neurons.

At P5, the B1-B9 cell group of raphe neurons can be well outlined with Tph2-immunostaining (Figure 2B-D), and EphA5-Tph2 co-localization could be evaluated quantitatively in the different sub-nuclei (Figure 3, tables 3-4). The highest co-localization index was found in the DR-B7 group where more than 50% 5-HT neurons expressed EphA5 (50.2% ± 2.2%, n= 3, Figure 3AD); while the lowest co-localization ratio was noted in the caudal raphe cell group (B1-B3) (Figure 3C, D). In the MnR (the B5 and B8 groups), although a strong expression of EphA5 was visible, only 14-22 % of the 5-HT neurons expressed EphA5 (Figure 3 B, D). Further heterogeneous expression was observed within the DR (B7) cell group where co-localization was compared from counts performed at 3 different levels (B7rostral, B7intermediate, B7caudal) and from the different DR subdivisions (DRD/B7dorsal, DRV/B7ventral, DRL/B7lateral) (Figure 3E and Table 4); these DR/B7 sub-divisions are based on differences in cytoarchitecture, connectivity or electrophysiological profiles(Crawford et al., 2010; Hale and Lowry, 2011; Fernandez et al., 2015; Muzerelle et al., 2016) . Thus the medially located neurons (B7d and B7v) showed higher co-expression than the lateral wings (B7lateral); and along the rostral to caudal axis, the middle levels of B7, B7i showed a higher % co-localization than the rostral or caudal B7 (Figure 3E, table 4). Overall, these results stressed the fact that EphA5 is topographically distributed in the 5-HT raphe subgroups with a rostral to caudal and a medial to caudal decreasing gradient of expression. These expression gradients suggest a possible role of EphA5 in differential targeting of 5-HT neurons from different raphe regions.

Collapse response of 5-HT raphe neurons after the ephrinA application.

EphA receptors can mediate repulsive or attractive signals according to whether they mediate forward or reverse signaling. To examine the functional role of ephA5 expression on 5-HT axon outgrowth, we analyzed the collapse response of raphe neurons. We took advantage of the clear-cut differential expression of EphA5 between the rostral and caudal clusters of 5-HT neurons at embryonic ages to compare their response to application of the ligand EphrinA5. Raphe explants from E12 hindbrains, were separated into rostral and caudal raphe based on fiducial marks (Figure 4A). Explants were grown 48 hrs on glass coverslips and EphrinA5-FC was applied to the cultures at different concentrations. In explants from the rostral raphe, the 5-HT labeled growth cones had a characteristic fan-shaped morphology (Figure 4 B3); EphrinA5-FC induced the collapse of a large fraction of 5-HT growth cones, some of which had a long

trailing process and an actin rich retraction bulb (Figure 4-B5), while others had a short trailing process and many filopodia (Figure 4-B4); A dose dependent effect was noted as 71.3% ± 4.5% of the 5-HT growth cones were collapsed at the highest concentration tested (500ng/ml), 45-50% at intermediate concentrations (50-250 ng/ml) and 20% at the lowest concentration (5ng/ml),which is similar to controls (Figure 4D). In caudal raphe explants, EphrinA5 application did not induce a significant collapse response compared to controls at any of the doses tested (Figure 4C); growth cones showed a normal morphology (Figure 4-B2). Because EphA5 is also expressed in a large number of non-HT neurons in both the rostral and caudal raphe areas (table 3), we also evaluated the collapse responses of the non-5-HT axons. The non-5-HT growth cones showed a significant dose-dependent collapse response in both rostral and caudal explants (Figure 4 E, F), thus showing less regional selectivity than the 5-HT growth cones.

Overall, these experiments demonstrated that EphA5 expression in 5-HT raphe neurons correlates with a repulsive response to the application of ephrinA5-FC. Interestingly there was a dose response effect suggesting that differences in the ligand/receptor ratio could contribute to a differential targeting of raphe neurons.

5-HT innervation is reduced by ectopic ephrinA expression in the amygdala and piriform cortex.

Next, we investigated the effects of ephrinA ligands for in vivo 5-HT axon targeting using an over-expression strategy. We focused on the amygdala and piriform cortex which express only very low levels of ephrinA2, ephrinA3 and ephrinA5 (Allen Brain Atlas, http://developingmouse.brain-map.org/gene/show/13415, 13416, 13418) (Deschamps et al., 2010), which are the preferential ligands of EphA5. Thus, the amygdala and piriform codices could be permissive for the ingrowth of DR axons which express high level of EphA5 receptors. To examine this possibility, we used an in utero electroporation strategy.

An ephrinA3 cDNA fragment was sub-cloned into a pCIG-Tdtomato vector; the plasmid with or without the ephrinA3 insert was electroporated into the amygdala and piriform cortex at E12.5. Electroporated cells were visible in the basolateral amygdaloid nucleus (BLA), basolateral amygdaloid nucleus ventral part (BLV) and basomedial amygdaloid nucleus anterior part (BMA), and the piriform cortex in brains on the elecroporated side (Figure 5A, C, D). Measures of 5-HT fiber density showed a significant decrease of innervation on the electroporated side (0.07±0.01/ μm) compared

to the contralateral control side (0.21±0.03 / µm)(Figure 5B, 7C,). In contrast in cases electroporated with the control vector, the density of 5-HT fibers was unchanged compared to the non-elecroporated side (0.19±0.02/ µm). This result indicated that EphA5-ephrinA3 interaction can specifically reduce the 5-HT raphe-amygdala innervation during development. (n=5, $p < 0.01$).

EphrinA5 is required for the differential forebrain targeting of B7/B8 raphe neurons.

To investigate the role of endogenous ephrins in 5-HT axon targeting we turned to EphrinA5 -KO mice. EphrinA5-KO mice showed no major structural alterations in the morphology of the raphe nuclei. Anterograde tracing with AAV viral vectors expressing Td-tomato combined 5-HT immunohistochemistry allowed to determine the extent of transfection of the 5-HT neurons (Figure 6A) and to select cases in which transfection was limited to the DR with a similar extension in control and mutant mice (Figure 6B). Anterogradely labeled axons were further characterized as serotonergic (or not), using 5-HT transporter (SERT) immunocytochemistry (Figure 6 D', E').

To identify target areas in which DR-5-HT innervation might be altered we relied on previous immunocytochemical (Deschamps et al., 2010) and ISH observations (Cooper et al., 2009)(http://developingmouse.brain-map.org/gene/show/13418) correlating areas of high ephrinA5 expression with areas in which a differential 5-HT innervation from the DR and MnR have been demonstrated (Muzerelle et al., 2016). A remarkable target in this respect is the olfactory bulb (OB) where DR and MnR 5-HT axons target different layers (Figure 6C), namely the granule cell layer for the DR and the Glomerular layer (GL) for the MnR where EphrinA5 expression is high (Figure 6C'). Anterogradely labeled axons from the DR in WT mice had a characteristic distribution similar to previous reports: Td-tomato labeled axons, all of which were SERT+, were restricted to the granular cell layer (GCL) and appeared to be arrested at the edge of the mitral cell layer (ML) with only a few fibers entering into the external plexiform layer (EPL) (Figure 5D-D'). In the EphrinA5 KO mice, anterogradely labeled axons from the DR were also abundant in the CGL but did not seem to be arrested by the ML, which they crossed, arborizing into the EPL (Figure 6E-E'). To obtain quantitative measures normalized to the number of anterogradely labeled axons, we estimated the density of td tomato labeled fibers in the CGL and the EPL, and calculated the EPL/CGL ratio. This ratio was significantly increased in ephrinA5 KO mice compared to WT mice (Figure 6F). To

determine whether the overall density of 5-HT labeled axons was modified, we measured the density of SERT-labeled axons in the CGL and the EPL which indicated an overall increase in the density of 5-HT axons in the EPL but not in the CGL (Figure 6 G, H).

Next, we analyzed, in the same cases, DR anterograde labeling and global 5-HT innervation in two hypothalamic areas that show high ephrinA5 expression. Two areas appeared to be of particular interest in this respect, the ventromedial hypothalamic (VMH) (Figure 7A) and the suprachiasmatic nuclei (Figure 7F). Both nuclei show a high level of ephrinA5 at P5 (Figure 7A, F). In WT mice, anterograde labeling from the DR shows that both the VMH and the suprachiasmatic are not targeted by DR axons (Figure 7B', G') confirming previous observations. However, these areas contain a very high density of SERT+ labeled terminals that originate from the MR (for the suprachiasmatic nucleus) or from both the MR and DRD for the VMH. In the EphrinA5 KO mice, the density of DR anterograde projection was substantially increased in both the VMH (Figure 7C', E) and the suprachiasmatic nuclei (Figure 7H', J). Double labeling showed that both 5-HT and non 5-HT DR axons contributed to this increase (Figure 7C", H"). Comparison of the density of SERT+ labelled fibers was also showed a significant difference in the total density of SERT fibers was noted in these hypothalamic areas (Figure 7E, I).

Discussion (1513 words)

Our results demonstrate for the first time a role of ephrin A signaling for the selective targeting of serotoninergic raphe nuclei. We show that EphA5 is differentially expressed across the different hindbrain raphe nuclei, and that this correlates with a different repulsive action of ephrinA on 5-HT axon growth. Ectopic expression of ephrin-A inhibits the ingrowth of 5-HT raphe axons in main targets of the dorsal raphe 5-HT neurons and Ephrin-A5 loss of function causes a mis-targeting of dorsal raphe 5-HT axons resulting in localized increases in 5-HT innervation.

The development of raphe neurons has been well outlined by classical morphological studies (Lidov and Molliver, 1982; Wallace and Lauder, 1983), however, only few insights have been obtained to date into the molecular control of axon guidance in this system. Wnt signals have been implicated in the polarity of 5-HT neurons

(Fenstermaker et al., 2010) and Slit/Robo signaling influences 5-HT axon tract organization in the medial forebrain bundle (Bagri et al., 2002), but hardly anything is known about the molecular control of selective 5-HT axon targeting. This knowledge gap is likely due to a prevailing view of 5-HT neurons as a diffuse highly collateralized system with limited specificity (Agnati et al., 2006). However, increasing evidence showed that raphe 5-HT neurons are in fact heterogeneous in their molecular identities (Wylie et al., 2010; Fernandez et al., 2015; Okaty et al., 2015), their physiology (Calizo et al., 2011; Fernandez and Gaspar, 2012) , their genetic determinants (Kiyasova et al., 2011), and their connectivity (Azmitia and Segal, 1978; Commons, 2015; Muzerelle et al., 2016). In addition to the established di- vergence of axons arising from the rostral and caudal 5-HT neuron clusters (directed toward the forebrain and the spinal cord respectively), there is a distinct topographic organization within the ascending forebrain projections. 5-HT axons originating from the DR and MnR occupy complementary terminal territories in the forebrain (Bobillier et al., 1976; 18 Azmitia and Segal, 1978; Jacobs et al., 1978; Vertes et al., 1999; Muzerelle et al., 2016). Coinciding with this topographic anatomical organization, our study revealed a gradient of EphA5 gene expression with higher EphA expression in the DR than in the MnR, and in addition a clear rostral to caudal and medial to lateral expression gradient. Thus, high EphA5 expression in DR neuronal subsets could explain why DR 5-HT neurons do not innervate brain areas that have high expression of ephrinA, which are instead innervated by 5-HT neurons from the MnR. This is particularly clear in the case of the olfactory bulb (OB), where DR and MnR 5-HT neurons are located respectively in the central (GCL) or outer (EPL, GL) layers of the OB (Steinfeld et al 2015; Muzerelle et al., 2016). The EphrinA3/5 expressing mitral cell layer might then act as a barrier to prevent DR 5-HT axons from crossing into the outer OB layers. Similarly, hypothalamic nuclei that normally receive all (suprachiasmatic) or a majority (VMH) of their 5-HT innervation from the MnR (Bang et al., 2012; Muzerelle et al., 2016) show high levels of ephrin A expresion during development. The implication of ephrin A was supported by altered distribution of DR axons. In both the OB and the hypothalamus, serotonin innervation was increased and anterogradely labeled axons from the DR were mispositioned as though an inhibitory barrier was removed. Conversely, when ephrinA ligand was ectopically expressed in a structure such as the amygdala, which is a preferential target of the DR 5-HT innervation (Muzerelle et al., 2016), the ingrowth of 5-HT raphe axons was significantly reduced. Thus, our results indicate that ephrinA5 signaling contributes to the selective of targeting of 5- HT axons in

the forebrain by repelling the ingrowth of 5-HT axons originating from the DR, in brain regions that are normally targeted by the MnR.

Other aspects of the topography of DR may also be influenced by EphrinA signaling; this is suggested by our observation of a medial to lateral gradient of EphA5 expression in the DR which coincides with differential anatomical projections. For instance, 5-HT neurons in the lateral wings of the DR show a low level of EphA expression and project to regions with high ephrinA5 expression such as the lateral geniculate nucleus (Muzerelle et al. 2016, Wilks et al. 2010). It will also be interesting to determine in the future how the combination of axon guidance molecules in raphe targets contribute to attracting subsets of 5-HT axons to defined brain areas/layers. In particular we do not know what factors attract the MnR axons to the areas that are avoided by the DR. Intriguingly 5-HT itself could contribute to this growth-promoting effects, as a defective innervation of the SCN was observed in Tph2-KO mice (Migliarini et al., 2013). The mis-targeting of DR axons in the hypothalamus of EphrinA5 KO mice concerned both 5-HT and non 5-HT neurons of the DR, indeed as noted in the present study, both cell types express EphA5. These common axon guidance cues are consistent with shared connectivity profiles; indeed, previous anatomical tracing studies showed that DR afferents frequently contain a mix of 5-HT and non 5-HT neurons (Steinbusch and Nieuwenhuys, 1981; Kiyasova et al., 2011), the latter could include glutamatergic Vglut3+ (Hioki et al., 2010) and GABAergic neurons (Bang et al., 2012). Thus DR neurons could share similar axon guidance mechanisms, independent of their neurotransmitter content.

EphA-EphrinA signaling has been implicated in several neuronal developmental processes from cell migration to synaptic maturation, (Cramer and Miko, 2016; Kania and Klein, 2016) although its best known implication in neural development is for axon guidance, where both repulsive and attractive interactions have been described. Our current studies indicated a main inhibitory effect of the ephrinA ligands on 5-HT axon growth: in vitro, ephrin5 induced a collapse of the growth cones and in vivo ectopic expression of EphrinA3 inhibited 5-HT axon ingrowth. This corresponds to the classic repulsive forward signaling of EphA receptor activation (Kania and Klein, 2016), and is most likely due to the EphA5 receptor according to the present localization studies. However we cannot exclude the implication of other EphAs since transcriptional profiling

of raphe neurons in embryonic and postnatal brains reported also the presence of other EphA (Wylie et al., 2010; Okaty et al., 2015), but likely expression is at levels too low for our ISH detection. Moreover, the loose specificity of the EphA5 receptors for ephrinA ligands and the redundancy of ephrinA expression in several brain targets (such as the mitral cells in the OB) suggest that the defects of 5-HT axon targeting observed in the ephrinA5 KO might be more pronounced in double or triple ephrinA KO mice. Such redundancy has previously been observed in the visual system (Feldheim et al., 2000).

In the visual and auditory sensory maps Eph-ephrinA signaling acts to build a continuous topographic map (Cramer and Miko, 2016) however this does not appear to be the case in the 5-HT raphe system where topography is much looser. EphrinA signaling would here rather appear to act in a target selection process, by generating non permissive boundaries for the ingrowth of DR 5-HT raphe subtypes. This effect is reminiscent of that observed for the motor neurons when choosing a dorsal/ventral muscle targets during development (Eberhart et al., 2004).

EphA5 expression in 5-HT raphe neurons was dynamically expressed, being maximal during axon growth and target reaching and showing decreased expression, as reported for EphrinA5 expression (Deschamps et al., 2010). Given the potential of 5-HT neurons to regenerate and grow, it will be interesting to know whether the present developmental mechanisms are reactivated after a lesion, and whether the propensity of serotonin axons to regrow (Mullner et al., 2008) could be linked to their EphA content.

What could be the pathophysiological consequences of targeting defects of raphe neurons in the olfactory bulb or the hypothalamus? Our observations in ephrinA5 KO showed that mis-targeting of the DR axons was correlated with a general increase of 5-HT innervation in these regions, suggesting that excitatory/inhibitory balance is compromised in these brain nuclei. Interestingly, behavioral observations conducted in the EphrinA5 and EphA5 KO mice showed some common phenotypes that could relate to our observations. Both studies report a reduction in inter-male aggression (Mamiya et al., 2008; Sheleg et al., 2015) and increase of 5-HT levels in the hypothalamus was shown in the EphA5 KO (Mamiya et al., 2008) consistent with our observations of increased 5-HT innervation in this brain region.. Interestingly the increased 5-HT innervation that we observed in the EphrinA5 KO was concentrated in the ventrolateral

part (VMHVL) which has specifically been implicated in modulating aggression (Martinez et al 2008; Silva et al. 2016). Clearly the possible pathophysiological consequences of SCN hyper- innervation calls for further studies on the circadian rhythms of these mutants, given the implication of 5-HT innervation to the SCN in entraining circadian rhythmicity (Versteeg et al., 2015)

Given the implication of 5-HT in a wide range of behaviors, and psychiatric disorders, our study point to new gene targets that may indirectly affect 5-HT functions by changing the targeting of raphe neurons and inducing modifications of 5-HT inputs in selected brain regions.

References

Agnati LF, Leo G, Zanardi A, Genedani S, Rivera A, Fuxe K, Guidolin D (2006) Volume transmission and wiring transmission from cellular to molecular networks: history and perspectives. Acta physiologica (Oxford, England) 187:329-344.

Alonso A, Merchan P, Sandoval JE, Sanchez-Arrones L, Garcia-Cazorla A, Artuch R, Ferran JL, Martinez-de-la-Torre M, Puelles L (2013) Development of the serotonergic cells in murine raphe nuclei and their relations with rhombomeric domains. Brain structure & function 218:1229-1277.

Azmitia EC, Segal M (1978) An autoradiographic analysis of the differential ascending projections of the dorsal and median raphe nuclei in the rat. The Journal of comparative neurology 179:641-667.

Bagri A, Marin O, Plump AS, Mak J, Pleasure SJ, Rubenstein JL, Tessier-Lavigne M (2002) Slit proteins prevent midline crossing and determine the dorsoventral position of major axonal pathways in the mammalian forebrain. Neuron 33:233-248.

Bang SJ, Jensen P, Dymecki SM, Commons KG (2012) Projections and interconnections of genetically defined serotonin neurons in mice. The European journal of neuroscience 35:85-96.

Bobillier P, Seguin S, Petitjean F, Salvert D, Touret M, Jouvet M (1976) The raphe nuclei of the cat brain stem: a topographical atlas of their efferent projections as revealed by autoradiography. Brain research 113:449-486.

Brust RD, Corcoran AE, Richerson GB, Nattie E, Dymecki SM (2014) Functional and developmental identification of a molecular subtype of brain serotonergic neuron specialized to regulate breathing dynamics. Cell reports 9:2152-2165.

Calizo LH, Akanwa A, Ma X, Pan YZ, Lemos JC, Craige C, Heemstra LA, Beck SG (2011) Raphe serotonin neurons are not homogenous: electrophysiological, morphological and neurochemical evidence. Neuropharmacology 61:524-543.

Commons KG (2015) Two major network domains in the dorsal raphe nucleus. The Journal of comparative neurology 523:1488-1504.

Cooper MA, Kobayashi K, Zhou R (2009) Ephrin-A5 regulates the formation of the ascending midbrain dopaminergic pathways. Developmental neurobiology 69:36-46.

Cramer KS, Miko IJ (2016) Eph-ephrin signaling in nervous system development. F1000Research 5.

Crawford LK, Craige CP, Beck SG (2010) Increased intrinsic excitability of lateral wing serotonin neurons of the dorsal raphe: a mechanism for selective activation in stress circuits. Journal of neurophysiology 103:2652-2663.

Deakin JF, Graeff FG (1991) 5-HT and mechanisms of defence. Journal of psychopharmacology (Oxford, England) 5:305-315.

Deschamps C, Faideau M, Jaber M, Gaillard A, Prestoz L (2009) Expression of ephrinA5 during development and potential involvement in the guidance of the mesostriatal pathway. Experimental neurology 219:466-480.

Deschamps C, Morel M, Janet T, Page G, Jaber M, Gaillard A, Prestoz L (2010) EphrinA5 protein distribution in the developing mouse brain. BMC neuroscience 11:105.

Eberhart J, Barr J, O'Connell S, Flagg A, Swartz ME, Cramer KS, Tosney KW, Pasquale EB, Krull CE (2004) Ephrin-A5 exerts positive or inhibitory effects on distinct subsets of EphA4-positive motor neurons. The Journal of neuroscience : the official journal of the Society for Neuroscience 24:1070-1078.

Feldheim DA, Kim YI, Bergemann AD, Frisen J, Barbacid M, Flanagan JG (2000) Genetic analysis of ephrin-A2 and ephrin-A5 shows their requirement in multiple aspects of retinocollicular mapping. Neuron 25:563-574.

Fenstermaker AG, Prasad AA, Bechara A, Adolfs Y, Tissir F, Goffinet A, Zou Y, Pasterkamp RJ (2010) Wnt/planar cell polarity signaling controls the anterior-posterior organization of monoaminergic axons in the brainstem. The Journal of neuroscience : the official journal of the Society for Neuroscience 30:16053-16064.

Fernandez SP, Gaspar P (2012) Investigating anxiety and depressive-like phenotypes in genetic mouse models of serotonin depletion. Neuropharmacology 62:144-154.

Fernandez SP, Cauli B, Cabezas C, Muzerelle A, Poncer JC, Gaspar P (2015) Multiscale single-cell analysis reveals unique phenotypes of raphe 5-HT neurons projecting to the forebrain. Brain structure & function.

Frisen J, Yates PA, McLaughlin T, Friedman GC, O'Leary DD, Barbacid M (1998) Ephrin-A5 (AL-1/RAGS) is essential for proper retinal axon guidance and topographic mapping in the mammalian visual system. Neuron 20:235-243.

Hale MW, Lowry CA (2011) Functional topography of midbrain and pontine serotonergic systems: implications for synaptic regulation of serotonergic circuits. Psychopharmacology 213:243-264.

Hioki H, Nakamura H, Ma YF, Konno M, Hayakawa T, Nakamura KC, Fujiyama F, Kaneko T (2010) Vesicular glutamate transporter 3-expressing nonserotonergic projection neurons constitute a subregion in the rat midbrain raphe nuclei. The Journal of comparative neurology 518:668-686.

Huang TN, Chuang HC, Chou WH, Chen CY, Wang HF, Chou SJ, Hsueh YP (2014) Tbr1 haploinsufficiency impairs amygdalar axonal projections and results in cognitive abnormality. Nature neuroscience 17:240-247.
Imai H, Matsukawa M, Okado N (2004) Lamina-selective changes in the density of synapses following perturbation of monoamines and acetylcholine in the rat medial prefrontal cortex. Brain research 1012:138-145.
Jacobs BL, Azmitia EC (1992) Structure and function of the brain serotonin system. Physiological reviews 72:165-229.
Jacobs BL, Foote SL, Bloom FE (1978) Differential projections of neurons within the dorsal raphe nucleus of the rat: a horseradish peroxidase (HRP) study. Brain research 147:149-153.
Jensen P, Farago AF, Awatramani RB, Scott MM, Deneris ES, Dymecki SM (2008) Redefining the serotonergic system by genetic lineage. Nature neuroscience 11:417-419.
Kania A, Klein R (2016) Mechanisms of ephrin-Eph signalling in development, physiology and disease. Nature reviews Molecular cell biology 17:240-256.
Kiyasova V, Gaspar P (2011) Development of raphe serotonin neurons from specification to guidance. The European journal of neuroscience 34:1553-1562.
Kiyasova V, Fernandez SP, Laine J, Stankovski L, Muzerelle A, Doly S, Gaspar P (2011) A genetically defined morphologically and functionally unique subset of 5-HT neurons in the mouse raphe nuclei. The Journal of neuroscience : the official journal of the Society for Neuroscience 31:2756-2768.
Klein R, Kania A (2014) Ephrin signalling in the developing nervous system. Current opinion in neurobiology 27:16-24.
Lidov HG, Molliver ME (1982) Immunohistochemical study of the development of serotonergic neurons in the rat CNS. Brain research bulletin 9:559-604.
Lucki I (1998) The spectrum of behaviors influenced by serotonin. Biological psychiatry 44:151-162.
Mamiya PC, Hennesy Z, Zhou R, Wagner GC (2008) Changes in attack behavior and activity in EphA5 knockout mice. Brain research 1205:91-99.
Migliarini S, Pacini G, Pelosi B, Lunardi G, Pasqualetti M (2013) Lack of brain serotonin affects postnatal development and serotonergic neuronal circuitry formation. Molecular psychiatry 18:1106-1118.
Miko IJ, Nakamura PA, Henkemeyer M, Cramer KS (2007) Auditory brainstem neural activation patterns are altered in EphA4- and ephrin-B2-deficient mice. The Journal of comparative neurology 505:669-681.
Mullner A, Gonzenbach RR, Weinmann O, Schnell L, Liebscher T, Schwab ME (2008) Lamina-specific restoration of serotonergic projections after Nogo-A antibody treatment of spinal cord injury in rats. The European journal of neuroscience 27:326-333.
Muzerelle A, Scotto-Lomassese S, Bernard JF, Soiza-Reilly M, Gaspar P (2016) Conditional anterograde tracing reveals distinct targeting of individual serotonin cell groups (B5-B9) to the forebrain and brainstem. Brain structure & function 221:535-561.
O'Leary DD, Wilkinson DG (1999) Eph receptors and ephrins in neural development. Current opinion in neurobiology 9:65-73.
Okaty BW, Freret ME, Rood BD, Brust RD, Hennessy ML, deBairos D, Kim JC, Cook MN, Dymecki SM (2015) Multi-Scale Molecular Deconstruction of the Serotonin Neuron System. Neuron 88:774-791.
Pflieger JF, Clarac F, Vinay L (2002) Postural modifications and neuronal excitability changes induced by a short-term serotonin depletion during neonatal development in the rat. The Journal of neuroscience : the official journal of the Society for Neuroscience 22:5108-5117.
Prakash N, Vanderhaeghen P, Cohen-Cory S, Frisen J, Flanagan JG, Frostig RD (2000) Malformation of the functional organization of somatosensory cortex in adult ephrin-A5 knock-out mice revealed by in vivo functional imaging. The Journal of neuroscience : the official journal of the Society for Neuroscience 20:5841-5847.
Prestoz L, Jaber M, Gaillard A (2012) Dopaminergic axon guidance: which makes what? Frontiers in cellular neuroscience 6:32.
Remedios R, Subramanian L, Tole S (2004) LIM genes parcellate the embryonic amygdala and regulate its development. The Journal of neuroscience : the official journal of the Society for Neuroscience 24:6986-6990.
Schmidt BJ, Jordan LM (2000) The role of serotonin in reflex modulation and locomotor rhythm production in the mammalian spinal cord. Brain research bulletin 53:689-710.
Scott MM, Wylie CJ, Lerch JK, Murphy R, Lobur K, Herlitze S, Jiang W, Conlon RA, Strowbridge BW, Deneris ES (2005) A genetic approach to access serotonin neurons for in vivo and in vitro studies. Proceedings of the National Academy of Sciences of the United States of America 102:16472-16477.
Sheleg M, Yochum CL, Richardson JR, Wagner GC, Zhou R (2015) Ephrin-A5 regulates inter-male aggression in mice. Behavioural brain research 286:300-307.

Sheleg M, Yu Q, Go C, Wagner GC, Kusnecov A, Zhou R (2016) DECREASED MATERNAL BEHAVIOR AND ANXIETY IN EPHRIN-A5-/- MICE. Genes, brain, and behavior.
Sousa VH, Miyoshi G, Hjerling-Leffler J, Karayannis T, Fishell G (2009) Characterization of Nkx6-2-derived neocortical interneuron lineages. Cerebral cortex (New York, NY : 1991) 19 Suppl 1:i1-10.
Steinbusch HW, Nieuwenhuys R (1981) Localization of serotonin-like immunoreactivity in the central nervous system and pituitary of the rat, with special references to the innervation of the hypothalamus. Advances in experimental medicine and biology 133:7-35.
Teissier A, Chemiakine A, Inbar B, Bagchi S, Ray RS, Palmiter RD, Dymecki SM, Moore H, Ansorge MS (2015) Activity of Raphe Serotonergic Neurons Controls Emotional Behaviors. Cell reports 13:1965-1976.
Versteeg RI, Serlie MJ, Kalsbeek A, la Fleur SE (2015) Serotonin, a possible intermediate between disturbed circadian rhythms and metabolic disease. Neuroscience 301:155-167.
Vertes RP, Fortin WJ, Crane AM (1999) Projections of the median raphe nucleus in the rat. The Journal of comparative neurology 407:555-582.
Wallace JA, Lauder JM (1983) Development of the serotonergic system in the rat embryo: an immunocytochemical study. Brain research bulletin 10:459-479.
Wilks TA, Rodger J, Harvey AR (2010) A role for ephrin-As in maintaining topographic organization in register across interconnected central visual pathways. The European journal of neuroscience 31:613-622.
Wylie CJ, Hendricks TJ, Zhang B, Wang L, Lu P, Leahy P, Fox S, Maeno H, Deneris ES (2010) Distinct transcriptomes define rostral and caudal serotonin neurons. The Journal of neuroscience : the official journal of the Society for Neuroscience 30:670-684.

Figure 1

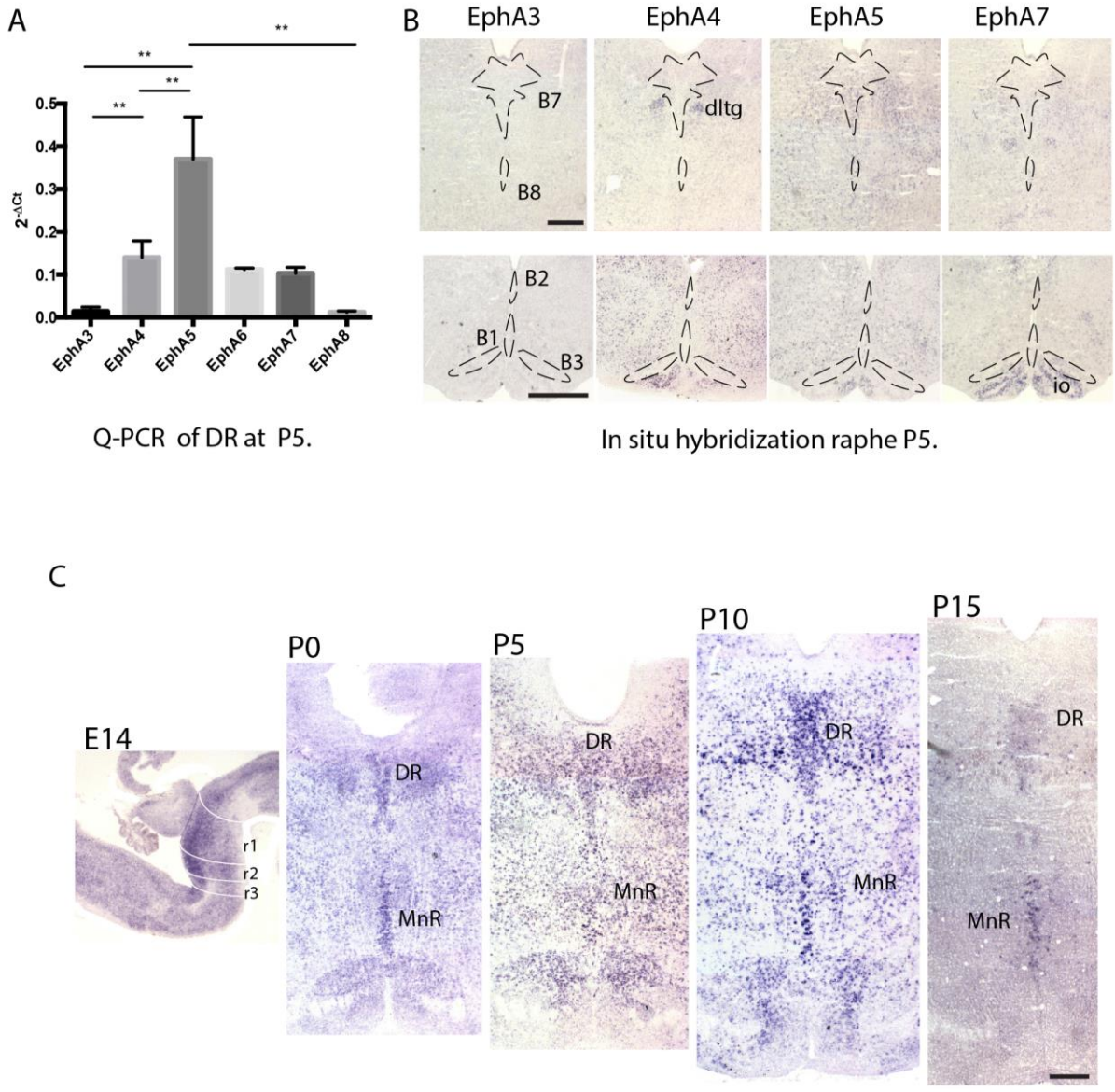

Figure 1 - EphA receptor gene expression in the developing mouse raphe.

A, Q-PCR of EphA3, EphA4, EphA5, EphA6, EphA7 and EphA8 mRNAs in DR extracts from P5 mice (n=4 mice /experiment, 3 experiments) Relative mRNA expression was calculated as $2^{-\Delta Ct}$. Data are presented as mean ± SEM, one-way anova, *p<0.05.

B, In situ hybridization of EphA3, EphA4, EphA5 and EphA7 mRNAs on coronal sections through the rostral raphe groups, including the DR (B7) and MnR (B8) cell groups, and through the caudal raphe cell groups, including raphe pallidus (B1), obscurus (B2), and magnus (B3), that are outlined with dashed lines. EphA5 labeling is visible in the DR and MnR, whereas other EphA are only detected in areas neighboring the raphe cell groups

such ad the dorsal lateral tegmental nucleus (dltg) or the inferior olive (io). Scale bar= 250um

C, Time course of EphA5 expression in the developing raphe was analyzed on sagittal (E14) and coronal (P0, P5, P10, P15) sections through the raphe nuclei. Note the decrease in EphA5 expression by P15. Scale bar=500um

Figure 2

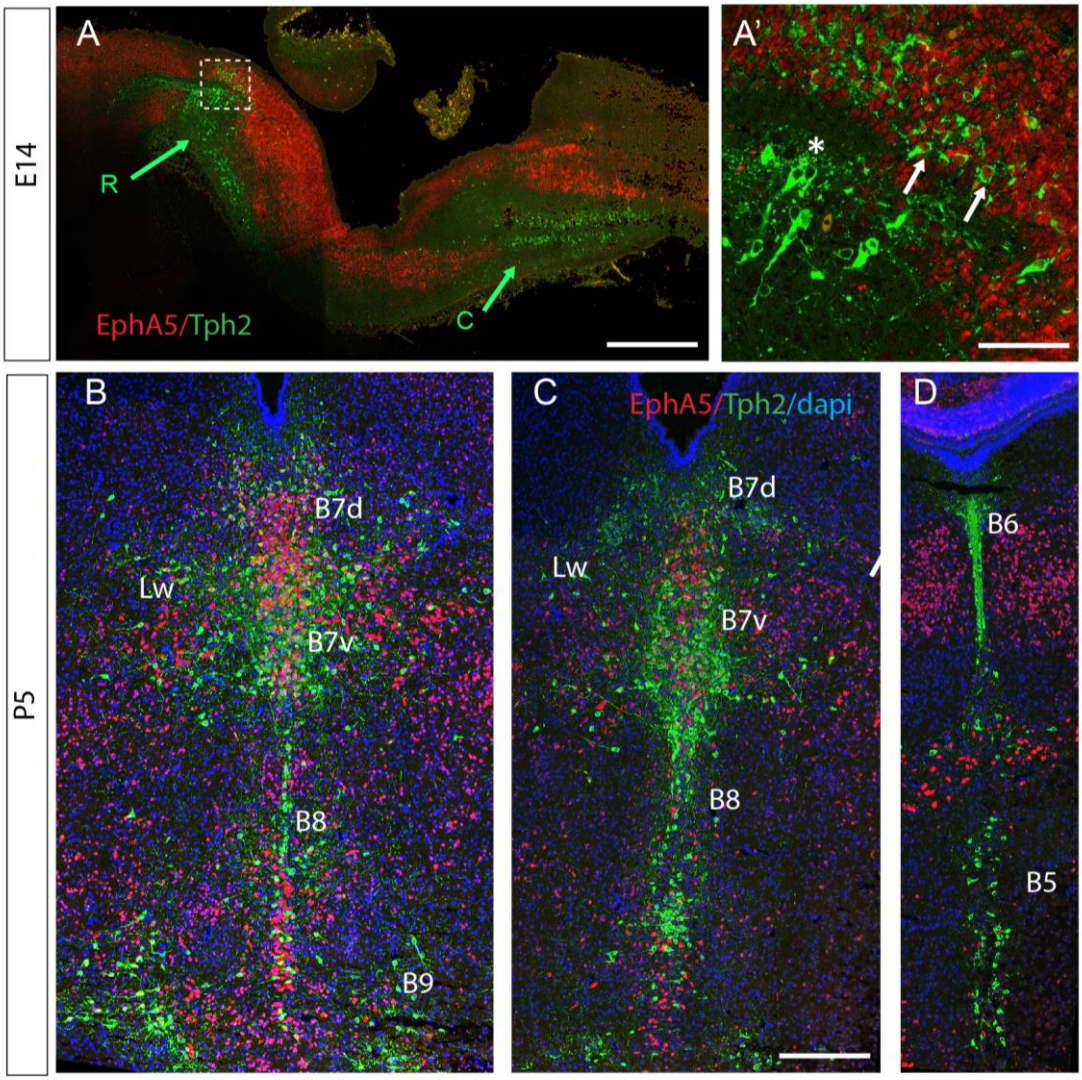

Figure 2- EphA5 is expressed in serotonergic neurons during embryonic and postnatal development.

Co-localization was visualized on confocal images after Tph2-immunostaining (green) and EphA5 ISH (red).

A, Sagittal section of E14 mouse brain through the rostral (R) and caudal (C) raphe clusters that are indicated with arrows. Note that the dorsal part of the rostral cluster in the alar plate overlaps with EphA5 labeling, whereas the ventral part does not. A', shows a higher power image of the boxed area in 2A. Arrows indicate co-localized neurons, and the asterisk shows Tph2 + neuron with no EphA5 expression. Scale bar=1000um (A), 100um (A')

B, C, D, Coronal sections of a P5 mouse hindbrain at 3 a rostral (B), intermediate (C) and caudal (C) levels of the raphe. Sections were counter-stained with DAPI. Scale bar=500um

Figure3

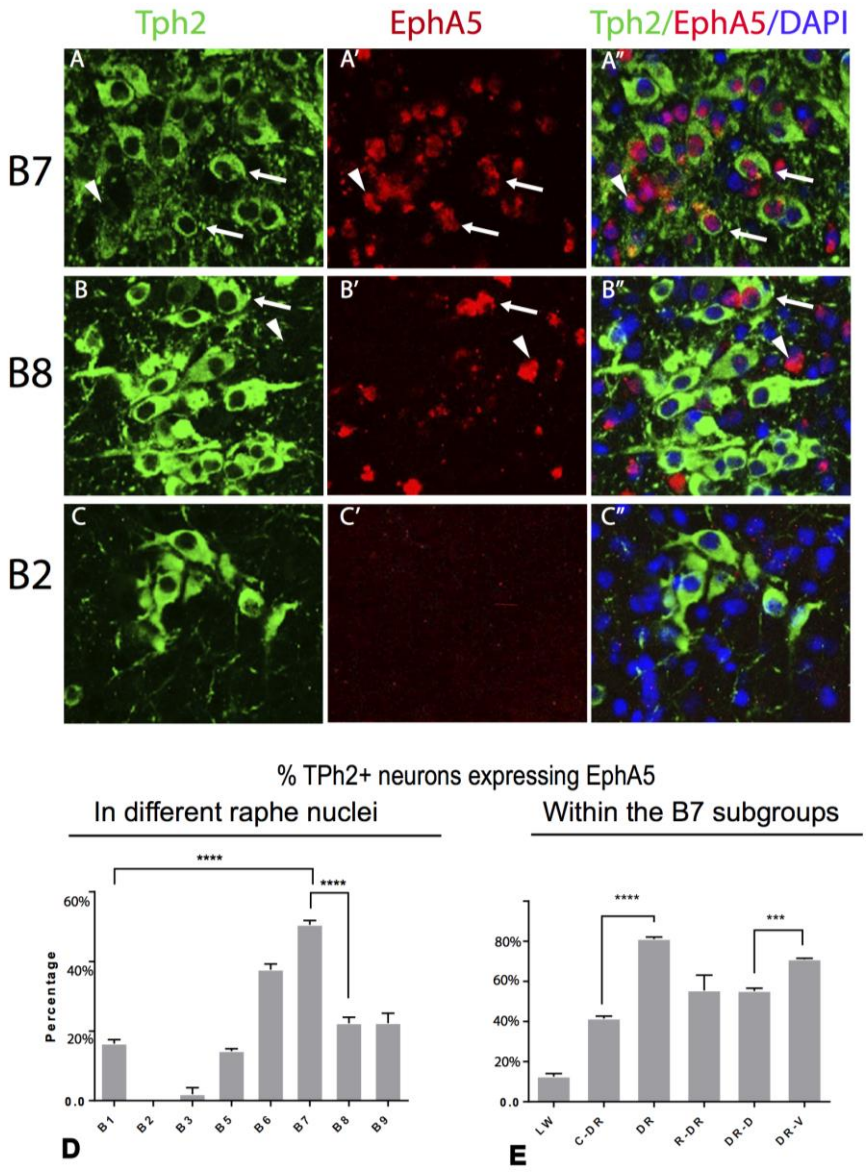

Figure 3- Quantification of co-localization in distinct raphe nucleus.

A-C, High power confocal images in B7, B8 and B2. These examples to show the difference in co-localization in different raphe nuclei. White arrows point to Tph2+EphA5 co-localized neurons whereas the arrowheads show neuron containing only EphA5. Scale bar=50um

D, E, Histograms summarizing the % co-localization among the different raphe B1-B9 raphe nuclei (D) and within the different sub-nuclei of B7 (E). Data are presented as mean ± SEM (n=3), one-way anova, **p< 0.01, ***p<0.005 and ****p<0.001.

Figure 4

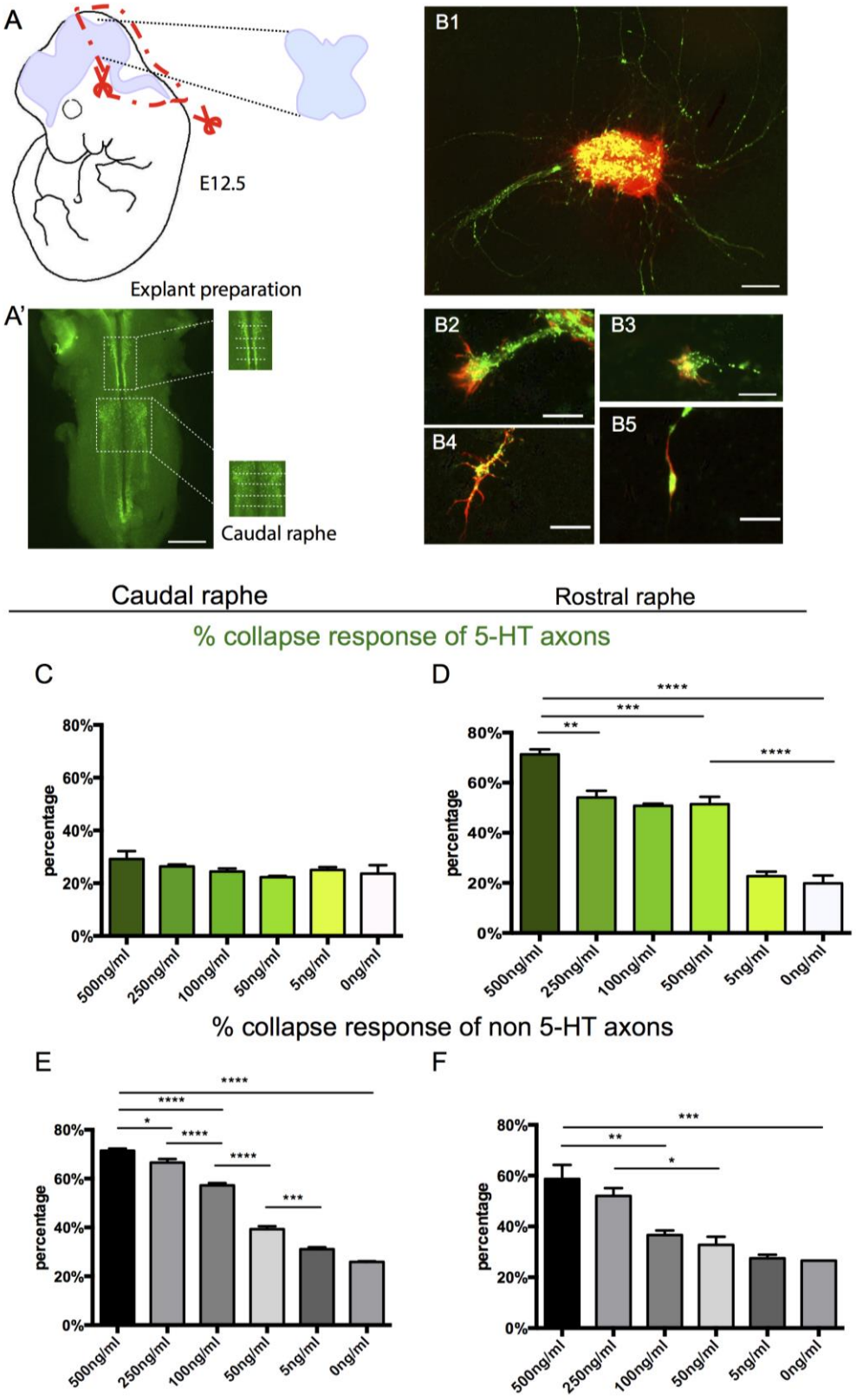

Figure 4- EphrinA5 induces collapse of rostral raphe serotonin axons in vitro.

A, Explant preparation: hindbrain was dissected as an ‘open book’ from E12 embryos; the

rostral and caudal raphe were dissected as depicted on a whole mount E12 hindbrain stained for 5-HT. Scale bar=2mm.

B; Raphe explants (3DIV) were stained for 5-HT (green) and phalloidin (red). B1- shows 5-HT+ axons emerging from the explant; B2-B3, 5-HT+ growth cones displaying a normal fan-like morphology. B4, Collapsed growth cone has a short trailing process which a branch-like morphology. B5, collapsed axon with a long trailing process and an actin rich retraction bulb. Scale bar=100um (B1), 10um (B2-B5)

C, D, E, F, Histograms show the % of collapsed growth cones when explants are exposed to different concentrations of EphrinA5. C-D) 5-HT-labeled axons from caudal (C) and rostral (D) explants; E-F) non-5-HT axons from caudal (E) and rostral (F) explants. (> 5 explants and >100 growth cones per condition). Data are presented as mean ± SEM, one-way anova, *$p<0.05$, **$p<0.01$, ***$p<0.005$ and ****$p<0.001$.

Figure 5

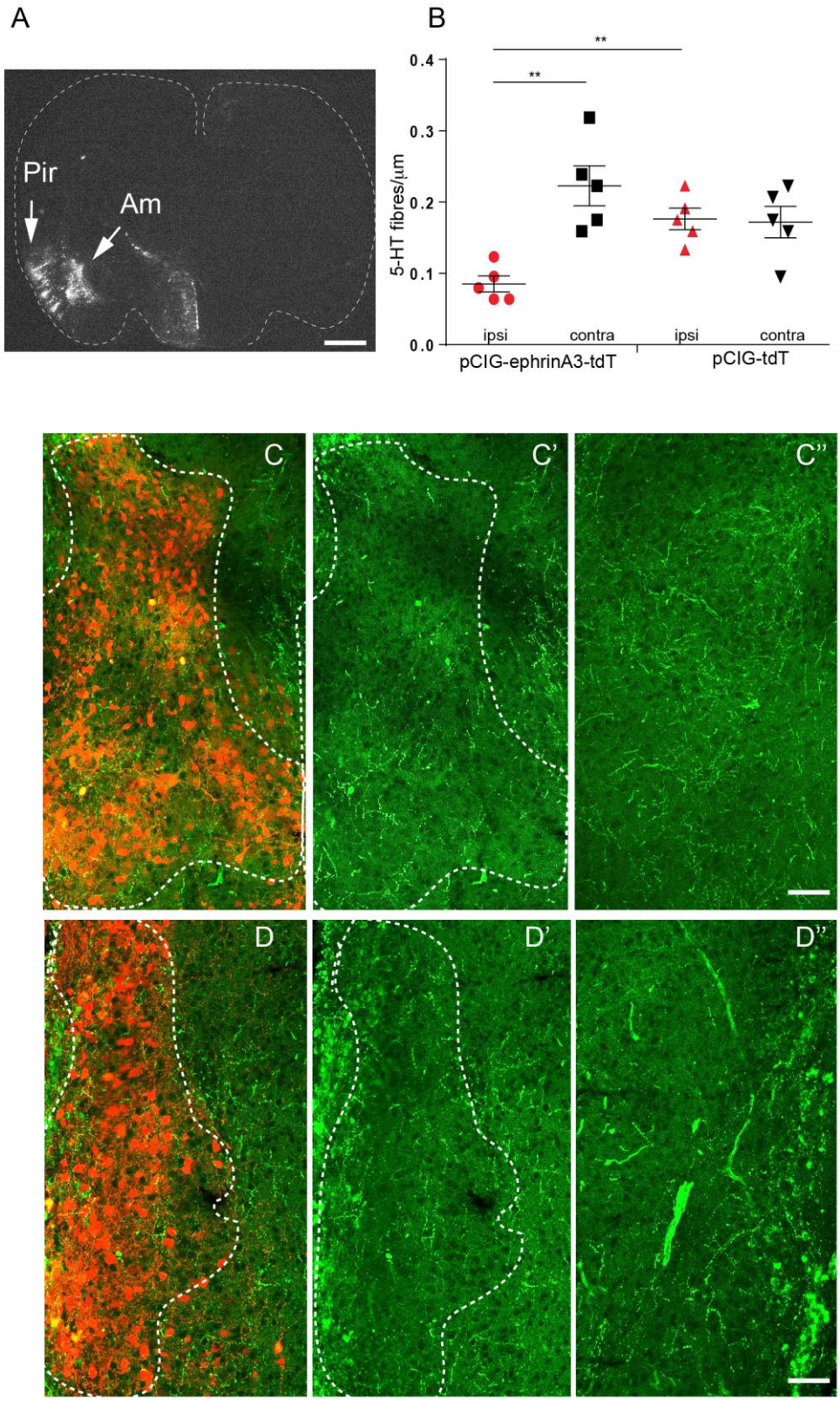

Figure 5- Overexpression of ephrinA3 down regulates serotonergic innervation in the amygdala.

A, Target of electroporation (td-tomato) on a coronal section of P5 mouse brain at the level of amygdala. Arrows show electroporated Am and Pir. Scale bar=1000um

B, Scattergram shows serotonergic fiber density per µm in the electroporated (red) versus non

electroporated (black) amygdala, using either the ephrinA3 (pCIG-ephrinA3-tdT) or the control (pCIG-tdT) plasmid. Overexpression of ephrinA3 resulted in a significant decrease of 5-HT fiber density compared to the control groups. (n=5) Data are presented as mean ± SEM, unpaired t test was used for pCIG-ephrinA3-tdT vs. pCIG-tdT and paired t test was used for ipsi vs. contra, **p<0.01.

C-C", D-D", Electroporated neurons were revealed by td-tomato in cases with the ephrinA3 (C1) and control (D) plasmid. Corresponding 5-HT immunocytochemistry from the elecotrporated (C', D') and non electroporated (C", D") sides. Note the decrease of 5-HT fibers in the outlined area compared to the control side. Scale bar=50um

Figure 6

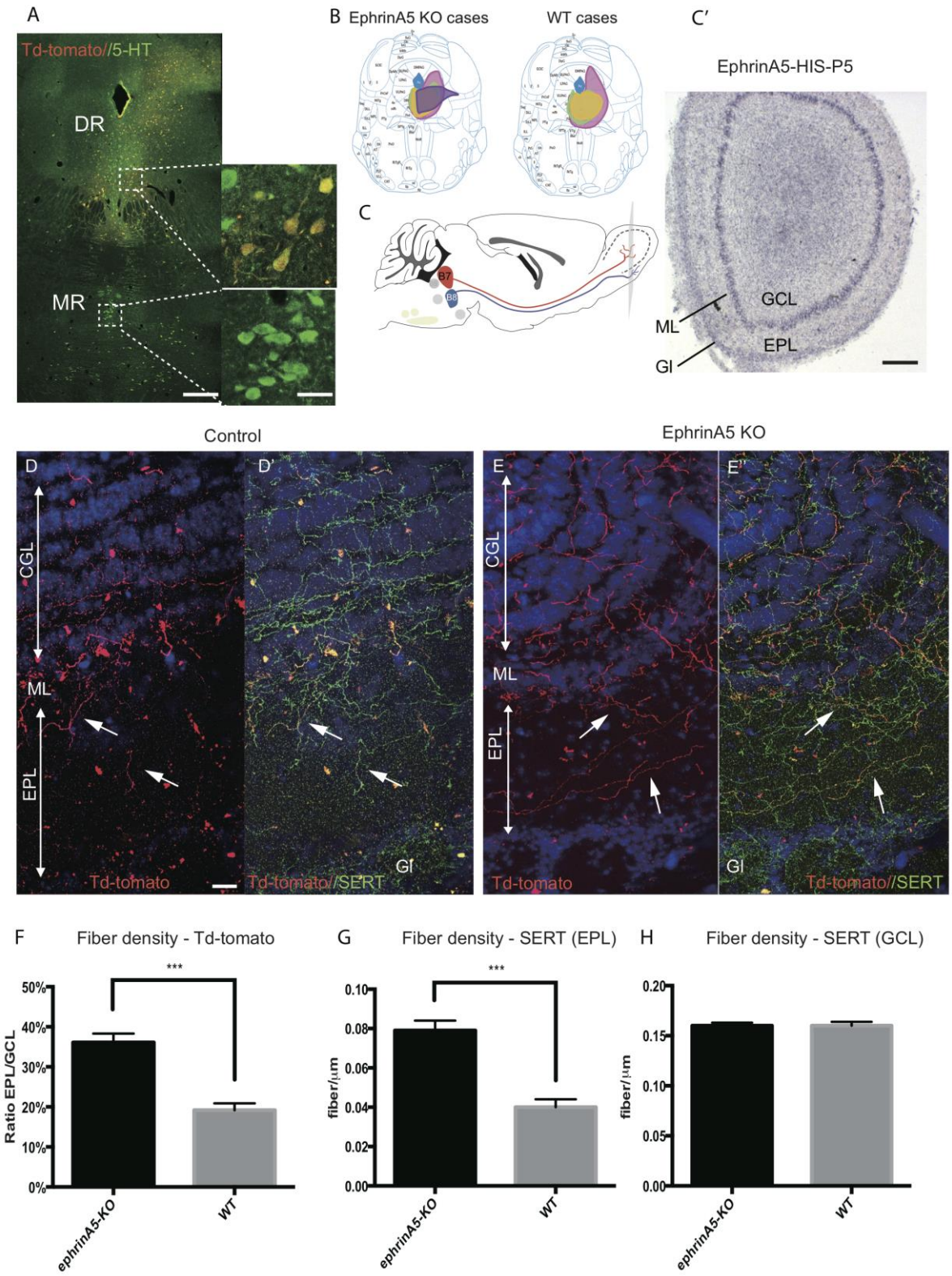

Figure 6- Anterograde tracing from dorsal raphe to olfactory bulb in ephrinA5-/-mice.

A, AAV-tdtomato virus was injected in the DR. Injection sites were checked with 5-HT immunohistochemistry on the coronal raphe sections, neurons co-labeled by 5-HT and td-tomato were

detected only in the DR and not in the MnR (A). Scale bar=500um (A left), 50um (A right)

B, The scheme shows the extent of transfection in the WT and EphrinA5 cases; injection occupied regions were drawn manually on coronal raphe sections (Bregma: -4.60mm)

C, Sagittal mouse brain scheme showing the projections from DR and MnR to GCL and GL respectively.

C', Coronal section of the OB, In situ hybridization of ephrinA5 mRNA shows the expression of ephrinA5 mainly in the ML and GL. Scale bar=250um

D-E', Anterogradely labeled axons (td-tomato) and SERT+ fibers in the OB of WT (D, D') and EphrinA5 KO mice (E,E'). Most of the td-tomato were co-labeled with SERT. More co-labeled fibers were detected in the EPL of ephrinA5-/- mice, compared to WT. Scale bar=50um.

F-H, Histograms show the fiber densities anterogradely labeled and 5-HT axons. (F) The density of td tomato fibers was normalized by calculating the of EPL/GCL fiber density ratio. The density of 5-HT axons was measured as linear density in the EPL (G) and CGL (H) (***$p<0.005$)

Figure 7

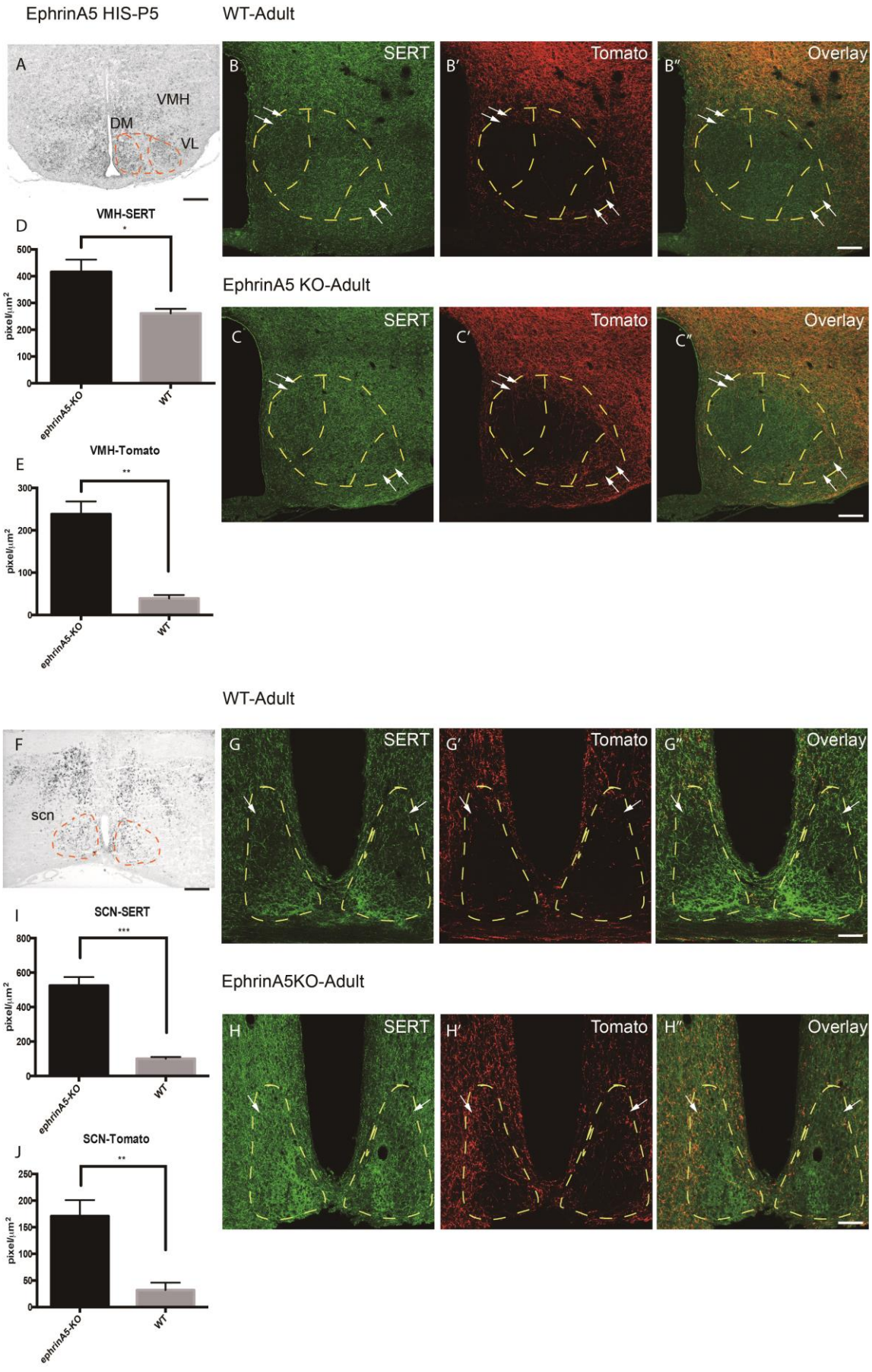
EphrinA5 HIS-P5
WT-Adult
A
VMH
DM
VL
B
SERT
B′
Tomato
B″
Overlay
D
VMH-SERT
*
pixel/μm²
500
400
300
200
100
0
ephrinA5-KO
WT
EphrinA5 KO-Adult
C
SERT
C′
Tomato
C″
Overlay
E
VMH-Tomato
**
pixel/μm²
300
200
100
0
ephrinA5-KO
WT
WT-Adult
F
scn
G
SERT
G′
Tomato
G″
Overlay
I
SCN-SERT
***
pixel/μm²
800
600
400
200
0
ephrinA5-KO
WT
EphrinA5KO-Adult
H
SERT
H′
Tomato
H″
Overlay
J
SCN-Tomato
**
pixel/μm²
250
200
150
100
50
0
ephrinA5-KO
WT

Figure 7- EphrinA5 expression modulates the DR innervation in forebrain target.

A, F, Expression of ephrinA5 in VMH (A), SCN (F) in coronal brain section of P5 mice. High level of ephrinA5 were detected in the VL and DM part of VMH. Scale bar=500um

B-B", C-C", G-G", H-H', immunofluorescence images show SERT labeling and anterograde labeling of DR in adult in control (B-B", G-G") and EphrinA5 KO mice (C-C", H-H"). Arrows show few fibers were detected in VMH and SCN in the control cases whereas labelled fibers were detected in larger amounts in the VMH and SCN of the EphrinA5 KO. Scale bar=100um (B-C"), 50um (G-H").

D, E, I, J, Histograms show the fiber densities anterogradely labeled and 5-HT axons. Fiber density was calculated by pixel per um^2 and data are presented as mean ± SEM, unpaired t test, *p<0.05, **p<0.01 and ***p<0.005.

Table 1. Enzymes for mRNA probe synthesization

	Restriction enzyme		Polymerase	
	Sense	**Anti-sense**	**Sense**	**Anti-sense**
EphA3	HindIII	EcoRI	T7	T3
EphA4	SacI/SacII	XhoI/BamHI	T7	T3
EphA5	XbaI	BamHI	T3	T7
EphA7	BamHI	XhoI	T7	SP6
ephrinA2	HindIII	EcoRV	SP6	T7
ephrinA3	XhoI	BamhI	T7	SP6
ephrinA5	HindIII	XbaI	T3	T7

Table 1. Enzymes for mRNA probe synthesization

Table lists enzymes that were used for mRNA probe synthesization. Expressions of different EphA receptors and ephrinA ligands were examined by performing an ISH. mRNA probes were synthesized by using specific restriction enzymes and polymerase on the selected restriction site and polymerase active site which were listed in table1. Sense and anti-sense means the different direction of the synthesization which are 5'-3' (anti-sense) and 3'-5' (sense).

Table 2. RT-QPCR primers

	mRNA variant	Primer info	Forward primer	Reverse primer
EPHA3	NM_010140	Product length 116	TGCGGGACTGTAACAGCATT	CGTGAACTGATGCTCTCGGA
EPHA4	NM_007936	Product length 90	GAGGCTCCTGTGTCAACAACT	AGTTGCCAATGGGTACCAGC
EPHA5	NM_007937	Product length 98	TTGGCTGTTGACCAGTTGGA	GTCCTCCAGGAAGGCTGTTG
EPHA6	NM_007938	Product length 90	ACTGAAATCCGTGAGGTGGG	GACTGAGACCAGAGCGATGC
EPHA7	NM_010141	Product length 98	TCCTCCTTAGTCGAGGTCCG	GCCACTCTCCTTCTGCACTG
EPHA8	NM_007939	Product length 95	CATTGCTTTCCGCACGTTCT	TCCAGTAGGGTCGTTCACCA

Table 2. RT-QPCR primers

Table shows several informations refer to the primers that were used for Q-PCR analysis. Primer sequences of different EphA receptors were kindly provided by Dr. Micheal Rober. References of mRNA variant refers to the mRNA sequence in NCBI (http://www.ncbi.nlm.nih.gov/). Forward and reverse primers for Q-PCR were orderd from Eurofins Genomics with the sequences listed in table2. Primers were synthesized with a ‘salt free’ purification and final concentration of 50pmol/ul in H_2O.

Table 3. Expressions of Tph2 and EphA5 in distinct subpopulation of raphe neurons (n=3, mean ± SEM)

		B1	B2	B3	B5
[1] Tph2+	EphA5+	4±0,6	0	0,3±0,3	4,3±0,3
[2] Tph2+	EphA5-	21,3±2,8	8,3±0,3	22±2,6	26±0,9
[3] Tph2-	EphA5+	54±9,9	10±5	8,4±4,4	53,3±1,2
[4] CO/Tph2		16,3%±1%	0	1,8%±1,9%	14,3%±0,7%
		B6	**B7**	**B8**	**B9**
Tph2+	EphA5+	69±3,8	187±13,2	10±1	28,6±4,4
Tph2+	EphA5-	115±11,6	184±30,6	35±3,6	100±11,5
Tph2-	EphA5+	178±17,3	582,3±73,8	160,3±14,8	26,4±15,8
CO/Tph2		37,6%±1,6%	50,5%±1,2%	22,3%±0,2%	22,3±2,8

Table 3. Expressions of Tph2 and EphA5 in distinct subpopulation of raphe neurons (n=3, mean ± SEM)

Table exhibits the different cell numbers in subnuclei of raphe neurons which correspond to the expression of Tph2 and EphA5. Cells were counted with cell counter plugin of image J. A 150um X 150um squared mask was used for region selection. Cells (validated by DAPI staining) that located within the mask and on the upper and right edges of the mask were counted. Cell numbers were listed in the table and exhibited as mean ± SEM.

Remarks:

1: Cell numbers of both Tph2+ and EphA5+.

2: Cell numbers of Tph2+ cells only.

3. Cell numbers of EphA5+ cells only.

4. Percentage of co-localization cells in total 5-HT neurons.

Table 4. Expressions of Tph2 and EphA5 in distinct sub-nuclei within B7 (n=3, mean ± SEM)

		LW	B7c	B7m	B7r	B7d	B7v
Tph2+	**EphA5+**	10,3±1,7	44,3±6,4	98,3±8,7	34±2,1	66,7±8,1	76±7
Tph2+	**EphA5-**	71,3±8,2	62,3±13,8	22,7±9,5	29±6	53,6±12,6	31,3±10,7
Tph2-	**EphA5+**	349,7±22,2	79,3±21,7	131,7±26	21,6±9,3	129,9±21,1	81±26,8
CO/Tph2		12,6%±1,5%	41,5±1,2	81,1% ± 1%	44,4%±7,7%	55,2%±1,4%	70,9%±0,6%

Table 4. Expressions of Tph2 and EphA5 in distinct sub-nuclei within B7 (n=3, mean ± SEM)

Table exhibits the different cell numbers of different subnuclei within B7. The way of analysis was as same as described in table3.

Part 2: Study of serotonin raphe neurons projections during development with an IDISCO method

In mice, serotonin midbrain neurons are born from embryonic day 10 to 12, and start extending axons, shortly after neurogenesis, both rostrally to the telencephalon and caudally to the brainstem. The development of these 5-HT midbrain neurons has been studied in a number of invertebrates. Early studies focused on the development 5-HT neurons in the rats and more recent studies analyzed development in the zebrafish. However there are no systematic detailed developmental studies in mice, which are the most extensively used model, in particular for genetic studies. Such data are important to gather in order to analyze the effects of mouse mutations on defined molecular pathway of serotonin neurons.

Another reason for performing a developmental study of 5-HT innervation is that we wanted to know how the dorsal and median raphe nuclei target to different forebrain regions during development. Indeed our analysis of the role of ephrinA signalling in raphe neurons showed that targeting of the dorsal and medial raphe axons to different layers of the olfactory bulb is altered in ephrinA5 KO mice. However we do not know at what developmental stage these alterations occur, in particularly, whether this reflects an alteration in the orientation of ascending fibre tracts, or whether this reflects late developmental maturation when raphe axons collateralize and branch in specific target regions.

In order to analyse embryonic development of the 5-HT innervation, we have taken advantage a new morphological method, which allows analysing immunocytochemical labelling in whole brain. This involves a transparization method after in total immunocytochemistry (whole embryos, whole heads or dissected mouse brains.

I have first optimized a published method for in total immunocytochemistry to test optimal antibody labelling of the serotonin neurons at the different developmental stages. I have then compared 5-HT immunolabelling in the brains of control and ephrinA5 KO mice

Materials and methods

Animals:

Developmental analyses were all performed on mice of the Swiss background (RjOrl:SWISS) purchased from a commercial breeder (Centre d'Elevage R. Janvier). E0.5 was defined as the plug date, and P0 as the date of birth.

The ephrinA5-KO mouse line was a gift of the Frisen lab to Dr Afsaneh Gaillard and maintained on a C57Black6 background. Briefly these mice have a PGK-neo cassette replacing the 5' acceptor splicing site and the sequences encoding amino acid residues 42–129. The PCR primers for genotype are as follows: primer 1 (TCCAGCTGTGCAGTTCTCCAAAACA) and primer 2 (ATTCCAGAGGGGTGACTACCACATT) for wild-type sequences (397 bp) and primers 1 and primer 3 (AGCCCAGAAAGCGAAGGAGCAAAGC) for mutant sequences (513 bp).

All experiments were performed were in compliance with the standard ethical guidelines (European Community Guidelines and French Agriculture and Forestry Ministry Guidelines for Handling Animals decree 87849). All efforts were made to reduce the number of animals used and their suffering.

Idisco (adapted from the protocol of Nicolas Renier et al., 2014):

Sample collection

The day of vaginal plug was defined as E 0. Embryos were collected at E12, E14, E16 and E18 were collected in ice-cold PBS 1X. To better preserve the skin and avoid air bubble formation, embryos were manipulated with extra care, and contact with tweezers tip avoided. The umbilical cord was regularly trimmed to help drain as much blood as possible from embryos.

Sample pre-treatment with methanol

Embryos were washed in PBS for 1h (or 4°C overnight), then in 25% methanol (in PBS) for 1h, in 50% methanol (in PBS) for 1h, 75% methanol for 1h,

100% methanol for 1h twice. Samples were then bleached with 5% H2O2 in 20%DMSO/methanol (1 volume 30%H2O2/1 volume DMSO/4 volume methanol, ice cold) at 4°C overnight. After bleaching, samples were washed in 100% methanol for 1h twice, then in 20%DMSO/methanol for 1h twice, then in 75% methanol for 1h, 50% methanol for 1h, 25% methanol for 1h, PBS for 1h, and finally in PBS/0.2% TritonX-100 for 1h twice before further staining procedures.

Immunolabeling protocol

Pre-treated samples were incubated in PBS/0.2% TritonX-100/20% DMSO/0.3M glycine at 37°C overnight, and then blocked in PBS/0.2% TritonX-100/10% DMSO/6% horse Serum at 37°C for indicated time (Table 3). After blocking, samples were washed in PBS/0.2% TritonX-100 for 1h twice, then incubated in 5-HT anti (1/1000) in PBS/0.2% TritonX-100/10% DMSO/3% horse Serum at 37°C for indicated time (Table 3). After primary antibody, samples were washed in PBS/0.2% TritonX-100 for 1h twice, two hour twice and lasting for 1d, then incubated in secondary antibody Donkey anti-rabbit Alexa 488 (1/400) in PBS/0.2% TritonX-100/10% DMSO/3% horse Serum at 37°C for indicated time (Table 3). After secondary antibody, samples were finally washed in PBS 1X for 2d before clearing and imaging.

5-HT, SERT and Tph2 antibodies were used to label serotonergic neurons. Tests were made to verify the best antibody to label the serotonergic projection at the prenatal ages. Antibodies that are used for immunocytochemistry were list in the table 3.

Tissue clearing, and precautions with solvents

Immunolabeled tissues were cleared with a simplified version of the 3DISCO method (Ertürk et al., 2012a). Samples were incubated in a 5ml glass container with a silicon-coated cap overnight in 3ml of 50% Tetrahydrofuran/H2O (THF, Sigma 186562-12X100ML) on an agitator at room temperature. Samples were then incubated for 1h in 3ml of 80% THF/H2O and twice 1h in 100% THF. Samples were then incubated in Dichloromethane (DCM, Sigma 270997-12X100ML) until they sank the bottom of the vial for 5-10 mins. Finally, samples were incubated in 3ml of

DiBenzyl Ether (DBE, Sigma 108014-1KG) until clear (about 2h) and stored in DBE at room temperature. Organic solvents, in particular dichloromethane (DCM), were handled under a chemical hood with care, and disposed according to local health and safety regulations. DBE, which is used for storage and imaging (below) is a skin irritant exhibiting Toxicity Class II (moderate toxicity) according to the MSDS sheets, and should be handled with care, including wearing gloves, but with those precautions it can be used on an open bench for slide mounting and for microscopy.

Table3

TIMING OF PRE-IMMUNOSTAINING				
AGES	BLOCKING	1ST AB	RINSE	2ND AB
E12-E14	2 DAYS	1 WEEK	1 DAY	1 WEEK
E16-E18	4 DAYS	2 WEEKS	2 DAYS	2 WEEKS

ANTIBODIES FOR IDISCO		
NAME	DILUTION	MeOH
5-HT (RABBIT)	1/1000	YES
SERT (GOAT)	1/1000	YES
TPH2 (MOUSE)	1/500	NO
TPH2 (RABBIT)	1/500	YES

Results

In mice, the serotonergic neurons are born in two waves. The rostral cluster arises one day earlier then the caudal raphe neurons, and these waves during relatively brief period between embryonic day E9.5 and E11.5 (Briscoe et al. 1999; Pattyn et al. 2003).

To study the projection of serotonin raphe neurons, we performed a time course from embryo day 12 to 18, to analyze the developing topographic serotonin projections in the forebrain.

1. Development of serotonergic projection pattern

Embryonic day 12

At E12, we observed two distinct groups of labeled neurons in the rostral hindbrain, and the other in the medulla, with a gap in between. The caudal raphe group contains two clusters, one lateral, the B3 group that shows descending fiber tracts into the spinal cord bilaterally while the B1 and B2 group form 2 contiguous groups along the midline of the hindbrain. The rostral serotonergic cluster at E12 form 2 continuous band distributed on either side of the midline with no clear subdivision. There is a clear gap between rostral group and caudal group. The ascending projection from rostral cluster is still in the initial status, most of the ascending fibers are fasciculate passing oculomotor nucleus and arrives at the mid-hind brain boundary, whereas a small population of fibers which are not fasciculate course dorsally to the ascending fiber tract and reach the oculomotor nucleus at the level of the ventral tegmental area (VTA) (Figure 1).

Embryonic day 14

48 hours later, the rostral group starts to be subdivided into subgroups such as the dorsal and median raphe. This partition is due to the migration of the median raphe neurons. At the same time, both the dorsal and median raphe neurons starting to form connections with the caudal group brainstem – the periolivary nucleus at this stage. Moreover median raphe serotonergic descending fibers exhibit denser innervation in contrast to the dorsal. At this stage, the ascending 5-HT fibers cross the

midbrain and enter the forebrain. As the ascending 5-HT fibers reach the midbrain, they start to defasciculate from lateral-ventral to dorsal-median. They densely innervate the substantial nigra and ventral tegmental area. However serotonin axons do not cross the midline and remain on either side. The scattered fibers passing through the edge of the mammillotegmental tract innervate the subthalamic nucleus. Serotonergic fibers are also detected in the lateral hypothalamic area, medial forebrain bundle and lateral preoptic area (Figure 2).

Embryonic day 16

At E16, the ascending serotonin fiber that has already reached most of the baso-ventral forebrain targets. At this stage, serotonergic fibers densely innervate the optic tract and suprachiasmatic nucleus just above the optic chiasm but no fibers are detected in the optic chiasm. In the hypothalamus, 5-HT fibers were detected in the anterior hypothalamic nucleus and the ventrolateral part of ventromedial hypothalamic nucleus. A large fiber bundle extended along the medial forebrain bundle. Most of the regions of the amygdala are innervated by sparse fibers, in particular the basolateral, basomedial, lateral, central, anterior and cortical amygdala. Dense fibers were also detected in the lateral olfactory tract. More rostral, massive innervation is found in the olfactory tubercle and following the ventral hippocampal commissure and lateral septal nucleus. The most rostral, 5-HT fibers arrive close to the OB but instead of entering the OB, serotonergic fibers change direction, heading toward the frontal cortex. Most of the thalamic nuclei are dense innervated. In the frontal cortex, fibers seemed to branch in two directions: 1. Fibers were following the cortical plate, pass through the cingulate cortex and the motor cortex, and enter the somatosensory cortex. 2. Fibers that descend forward the hippocampal formation, following the dentate gyrus and fimbria, end in ventricular and subventricular zones. The cerebellum is also innervated densely at E16. (Figure 3)

Embryonic day 18

Embryonic day 18 ends the mouse embryonic stage (depending on the background of the mouse). At this stage, the serotonin fibers have reached all their targets and fibers are becoming denser in regions such as the amygdala and hypothalamus, the optic tract, olfactory tract, septal areas, thalamus nucleus,

hypothalamus and cerebellum. Additionally, a dense innervation begins to be detected in the lateral and medial habenular nucleus, and most of cortical regions: in the somatosensory cortex, piriform cortex and visual cortex. (Figure 4)

2. The development of serotonin projection to OB

It has been published that 5-HT plays a key role in the olfactory function. (Dugue & Mainen, 2009) Moreover, the dorsal raphe neuron and median raphe neurons innervate different layers of the OB (Muzerelle et al., 2016). Therefore, the timing of serotonin projection arrive to OB is important to know.

We performed histochemical analysis combining 5-HT immunocytochemistry (to label the serotonergic fibers) with DAPI staining (to label the rostral migratory steam, RMS) on embryo and postnatal mice brain sections, to analyze the development of serotonergic innervation in the OB. Our observations of the trajectory of the serotonergic projections at E16 showed an interesting phenotype: when serotonergic fibers reach the basoventral targets and start turning in the direction of the frontal cortex, the olfactory bulb is avoided.

At E16, serotonin fibers that arrive close to the OB changed their direction toward the frontal cortex, instead of entering the OB. This change in direction is correlated with the position of the rostral migratory steam (Figure 5A, A'). 24 hours later, a few serotonin fibers were found in the OB. 5-HT fibers which enter the OB at E17 can be divided into three groups depending on the distribution: one fascicle enters the OB along the basal plate that extend to the region of the forming glomeruli layer; the second group passes along the RMS; the remaining fibers are scattered in the rest part of the OB region (Figure 5B, B').

At P5, when all the different components (layers) of OB are mature, serotonergic fibers showed different morphology depending on the distribution in OB: fibers from the dorsal raphe were scattered in the granular cell layer (GCL), whereas punctate median raphe fibers distribute in the glomerular layer (GL). Serotonergic fibers enter the OB and distribute homogeneously in the GCL instead of surrounding the central region, which correlated to a retraction of the RMS (Figure 5 C, C'). By

the second postnatal week at P10, the innervation exhibits a mature aspect similar to adult.

3. Role of ephrinA5 in serotonin innervation organization in the RMS-OB region.

Our observations at E16 suggested that there could be a repellent signal produced by RMS that prevents 5-HT axons from entering the OB. We performed ISH of ephrinA5 mRNA probe and found a high level of eprhinA5 expression in the RMS, extending from the SVZ to the GCL in the OB. This expression pattern includes the region that repels the serotonin projections. At E17, when RMS undergoes shrinkage, the area of ephrinA5 expression region in the GCL is also reduced, which would then become permissive for the growth of 5-HT axons. At P5, there is no expression of ephrinA5 in the GCL but ML and GL, which resemble the pattern observed in the adult OB.

Overall ephrinA5 expression and the timing of serotonin innervation in the OB suggested that ephrinA5 plays a role during these developmental events. To test this hypothesis we analyzed serotonin innervation in ephrinA5-/- embryos.

In E16 EphrinA5 KO, a large population of serotonergic fibers was found altering pathway in the RMS and arrived at VZ and SVZ, whereas in WT serotonergic fiber avoid the RMS. Moreover few of the fibers were starting to enter the OB and on the coronal sections serotonin fibers were detected in the GCL whereas in the WT no fiber was detected in the OB (Figure 6).

Overall, ephrinA5 expression in the RMS and OB in the embryonic stage is involved in the guidance of ser otonin projections.

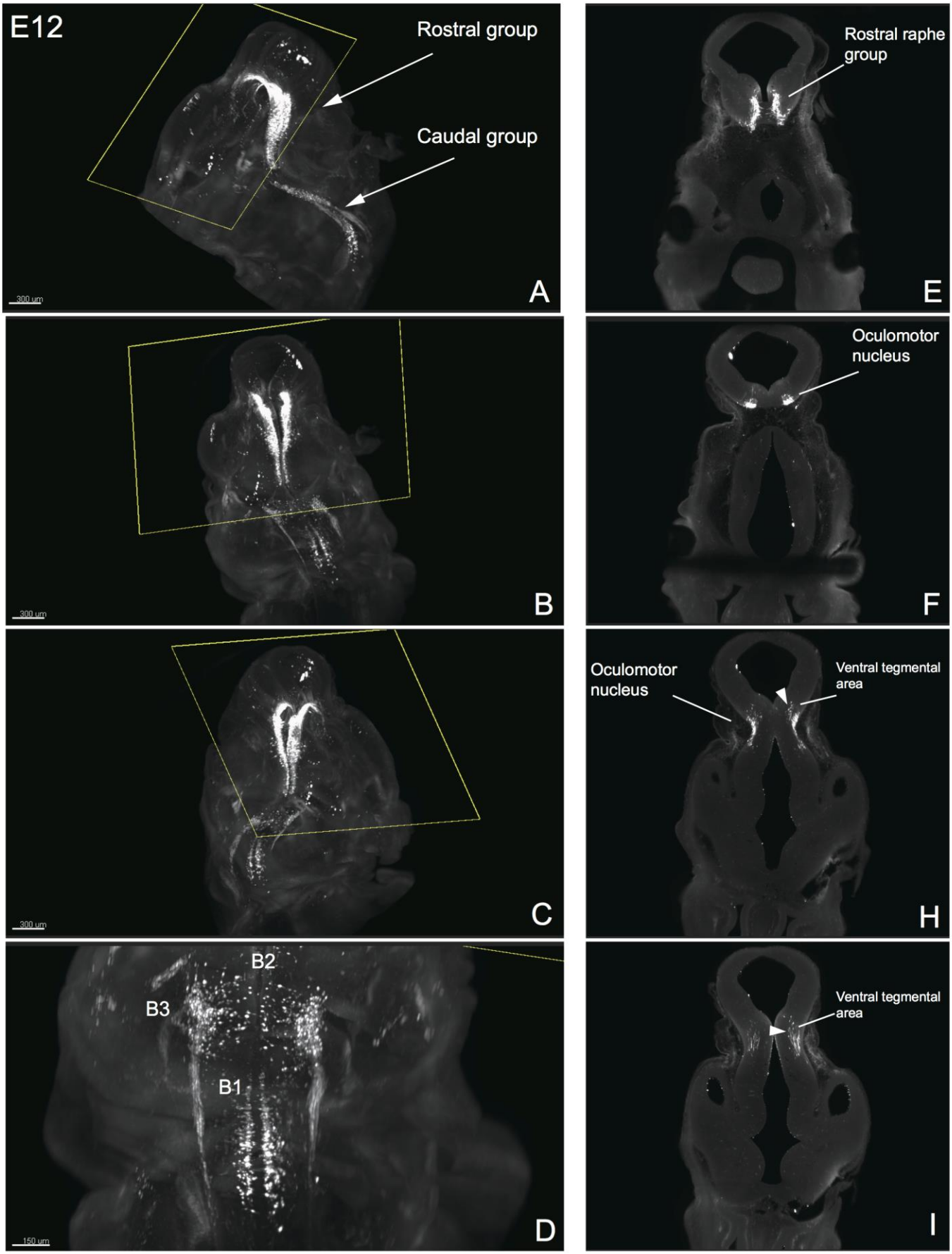

Figure 1. Serotonergic neurons and projections at E12.

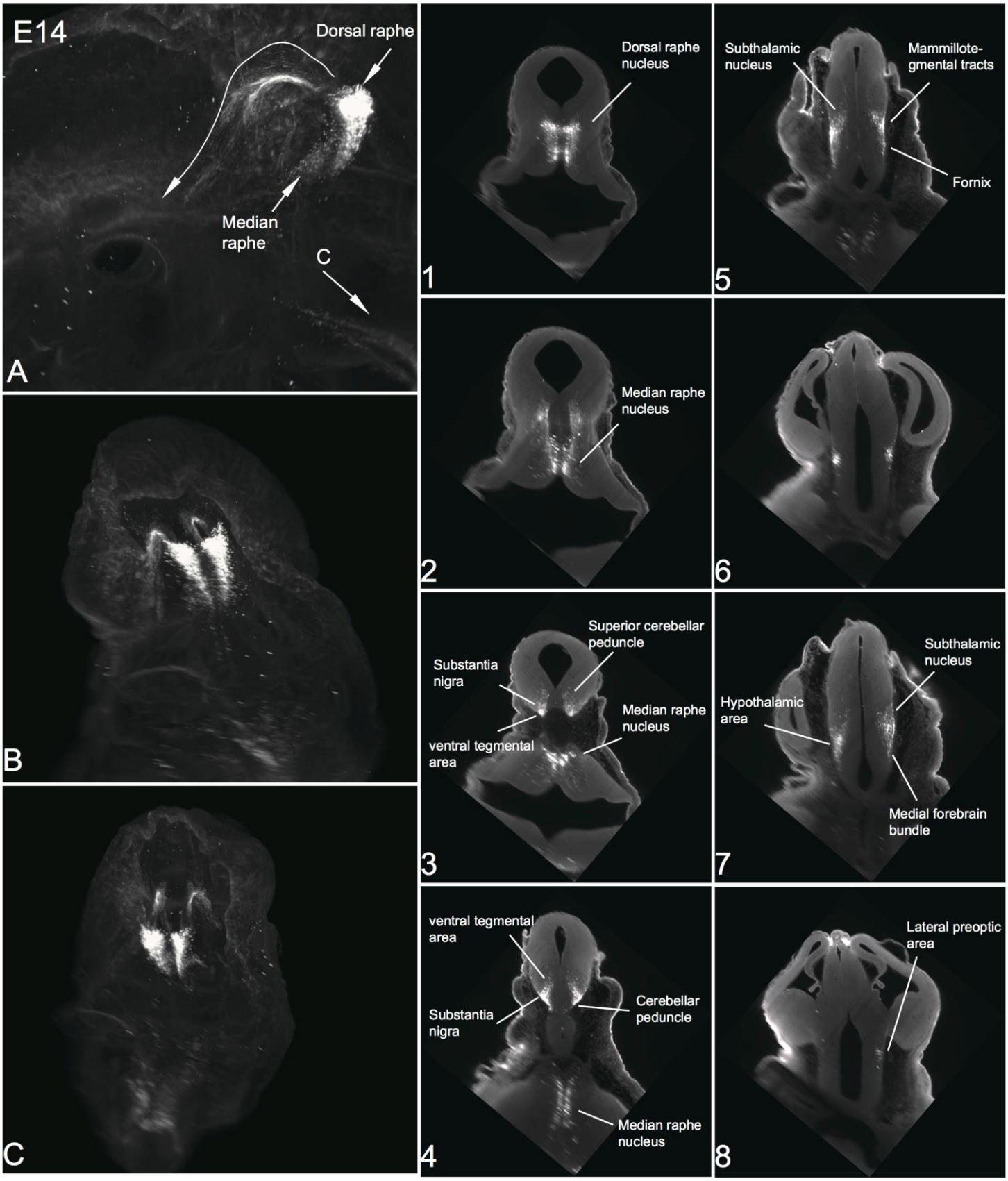

Figure 2. Serotonergic neurons and projections at E14.

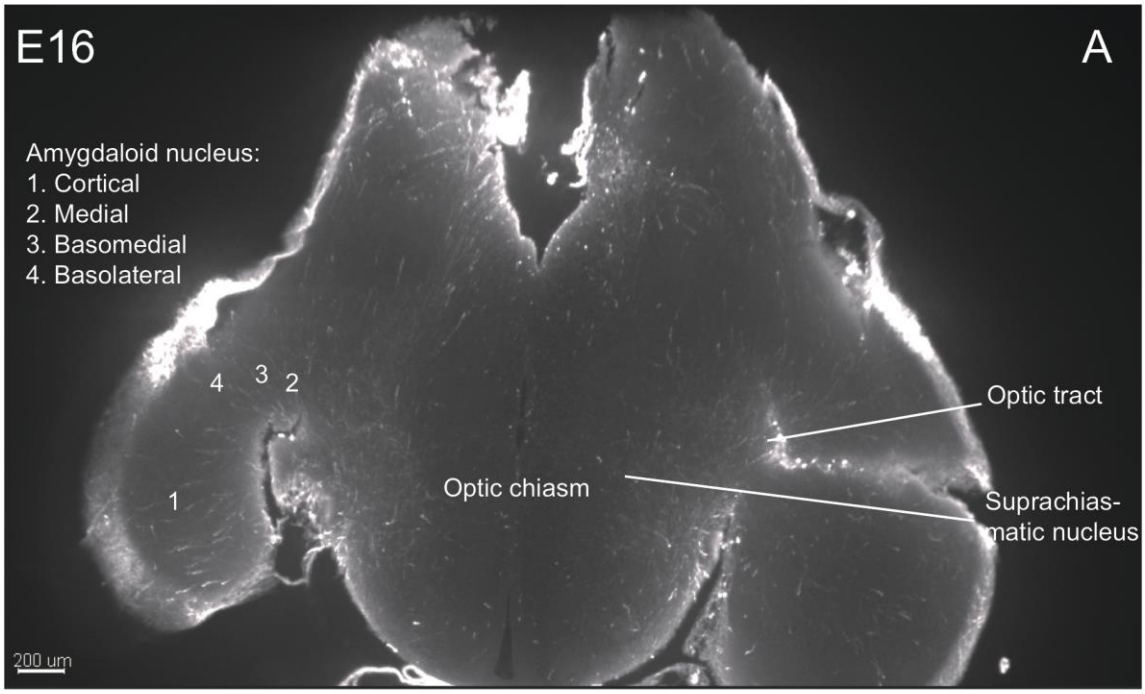
E16
A
Amygdaloid nucleus:
1. Cortical
2. Medial
3. Basomedial
4. Basolateral
4
3
2
1
Optic tract
Optic chiasm
Suprachias-
matic nucleus
200 um

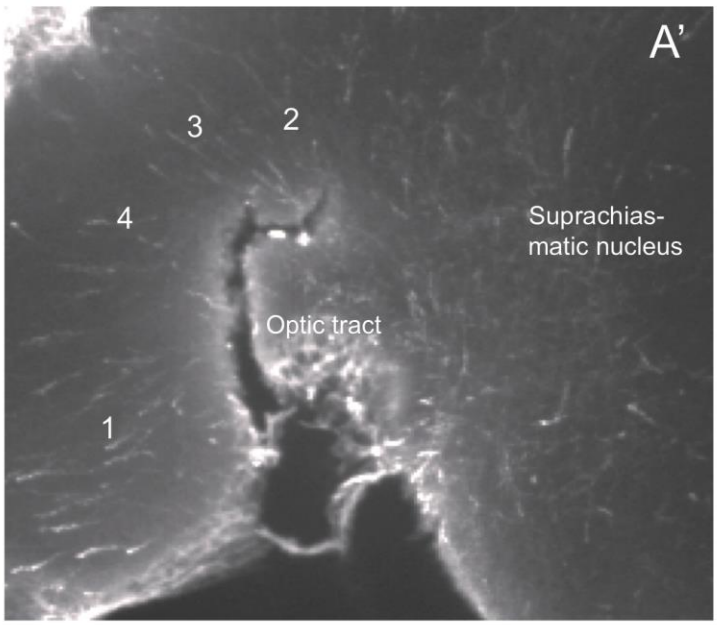
A'
3
2
4
Suprachias-
matic nucleus
Optic tract
1

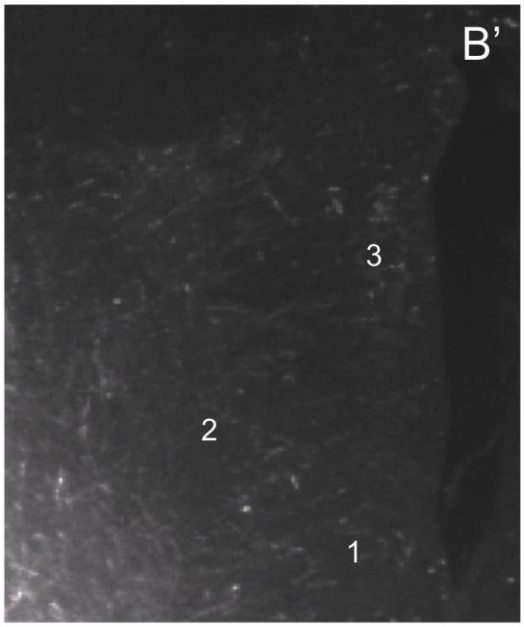
B'
3
2
1

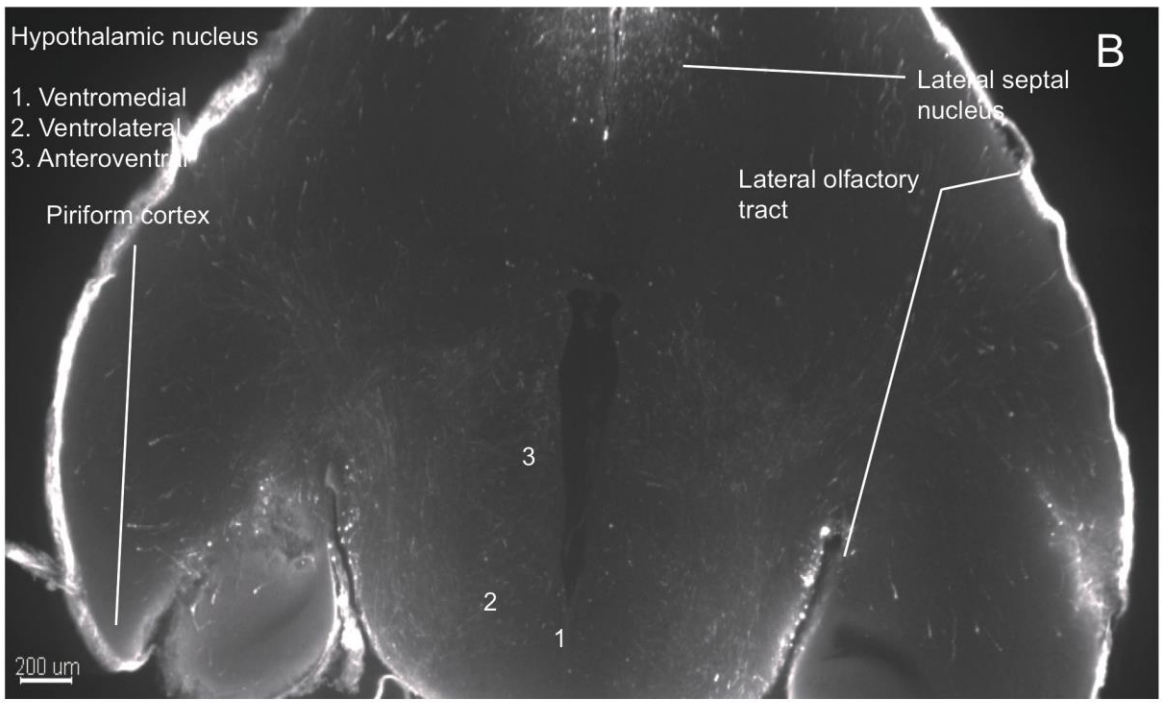
Hypothalamic nucleus
1. Ventromedial
2. Ventrolateral
3. Anteroventral
Piriform cortex
B
Lateral septal
nucleus
Lateral olfactory
tract
3
2
1
200 um

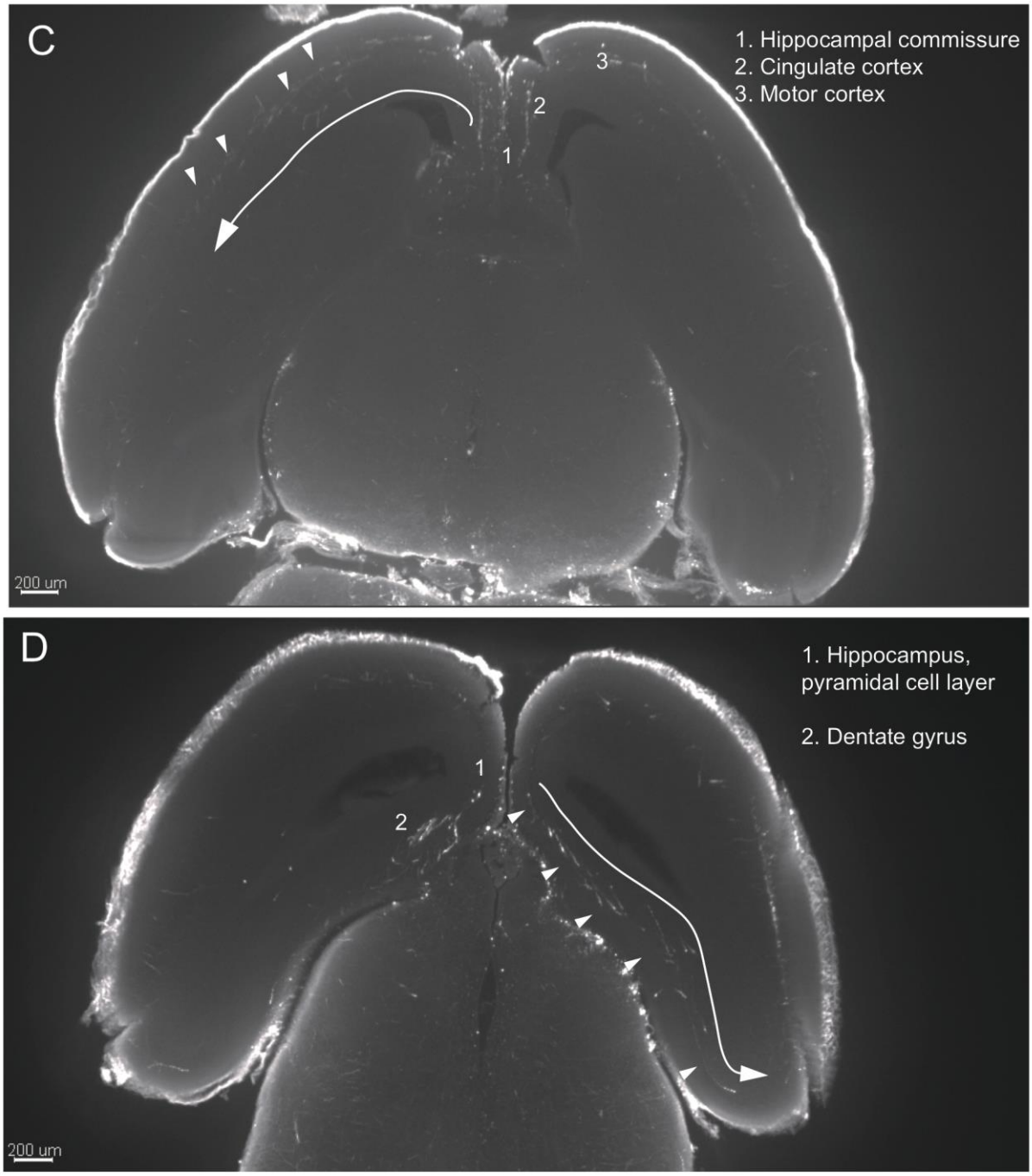

Figure 3. Serotonergic neurons and projections at E16.

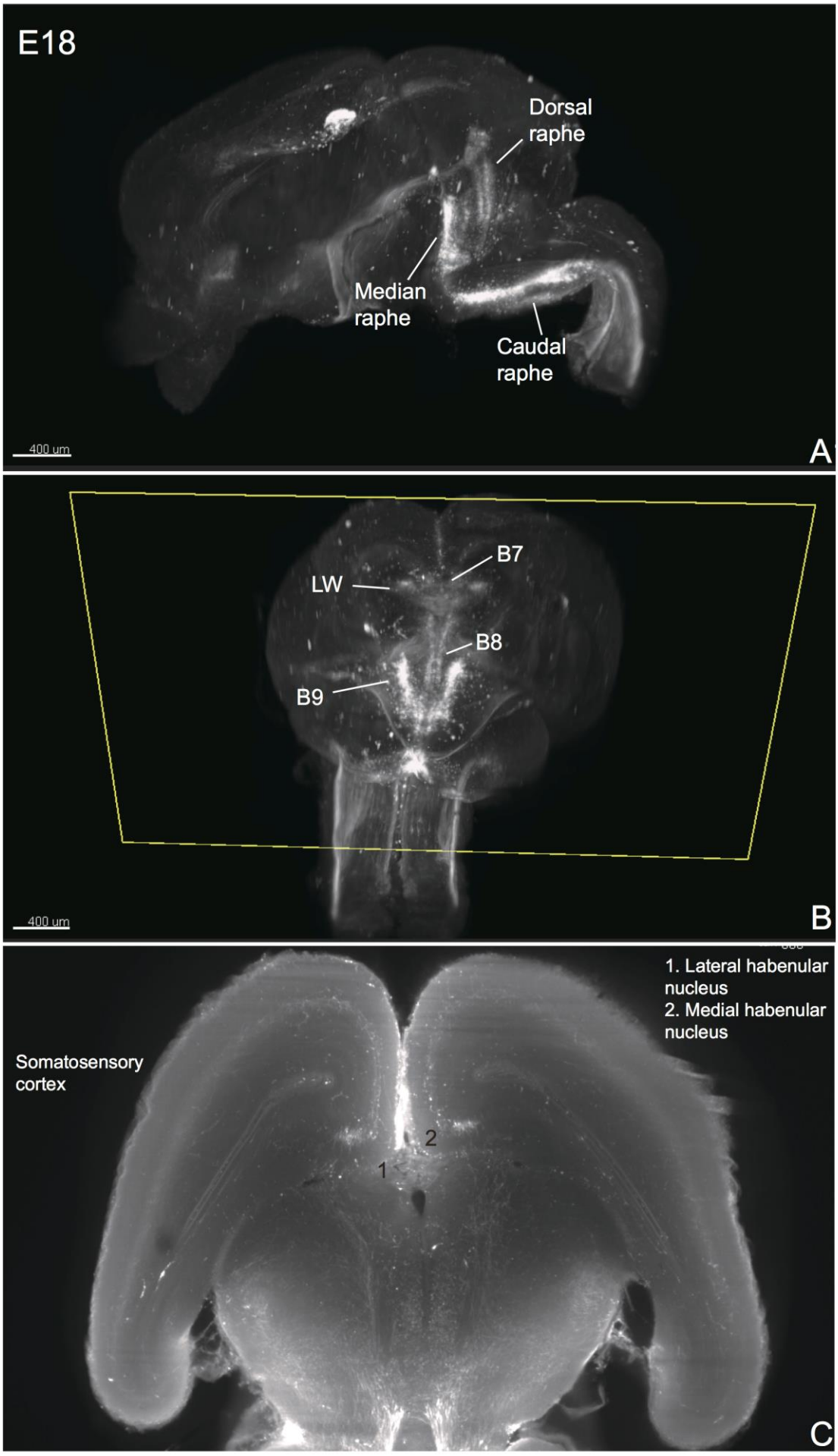

Figure 4. Serotonergic neurons and projections at E18.

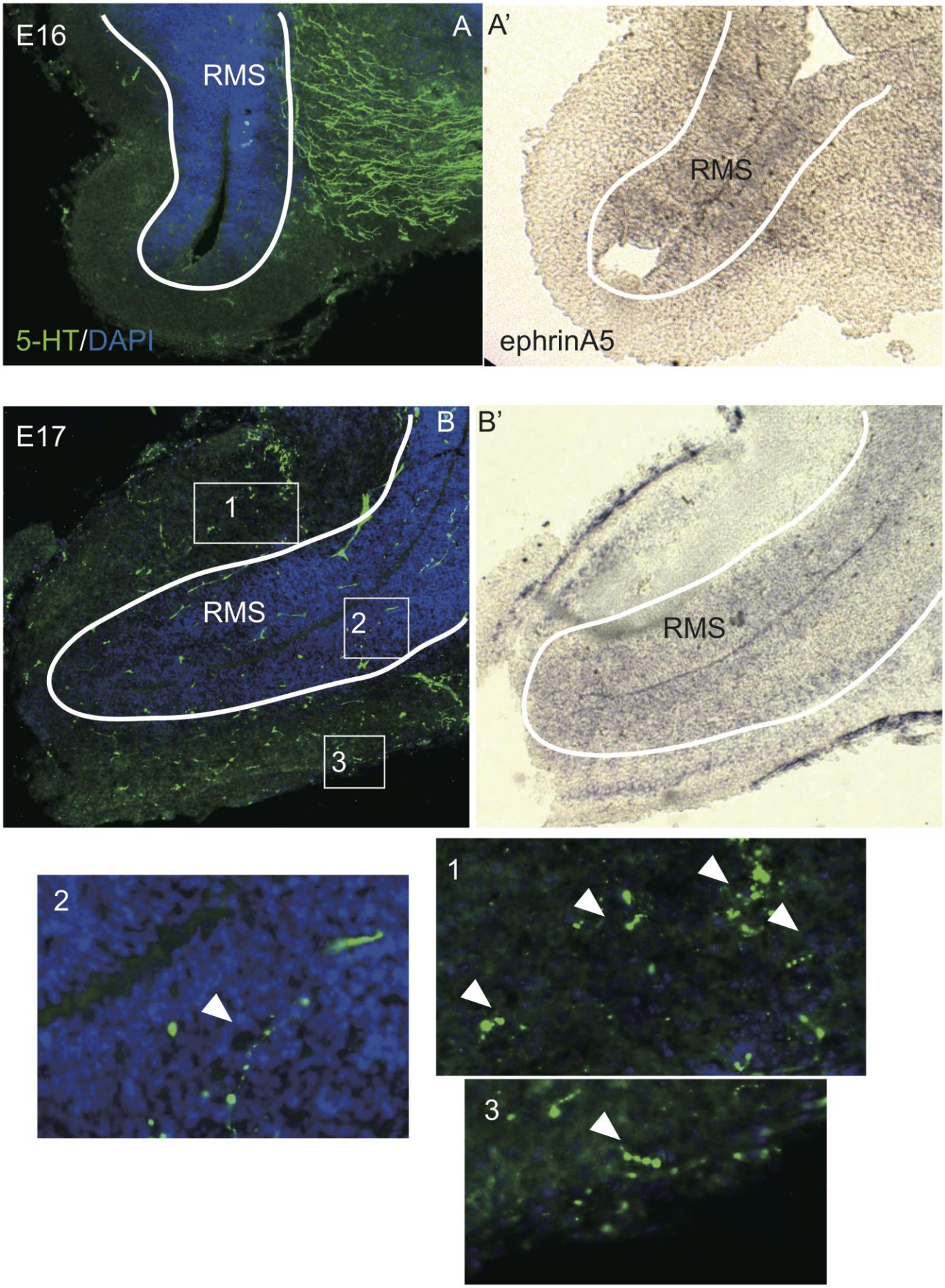
E16
A
RMS
5-HT/DAPI
A'
RMS
ephrinA5
E17
B
1
RMS
2
3
B'
RMS
2
1
3

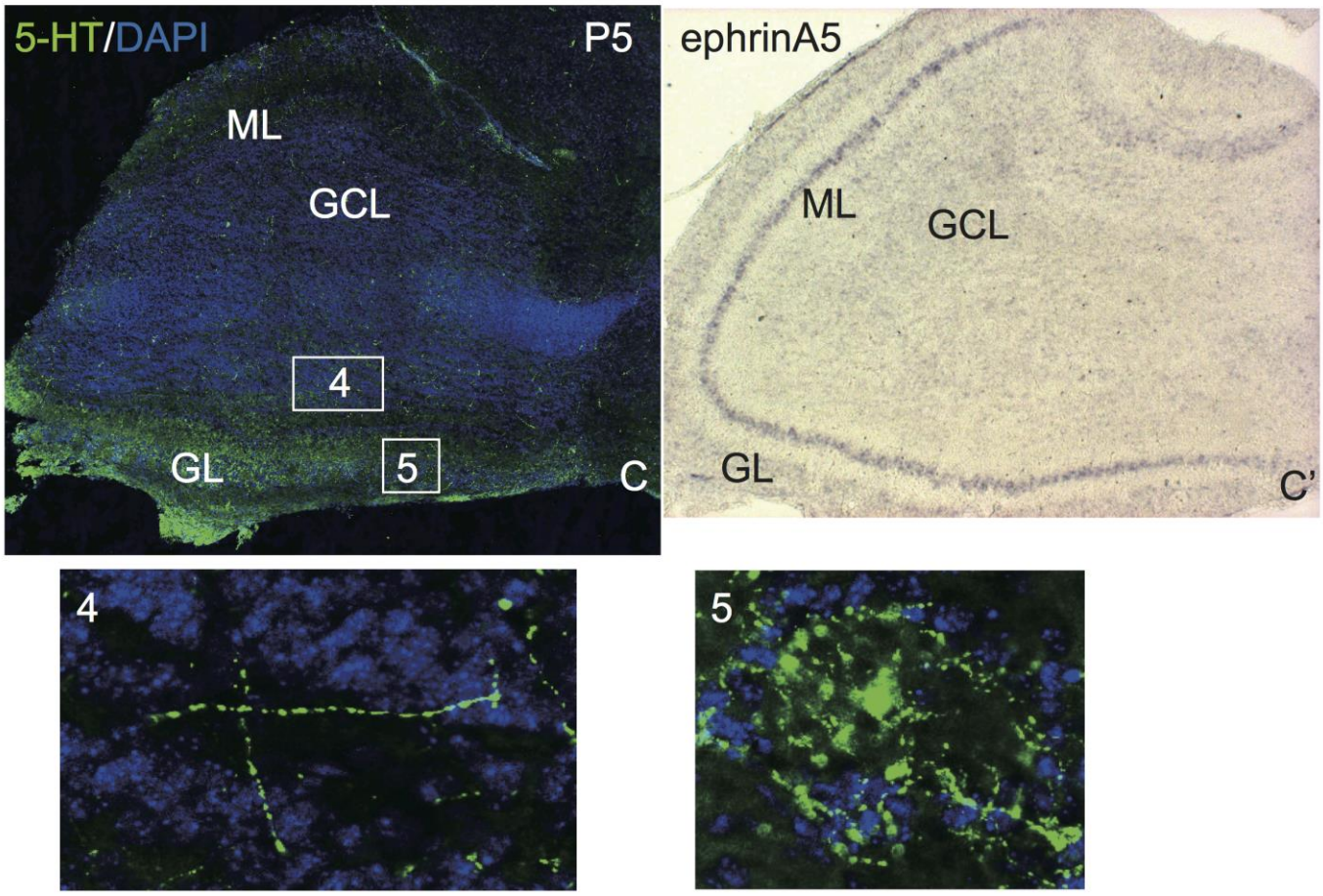

Figure 5. Development of the serotonergic innervation in OB.

A-A', E16 OB sagittal sections showed the 5-HT axons were repelled by RMS, ephrinA5 expressed within the RMS.

B-B', E17 OB sagittal sections showed the 5-HT axons start to enter the OB.

C-C', P5 OB sagittal sections showed the distribution of 5-HT axons in OB different layers and the change of ephrinA5 expression pattern

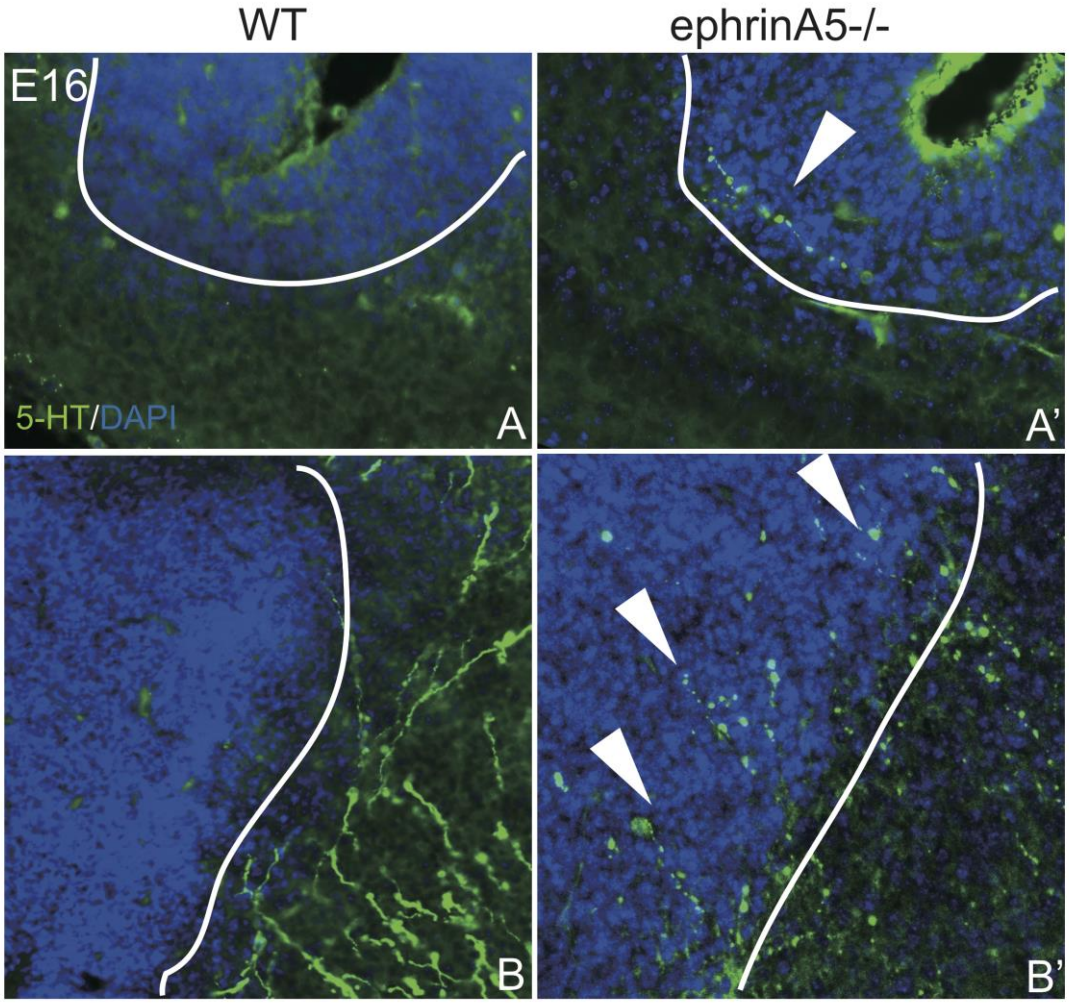

Figure 6. Lacking of ephrinA5 altered serotonergic innervation in OB and RMS

A-A', 5-HT axons were detected in OB of ephrinA5-/- in contrast to WT.

B-B', 5-HT axons were crossing the RMS in ephrinA5-/- in contrast to WT.

Discussion

Discussion

A large body of literature has indicated that serotonin plays a key role in the control of mood, fear, appetite, sleep, pain, vascular function, reproduction, feeding and aggressiveness. (Jacobs, 1992; Lucki, 1998; Fernandez & Gaspar. 2012) It has also been suggested that alterations of serotonin metabolism or of serotonergic projections, either during development or in adulthood, can lead to pathologies, such as depression, anxiety, autism, schizophrenia, sudden infant death syndrome and obsessive compulsive. (Gross and Han 2004;Scott and Deneris, 2005; Murphy, 2008; enoch, 2010; Takahashi, 2011; Waider, 2011) Thus, serotonin systems are an important target of pharmacological agents developed to treat these disorders. Moreover, serotonergic neurons are topographically organized, with anatomically distinct groups of serotonergic neurons that give rise to specific efferent to forebrain and brainstem structures. The patterns of afferent and efferent projections of these nuclei is highly organized, suggesting that there is precision in both the control of neuronal activity of subpopulations of serotonergic neurons and their output to forebrain and brainstem circuits. (Lowry, 2002; Michelsen, 2007; Hale and Lowry, 2011; Muzrelle el al. 2016). Over all, it is of great importance to understand how serotonergic projections develop and what are the molecular mechanisms of the specific serotonergic pathfinding that results in their distinct topographic organization.

In the first part of my thesis, I analyzed which guidance molecules are implicated in the serotonin signaling pathways. A previous genomic screen study in a transgenic mouse line provided us a list of candidate genes (Wylie et al. 2010). After validation of expression patterns of several Eph genes in the P5 mouse raphe nuclei, the EphA5 gene was selected as a gene of interest. Indeed, this tyrosine kinase receptor of the ephrinA subfamily, and was validated selectively as co-expressed in subpopulations of serotonergic neurons, mainly in the dorsal raphe complex. In vitro and in vivo experiments indicated that the EphA5 expressing serotonergic axonal growth cones responded by a retraction to the application of different doses of ephrinA5-FC. Moreover, ectopic expression of the ephrinA3 gene inhibited the ingrowth of serotonin innervation into the basolateral amygdala. The analysis of

anterograde racing in the ephrinA5-/- mice demonstrated that deletion of ephrinA5 led to the mistargetting of dorsal raphe serotonin projections to several forebrain targets, for instance, the ventromedial hypothalamus, suprachiasmatic nucleus, the bed nucleus of stria terminals, the subventricular zone and the olfactory bulb.

In the second part of our studies, we wanted to map the development of serotonin projections from embryonic day 12 to 18 and we found that serotonin projections passing though the midbrain to the forebrain bilaterally are already visible at E12-E14 and have reached most of their midbrain and basal forebrain targets at E16. Interestingly, at E16, the banner serotonin fibers have arrived in the OB but are repelled by the RMS and move towards the frontal cortex, instead of entering the OB. At E18, the serotonin projections have arrived to most of their targets in the forebrain. Regarding the special phenotype in the RMS-OB region at E16, we focused on the development of serotoninergic OB projections. We found that ephrinA5 was strongly expressed throughout the RMS and that, as expression became reduced, 5-HT axons invaded the RMS. This suggested that ephrinA5 could be the factor that repels the serotonin projections from the RMS and that this helps directing the serotoninergic projection to the OB.

1. Other EphA receptors expression in serotonin raphe neurons

Our results showed a specific expression pattern of EphA5 in the developing raphe continuing over the period of axonal maturation. ISH and Q-PCR experiments showed that in the P5 dorsal raphe, only EphA5 was expressed, EphA4 and EphA6 were also detected. On the other hand, EphA3 and EphA7 were not detected in the dorsal raphe. Whereas all these three receptors were detected in the median raphe.

The genom-wide expression analysis of Wylie et al. pointed out a list of guidance molecules expressed in the serotonin raphe neurons, among which the EphA3, EphA4, EphA5 and EphA7 are listed. In a more recent study, Okaty et al. using mRNA sequencing identify a number of EphA receptors genes in P21 serotonin neurons: EphA3, EphA4, EphA5, EphA6, EphA7, EphA8 and EhpA10. However, the level of expression is often very low. Using ISH data from the Allen brain atlas, we can group them in different ways. 1. Depending on the time of expression, EphA3 is

the only Eph expressed during embryonic development; EphA4, EphA5 and EphA7 are expressed both during embryonic development and the maturation of serotonin projection the early postnatal development EphA6, EphA8 and EphA10 only become expressed in the mature postnatal serotonin neurons. 2. Depending on the location, EphA3 is only expressed in the caudal raphe nuclei; EphA5 is mainly expressed in the DR, as well as EphA4 and EphA6, whereas the rest of the receptors exhibit a high level of expression in the MnR.

In conclusion, these expression patterns could imply specific roles of these receptors in the serotonin axon development and the targeting maturation. For instance, the EphA6, EphA8 and EphA10 might play an important role not for the development of the projection but for adult synaptic functions.

Functional topographic mapping alteration of dorsal raphe neuronal projections induced by the interaction of EphA5 and its ligands

Our findings using anterograde tracing analyses of the ephrinA5-/- mice showed an increase of DR innervation in certain targets. Immunostaining of the serotonin transporter (SERT) showed that this increase includes the serotonin innervation arising from the DR. These results suggest that the alteration of serotonin innervation in the ephrinA5-/- mice may be responsible for some of the behavioral changes observed in these mice.

2.1 Ventromedial hypothalamus could be a key structure explaining the aggression in ephrinA5-/- mice

In our results, one of the areas where DR 5-HT innervation is increased is the ventromedial hypothalamic nucleus (VMH), in particular, the ventrolateral part of the VMH. Interestingly, this region is a key structure in the control of inter male aggressive behavior. Furthermore, the possible molecular mechanism involved in this behavior, involve the serotonin transporter and the serotonin receptors. We thus hypothesize that increased DR innervation of the VMH of EphrinA5-/- mice could underlie a change in the aggressive behaviors of these mice.

The main evidence, which suggests this is provided by a study of inter-male mouse aggression in the ephrinA5-/- mouse line (Michal Sheleg et al., 2015). In their studies, the authors performed a series of behavioral test in male ephrinA5-/- mice and found that offensive aggression was severely reduced. This reduction of offensive aggression was not due to an inability to attack or to a lack of recognition of the presence of the intruder, since the ephrin-A5−/−mice exhibited increased target biting and testosterone levels and general olfaction were normal. A previous study of the same team demonstrated converging evidence showing that lack of EphA5 also leads to a decrease in male aggressive behavior in mice. (Pingchao et al., 2008) Overall, these 2 studies suggest that the EphA5 and ephrinA5 interaction plays a key role in regulating male mouse aggression.

Multiple previous studies showed aggressive behaviors are controlled by different regions of the mouse brain: the hypothalamus, the medial amygdala (MEA), the lateral septum (LAS), the periaqueductal gray (PAG) and the bed nucleus of the stria terminal (BNST), (Numan M.2014; Nelson RJ, 2007; Siegel A, 1999). All these regions are densely innervated by serotonin from different subpopulations of raphe serotonin neurons. (Hale and Lowry, 2011; Muzrelle and Scotto, 2016) Interestingly, our findings in the ephrinA5-/- mice show that DR innervation is increased in both the hypothalamus and the bed nucleus of the stria terminals. This increase involves both serotonin and non-serotonergic neurons. Within these targets, serotonergic ascending innervation arising from the DR was strongly increased in the ventomedial hypothalamic nucleus ventrolateral part (VL-VMH). Recent studies indicated that the VL-VMH region corresponds to the hypothalamic attack area (HAA) of the rat (Lin D, 2011), from which electrical and pharmacological stimulation elicited attacks and lesions reduced it.

2.1.1 How could increased serotonin innervation modulate male aggressive behavior?

Serotonin is considered as the most important neurotransmitter implicated in the neural control of aggressive behavior. It is generally thought to act as an inhibitor of aggression (Miczek et al., 1995; Carrillo, Ricci, Coppersmith, & Melloni, 2009). Numerous pharmacological and neurochemical investigations have provided evidence that the brain serotonin system is involved in controlling various types of aggressive

behaviors (Vishnivetskaya 2001; Popova 2004; Popova 1999) and clinical data have linked impulsivity, aggression, and self-harm attempts, regarded as self-directed aggression (J. Peddeer 1992), with reduced brain serotonin system activity (V. M. Linnoila and M. Virkkunen 1992; V. Arango 2003). Recently, the understanding of the mechanisms underlying the genetic regulation of aggressive behavior has attracted the view of researchers. In particular, the link between serotonin activity and aggression found strong support from mouse genetics, in mutations of specific genes that either directly or indirectly affect serotonin function. In humans and non human primates, impulsivity and high aggressiveness were correlated with low cerebrospinal fluid concentrations of HIAA, a 5-HT metabolite (Lesch, K.P. and Merschdorf, U. 2000). Pharmacological strategies increasing 5-HT levels, such as the use of 5-HT precursors, 5-HT reuptake inhibitors, or 5-HT1A and 5-HT1B receptor agonists are all able to reduce aggressive behavior in rodents (Olivier, B. et al. 1999; Miczek, K.A. et al. 1998; Fish, E.W. et al. 1999; Lyons, W.E. et al. 1999; Chiavegatto, S. et al. 2001)

2.1.2 The 5-HT1A/1B receptors are possible targets to study the mechanism of the aggression alteration in ephrinA5-/- mice

Previous studies indicated that the 5-HT1A receptor activation, with 5-HT1A agonist (eltoprazine and other agonists), decreases aggressive behavior (Olivier, B. et al. 1995; Miczek, K.A. et al. 1998). Interestingly, a finding consistent with the observation of increased postsynaptic 5-HT1A receptor availability in limbic and cortical regions of highly aggressive mice (Korte, S.M. et al. 1996). However 5-HT1A KO mice did not show modifications of aggressive behavior. Conversely, male mice that lack functional expression of the 5-HT1B receptor gene (5-HT1B−/−) are more aggressive than wild-type controls (Saudou, F. et al. 1994). Lactating female 5-HT1B−/− mice also attack unfamiliar male mice more rapidly and violently (Ramboz, S. et al.1996). Although both 5-HT1A and 5-HT1B receptors control the 5-HT tone, these two receptors probably have different contributions in particular brain areas that modulate the postsynaptic 5-HT inhibitory effects on aggression. Indeed, aggression evoked by electrical stimulation of the hypothalamus of rat is not affected by 5-HT1A agonist but reduced in a dose dependent manner by a treatment with 5-HT1B receptor agonist (Olivier B, 2005).

All these previous studies support the hypothesis that a reduction of inter-male aggression in the ephrinA5-/- mice may be caused by an increased in dorsal raphe innervation to the ventromedial hypothalamic nucleus.

2.2 Possible alteration of circadian rhythms in ephrinA5-/- mice induced by the role of EphA5-ephrinA5 interaction in serotonergic projections to the SCN

Another key target that could be interesting to investigate further is the SCN. Our findings showed a dense innervation from DR serotonin neurons in the SCN of the ephrinA5-/- mice in contract to wild type SCN. Although there is no related behavioral test performed in ephrinA5-/- mouse model as yet, such a strong increase of serotonergic innervation could increase the serotonin release in the SCN in ephrinA5-/- mice, which could in turn result in alterations of circadian rhythms.

The suprachiasmatic nucleus (SCN), is a main regulator of the circadian clock, it receives its major afferents from the median raphe nucleus (MRN) but not DR (Muzrelle et al. 2016). Serotonergic projections to the SCN are thought to be involved in non-photic phase shifting. Multiple previous studies indicated that increased 5-HT release in the SCN can influence circadian rhythms. For instance, the exposure to non-photic stimuli such as midday access to a novel running wheel, sleep deprivation or dark pulses all phase advance circadian rhythms of wheel running and elicit a large increase of 5-HT release in the SCN (Dudley et al., 1998; Grossman et al., 2000; Mendoza et al., 2008). Electrical stimulation of the MRN or DRN at midday induces 5-HT release at the SCN and results in phase advances of circadian locomotor rhythms (Meyer- Bernstein & Morin, 1999; Glass et al., 2000, 2003). Midday application of 5-HT or the 5-HT1A agonist 8-OH-DPAT to rat or mouse SCN slices results in phase advances of electrical firing (Prosser et al., 1990, 1993; Medanic & Gillette, 1992; Shibata et al., 1992; Prosser, 2003). Application of 8-OH-DPAT to the SCN in vivo in animals made supersensitive to 5-HT by constant light (Knoch et al., 2004) or by pretreatment with the 5-HT biosynthesis inhibitor p-CPA (Ehlen et al., 2001) elicits larger phase shifts than vehicle alone.

3. Independent or associate? The role of non-serotonergic dorsal raphe neurons in ephrinA5-/-

3.1 Dopaminergic raphe neurons

Dopaminergic neurons have an extension in the DR, essentially in the caudal linear nucleus (Hale and Lowry 2011). Interestingly, the dopaminergic raphe neurons project also to the BNST. In our study of Ephrin A5-/- mice, we detected an increase of DR fibers that included both serotonergic and non serotoninergic axons that may comprise dopaminergic axons. The BNST is a structure that is also involved in the aggressive circuit, which could suggest that dopaminergic raphe neurons projections also modulated the aggression in the ephrinA5-/-.

Dopamine's role in aggressive behavior is not yet precisely known. Growing evidence suggests the dopamine plays a role in aggressive behavior through the D1 and D2 receptors. One well-known example of such an inhibitory capacity is the D2 receptor antagonist risperidone, which is commonly used to reduce aggressive behavior associated with arousal and stress (Nelson & Trainor, 2007). Thus, it seems that dopamine modulates aggressive behavior but independently from serotonin.

3.2 GABAergic raphe neurons

GABAergic neurons are mainly located bilaterally to the dorsal raphe serotonin neurons, particularly, in the lateral wing. (Brandon, 2014) Our findings showed that, EphA5 is highly expressed in the LW where is overlaps with the location of GABAergic neurons, which means, GABAergic raphe neurons could also have a high rate of EphA5 co-expression. This could lead to more connectivity from GABAergic raphe neurons to the serotonergic raphe neurons in the ephrinA5-/- mice. GABA is well known as the main inhibitory neurotransmitter in the mammalian brain. Moreover GABA's involvement in aggressive behavior is mostly associated with its inhibitory action, Takahashi et al. (2010a) showed that pharmacological activation of GABAB receptors in the DRN plays an important role in the escalation of aggressive behavior. This is most likely related to the inhibition of presynaptic 5-HT1A autoreceptor on the serotonin raphe neurons, which could increase serotonin release.

GABA is well known to regulate serotonin levels because of high receptor expression in the DRN (Takahashi et al., 2010a, 2010b). Both GABAA and GABAB receptors are involved in the regulation of serotonin levels. The activation of GABAergic receptors on serotonergic neurons can lead to higher serotonin levels in the mPFC and, therefore, can decrease aggression. Notably, however, GABA receptors in the medial raphe nuclei (MRN) have no escalating effect on aggressive behavior, showing that serotonin neurons in the MRN and DRN play differential roles in aggressive behavior. (Mokler, 2009) Our finding suggesting the possibility in the increased GABA dorsal raphe projections in the ephrinA5-/- mice

Based on the available literature, GABA and serotonin thus appear to show a team work to regulate aggressive behaviors. This can suggest another way to figure out the decreased aggressive alteration in the ephrinA5-/- mice.

3.3 Glutamatergic raphe neurons

Glutamatergic neurons are densely distributed in the DR and median raphe, and previous observation showed that a majority of central 5-HT neurons express the vesicular glutamate transporter VGLUT3 (Fremeau et al., 2002; Gras et al., 2002; Scha¨fer et al., 2002; Takamori et al., 2002). VGLUT3 clearly fulfils the function of a vesicular glutamatergic transporter; its expression confers to neurons the ability to release glutamate. In addition to this expected function, VGLUT3 enhances striatal cholinergic neurotransmission at the presynaptic level (Gras et al., 2008) So far, whether glutamate plays a role in aggressive behavior, by itself or its transporters, is still unclear. Interestingly, a recent study of Amilhon et al. in 2010 indicated that 1. VGLUT3 deletion caused a significant decrease of 5-HT1A-mediated neurotransmission in the raphe nuclei; 2. VGLUT3 positively modulated 5-HT transmission of a specific subset of 5-HT terminals from the hippocampus and the cerebral cortex. These results unravel the existence of a novel subset of 5-HT terminals in limbic areas that might play a crucial role in anxiety-like behaviors. Moreover, 5-HT axon varicosities that contain the VGLUT3 were larger, in congruence with the previously reported data that larger 5-HT axon varicosities establish more synapses raising the hypothesis of higher synaptic incidence for 5-HT varicosities that contain the VGLUT3 (Smiley JF, 1996). These results suggest that glutamate may play a role in aggressive alteration, via VGLUT3, to regulate the 5-HT

tone or axonal synapses in projection areas or to decrease 5-HT1A autoreceptors-mediated transmission in the raphe. It seems the role of glutamatergic raphe neurons in the alteration of aggression may be associated with serotonin and non-serotonin raphe neurons.

4. Changes of ephrinA5 expression pattern modulate the development of serotonergic projections from raphe to olfactory bulb

In our results, we demonstrated that, during embryonic development of serotonergic projections, the ascending serotonergic fiber fascicles were repelled by the RMS and that this may be due to the expression of ephrinA5. The area occupied by the RMS changes during development, which could lead to a change of ephrinA5 expression patterns, and consequently lead the serotonergic fibers started to innervate distinct layer of OB.

We ask here 2 questions raised by these observations.

1. Why does the RMS show a change in the expression of ephrinA5 during development?

Neurogenesis occurs in the mouse subventricular zone (SVZ) throughout life and is a source of new interneurons for the olfactory bulb (OB) (Doetsch et al., 1997; Lledo and Saghatelyan, 2005; Lledo et al., 2008; Whitman and Greer, 2009). The pathway in which neuroblasts migrate tangentially to the OB is called the rostral migratory stream (RMS). (Loisand Alvarez-Buylla, 1994; Whitman et al., 2009)

In rat, the first cells of the RMS start to differentiate at about E14 in the LGE (equivalent to E11 in mouse), the initial differentiation of the RMS precedes the bulging of the OB at the anterior tip of the cerebral hemispheres. In addition, the emergence of the RMS occurs in advance of the formation of the olfactory ventricles, as an extension of the lateral ventricle into the OB. Furthermore, at E15-E17 as the OB and ventricle begin to form, the developing RMS lies laterally to the olfactory ventricle. E18 is the stage of the initial formation of the RMS, which means that neuroblasts start their migration from the SVZ to the OB. (Pencea, 2003) Neuroblasts from the SVZ migrate radially to the OB granule (GCL) and to the glomerular layers

(GL); they then differentiate, and become integrated into synaptic circuits (Carleton et al., 2003; Kelsch et al., 2010; Whitman and Greer, 2007b). Most of the surviving neurons differentiate into granule cells, although approximately 5% become periglomerular (PG) cells (Lemasson et al., 2005).

From the developing of RMS we can surmise that the RMS occupies the whole OB region, before the formation of the OB layers. Which means that from E11 to E16, in mouse, the OB is filled with RMS cell which express ephrinA5. As the differentiation proceeds, granule cells that do not express ephrinA5, begin replacing the RMS cells and thus reduce the zone of ephrinA5 expression.

2. What is the signaling mechanism that guide serotonin fibers into the different components? Indeed, EphrinA5 seems to modulate serotonergic projections to distinct layers but the mechanism is unclear.

Tracing studies showed that the serotonergic projections from the DR specifically target the granule cell layer of the OB whereas the median raphe serotonergic projections target the glomerular layer of the OB. Combined with our findings of the specific signaling pathway via EphA5-ephrinA5 interaction, we hypothesize that, during development, DR serotonergic fibers arrive to the OB earlier than median raphe and that they are initially repelled by ephrinA5 expression in the RMS, at E17; then as ephrinA5 regional expression is reduced, DR axons start to innervate the GCL of the OB avoiding the RMS, whereas the just arrived median raphe fibers enter the OB directly along the basal tract into the forming GL. The initial evidence for this hypothesis is our finding in the ephrinA5-/- mice that the front most serotonergic fibers enter the OB at E16 and do not seem repelled by the RMS.

Bibliography

Reference

Abrams JK, Johnson PL, Hay-Schmidt A, Mikkelsen JD, Shekhar A, Lowry CA (2005) Serotonergic systems associated with arousal and vigilance behaviors following administration of anxiogenic drugs. Neuroscience 133:983-997.

Acsady L, Halasy K, Freund TF (1993) Calretinin is present in non-pyramidal cells of the rat hippocampus--III. Their inputs from the median raphe and medial septal nuclei. Neuroscience 52:829-841.

Alonso A, Merchan P, Sandoval JE, Sanchez-Arrones L, Garcia-Cazorla A, Artuch R, Ferran JL, Martinez-de-la-Torre M, Puelles L (2013) Development of the serotonergic cells in murine raphe nuclei and their relations with rhombomeric domains. Brain structure & function 218:1229-1277.

Amin AH, Crawford TB, Gaddum JH (1954) The distribution of substance P and 5-hydroxytryptamine in the central nervous system of the dog. The Journal of physiology 126:596-618.

Anden NE (1965) Distribution of monoamines and dihydroxyphenylalanine decarboxylase activity in the spinal cord. Acta physiologica Scandinavica 64:197-203.

Arvidsson U, Ulfhake B, Cullheim S, Bergstrand A, Theodorson E, Hokfelt T (1991) Distribution of 125I-galanin binding sites, immunoreactive galanin, and its coexistence with 5-hydroxytryptamine in the cat spinal cord: biochemical, histochemical, and experimental studies at the light and electron microscopic level. The Journal of comparative neurology 308:115-138.

Arvidsson U, Cullheim S, Ulfhake B, Luppi PH, Kitahama K, Jouvet M, Hokfelt T (1994) Quantitative and qualitative aspects on the distribution of 5-HT and its coexistence with substance P and TRH in cat ventral medullary neurons. Journal of chemical neuroanatomy 7:3-12.

Azmitia EC (1999) Serotonin neurons, neuroplasticity, and homeostasis of neural tissue. Neuropsychopharmacology : official publication of the American College of Neuropsychopharmacology 21:33s-45s.

Azmitia EC, Segal M (1978) An autoradiographic analysis of the differential ascending projections of the dorsal and median raphe nuclei in the rat. The Journal of comparative neurology 179:641-667.

Azmitia EC, Gannon PJ (1986) The primate serotonergic system: a review of human and animal studies and a report on Macaca fascicularis. Advances in neurology 43:407-468.

Baker KG, Halliday GM, Halasz P, Hornung JP, Geffen LB, Cotton RG, Tork I (1991) Cytoarchitecture of serotonin-synthesizing neurons in the pontine tegmentum of the human brain. Synapse (New York, NY) 7:301-320.

Bang SJ, Jensen P, Dymecki SM, Commons KG (2012) Projections and interconnections of genetically defined serotonin neurons in mice. The European journal of neuroscience 35:85-96.

Baraban JM, Aghajanian GK (1981) Noradrenergic innervation of serotonergic neurons in the dorsal raphe: demonstration by electron microscopic autoradiography. Brain research 204:1-11.

Barkus C, Line SJ, Huber A, Capitao L, Lima J, Jennings K, Lowry J, Sharp T, Bannerman DM, McHugh SB (2014) Variation in serotonin transporter expression modulates fear-evoked hemodynamic responses and theta-frequency neuronal oscillations in the amygdala. Biological psychiatry 75:901-908.

Bashaw GJ, Klein R (2010) Signaling from axon guidance receptors. Cold Spring Harbor perspectives in biology 2:a001941.

Beg AA, Sommer JE, Martin JH, Scheiffele P (2007) alpha2-Chimaerin is an essential EphA4 effector in the assembly of neuronal locomotor circuits. Neuron 55:768-778.

Behzadi G, Kalen P, Parvopassu F, Wiklund L (1990) Afferents to the median raphe nucleus of the rat: retrograde cholera toxin and wheat germ conjugated horseradish peroxidase tracing, and selective D-[3H]aspartate labelling of possible excitatory amino acid inputs. Neuroscience 37:77-100.

Belin MF, Aguera M, Tappaz M, McRae-Degueurce A, Bobillier P, Pujol JF (1979) GABA-accumulating neurons in the nucleus raphe dorsalis and periaqueductal gray in the rat: a biochemical and radioautographic study. Brain research 170:279-297.

Bobillier P, Seguin S, Petitjean F, Salvert D, Touret M, Jouvet M (1976) The raphe nuclei of the cat brain stem: a topographical atlas of their efferent projections as revealed by autoradiography. Brain research 113:449-486.
Bocchio M, McHugh SB, Bannerman DM, Sharp T, Capogna M (2016) Serotonin, Amygdala and Fear: Assembling the Puzzle. Frontiers in neural circuits 10:24.
Bocchio M, Fucsina G, Oikonomidis L, McHugh SB, Bannerman DM, Sharp T, Capogna M (2015) Increased Serotonin Transporter Expression Reduces Fear and Recruitment of Parvalbumin Interneurons of the Amygdala. Neuropsychopharmacology : official publication of the American College of Neuropsychopharmacology 40:3015-3026.
Bonanomi D, Chivatakarn O, Bai G, Abdesselem H, Lettieri K, Marquardt T, Pierchala BA, Pfaff SL (2012) Ret is a multifunctional coreceptor that integrates diffusible- and contact-axon guidance signals. Cell 148:568-582.
Boularand S, Darmon MC, Ganem Y, Launay JM, Mallet J (1990) Complete coding sequence of human tryptophan hydroxylase. Nucleic acids research 18:4257.
Bouvier D, Corera AT, Tremblay ME, Riad M, Chagnon M, Murai KK, Pasquale EB, Fon EA, Doucet G (2008) Pre-synaptic and post-synaptic localization of EphA4 and EphB2 in adult mouse forebrain. Journal of neurochemistry 106:682-695.
Boyd AW, Lackmann M (2001) Signals from Eph and ephrin proteins: a developmental tool kit. Science's STKE : signal transduction knowledge environment 2001:re20.
Braak H (1970) [On the nuclei of the human brain stem. II. The raphe nuclei]. Zeitschrift fur Zellforschung und mikroskopische Anatomie (Vienna, Austria : 1948) 107:123-141.
Brambilla R, Klein R (1995) Telling axons where to grow: a role for Eph receptor tyrosine kinases in guidance. Molecular and cellular neurosciences 6:487-495.
Brose K, Bland KS, Wang KH, Arnott D, Henzel W, Goodman CS, Tessier-Lavigne M, Kidd T (1999) Slit proteins bind Robo receptors and have an evolutionarily conserved role in repulsive axon guidance. Cell 96:795-806.
Brown P, Molliver ME (2000) Dual serotonin (5-HT) projections to the nucleus accumbens core and shell: relation of the 5-HT transporter to amphetamine-induced neurotoxicity. The Journal of neuroscience : the official journal of the Society for Neuroscience 20:1952-1963.
Bruckner K, Pasquale EB, Klein R (1997) Tyrosine phosphorylation of transmembrane ligands for Eph receptors. Science (New York, NY) 275:1640-1643.
Brust RD, Corcoran AE, Richerson GB, Nattie E, Dymecki SM (2014) Functional and developmental identification of a molecular subtype of brain serotonergic neuron specialized to regulate breathing dynamics. Cell reports 9:2152-2165.
Bush JO, Soriano P (2012) Eph/ephrin signaling: genetic, phosphoproteomic, and transcriptomic approaches. Seminars in cell & developmental biology 23:26-34.
Caceres A, Banker GA, Binder L (1986) Immunocytochemical localization of tubulin and microtubule-associated protein 2 during the development of hippocampal neurons in culture. The Journal of neuroscience : the official journal of the Society for Neuroscience 6:714-722.
Calas A, Alonso G, Arnauld E, Vincent JD (1974) Demonstration of indolaminergic fibres in the media eminence of the duck, rat and monkey. Nature 250:241-243.
Calizo LH, Akanwa A, Ma X, Pan YZ, Lemos JC, Craige C, Heemstra LA, Beck SG (2011) Raphe serotonin neurons are not homogenous: electrophysiological, morphological and neurochemical evidence. Neuropharmacology 61:524-543.
Carvalho RF, Beutler M, Marler KJ, Knoll B, Becker-Barroso E, Heintzmann R, Ng T, Drescher U (2006) Silencing of EphA3 through a cis interaction with ephrinA5. Nature neuroscience 9:322-330.
Chan-Palay V (1981) Evidence for the coexistence of serotonin and substance P in single raphe cells and fiber plexuses: combined immunocytochemistry and autoradiography. Advances in experimental medicine and biology 133:81-97.
Chen HY, Lin YP, Lee EH (1992) Cholinergic and GABAergic mediations of the effects of apomorphine on serotonin neurons. Synapse (New York, NY) 10:34-43.
Clark MS, McDevitt RA, Neumaier JF (2006) Quantitative mapping of tryptophan hydroxylase-2, 5-HT1A, 5-HT1B, and serotonin transporter expression across the anteroposterior axis of the rat dorsal and median raphe nuclei. The Journal of comparative neurology 498:611-623.
Clark MS, McDevitt RA, Hoplight BJ, Neumaier JF (2007) Chronic low dose ovine corticotropin releasing factor or urocortin II into the rostral dorsal raphe alters exploratory behavior

and serotonergic gene expression in specific subregions of the dorsal raphe. Neuroscience 146:1888-1905.
Commons KG (2016) Ascending serotonin neuron diversity under two umbrellas. Brain structure & function.
Cordes SP (2005) Molecular genetics of the early development of hindbrain serotonergic neurons. Clinical genetics 68:487-494.
Correale P (1956) The occurrence and distribution of 5-hydroxytryptamine (enteramine) in the central nervous system of vertebrates. Journal of neurochemistry 1:22-31.
Cropper EC, Eisenman JS, Azmitia EC (1984) 5-HT-Immunoreactive fibers in the trigeminal nuclear complex of the rat. Experimental brain research 55:515-522.
Dahlstroem A, Fuxe K (1964) EVIDENCE FOR THE EXISTENCE OF MONOAMINE-CONTAINING NEURONS IN THE CENTRAL NERVOUS SYSTEM. I. DEMONSTRATION OF MONOAMINES IN THE CELL BODIES OF BRAIN STEM NEURONS. Acta physiologica Scandinavica Supplementum:Suppl 232:231-255.
Darmon MC, Guibert B, Leviel V, Ehret M, Maitre M, Mallet J (1988) Sequence of two mRNAs encoding active rat tryptophan hydroxylase. Journal of neurochemistry 51:312-316.
Day HE, Greenwood BN, Hammack SE, Watkins LR, Fleshner M, Maier SF, Campeau S (2004) Differential expression of 5HT-1A, alpha 1b adrenergic, CRF-R1, and CRF-R2 receptor mRNA in serotonergic, gamma-aminobutyric acidergic, and catecholaminergic cells of the rat dorsal raphe nucleus. The Journal of comparative neurology 474:364-378.
Deneris ES, Wyler SC (2012) Serotonergic transcriptional networks and potential importance to mental health. Nature neuroscience 15:519-527.
Descarries L, Watkins KC, Garcia S, Beaudet A (1982) The serotonin neurons in nucleus raphe dorsalis of adult rat: a light and electron microscope radioautographic study. The Journal of comparative neurology 207:239-254.
Descarries L, Berthelet F, Garcia S, Beaudet A (1986) Dopaminergic projection from nucleus raphe dorsalis to neostriatum in the rat. The Journal of comparative neurology 249:511-520, 484-515.
Deschamps C, Faideau M, Jaber M, Gaillard A, Prestoz L (2009) Expression of ephrinA5 during development and potential involvement in the guidance of the mesostriatal pathway. Experimental neurology 219:466-480.
Deschamps C, Morel M, Janet T, Page G, Jaber M, Gaillard A, Prestoz L (2010) EphrinA5 protein distribution in the developing mouse brain. BMC neuroscience 11:105.
DeVito JL, Anderson ME, Walsh KE (1980) A horseradish peroxidase study of afferent connections of the globus pallidus in Macaca mulatta. Experimental brain research 38:65-73.
Dickson BJ (2002) Molecular mechanisms of axon guidance. Science (New York, NY) 298:1959-1964.
Dinopoulos A, Dori I (1995) The development of the serotonergic fiber network of the lateral ventricles of the rat brain: a light and electron microscopic immunocytochemical analysis. Experimental neurology 133:73-84.
Dodelet VC, Pasquale EB (2000) Eph receptors and ephrin ligands: embryogenesis to tumorigenesis. Oncogene 19:5614-5619.
Doeppner TR, Bretschneider E, Doehring M, Segura I, Senturk A, Acker-Palmer A, Hasan MR, ElAli A, Hermann DM, Bahr M (2011) Enhancement of endogenous neurogenesis in ephrin-B3 deficient mice after transient focal cerebral ischemia. Acta neuropathologica 122:429-442.
Dong XW, Shen E (1986) Origin of monoaminergic innervation of the nucleus raphe magnus--a combined monoamine histochemistry and fluorescent retrograde tracing study in the rat. Scientia Sinica Series B, Chemical, biological, agricultural, medical & earth sciences / Chung-kuo k'o hsueh yuan, chu pan 29:599-608.
Dotti CG, Banker GA (1987) Experimentally induced alteration in the polarity of developing neurons. Nature 330:254-256.
Dugue GP, Mainen ZF (2009) How serotonin gates olfactory information flow. Nature neuroscience 12:673-675.
Egea J, Klein R (2007) Bidirectional Eph-ephrin signaling during axon guidance. Trends in cell biology 17:230-238.
Erspamer V, Asero B (1952) Identification of enteramine, the specific hormone of the enterochromaffin cell system, as 5-hydroxytryptamine. Nature 169:800-801.

Eswarakumar VP, Lax I, Schlessinger J (2005) Cellular signaling by fibroblast growth factor receptors. Cytokine & growth factor reviews 16:139-149.
Fawcett JP, Georgiou J, Ruston J, Bladt F, Sherman A, Warner N, Saab BJ, Scott R, Roder JC, Pawson T (2007) Nck adaptor proteins control the organization of neuronal circuits important for walking. Proceedings of the National Academy of Sciences of the United States of America 104:20973-20978.
Feldheim DA, Kim YI, Bergemann AD, Frisen J, Barbacid M, Flanagan JG (2000) Genetic analysis of ephrin-A2 and ephrin-A5 shows their requirement in multiple aspects of retinocollicular mapping. Neuron 25:563-574.
Feldheim DA, Vanderhaeghen P, Hansen MJ, Frisen J, Lu Q, Barbacid M, Flanagan JG (1998) Topographic guidance labels in a sensory projection to the forebrain. Neuron 21:1303-1313.
Felten DL, Cummings JP (1979) The raphe nuclei of the rabbit brain stem. The Journal of comparative neurology 187:199-243.
Fenstermaker AG, Prasad AA, Bechara A, Adolfs Y, Tissir F, Goffinet A, Zou Y, Pasterkamp RJ (2010) Wnt/planar cell polarity signaling controls the anterior-posterior organization of monoaminergic axons in the brainstem. The Journal of neuroscience : the official journal of the Society for Neuroscience 30:16053-16064.
Fernandez SP, Gaspar P (2012) Investigating anxiety and depressive-like phenotypes in genetic mouse models of serotonin depletion. Neuropharmacology 62:144-154.
Ferre S, Cortes R, Artigas F (1994) Dopaminergic regulation of the serotonergic raphe-striatal pathway: microdialysis studies in freely moving rats. The Journal of neuroscience : the official journal of the Society for Neuroscience 14:4839-4846.
Filosa A, Paixao S, Honsek SD, Carmona MA, Becker L, Feddersen B, Gaitanos L, Rudhard Y, Schoepfer R, Klopstock T, Kullander K, Rose CR, Pasquale EB, Klein R (2009) Neuron-glia communication via EphA4/ephrin-A3 modulates LTP through glial glutamate transport. Nature neuroscience 12:1285-1292.
Fitzpatrick PF (1999) Tetrahydropterin-dependent amino acid hydroxylases. Annual review of biochemistry 68:355-381.
Flanagan JG (2006) Neural map specification by gradients. Current opinion in neurobiology 16:59-66.
Forloni G, Grzanna R, Blakely RD, Coyle JT (1987) Co-localization of N-acetyl-aspartyl-glutamate in central cholinergic, noradrenergic, and serotonergic neurons. Synapse (New York, NY) 1:455-460.
Fremeau RT, Jr., Burman J, Qureshi T, Tran CH, Proctor J, Johnson J, Zhang H, Sulzer D, Copenhagen DR, Storm-Mathisen J, Reimer RJ, Chaudhry FA, Edwards RH (2002) The identification of vesicular glutamate transporter 3 suggests novel modes of signaling by glutamate. Proceedings of the National Academy of Sciences of the United States of America 99:14488-14493.
Frisen J, Yates PA, McLaughlin T, Friedman GC, O'Leary DD, Barbacid M (1998) Ephrin-A5 (AL-1/RAGS) is essential for proper retinal axon guidance and topographic mapping in the mammalian visual system. Neuron 20:235-243.
Fu W, Le Maitre E, Fabre V, Bernard JF, David Xu ZQ, Hokfelt T (2010) Chemical neuroanatomy of the dorsal raphe nucleus and adjacent structures of the mouse brain. The Journal of comparative neurology 518:3464-3494.
Gale NW, Holland SJ, Valenzuela DM, Flenniken A, Pan L, Ryan TE, Henkemeyer M, Strebhardt K, Hirai H, Wilkinson DG, Pawson T, Davis S, Yancopoulos GD (1996) Eph receptors and ligands comprise two major specificity subclasses and are reciprocally compartmentalized during embryogenesis. Neuron 17:9-19.
Gao WQ, Shinsky N, Armanini MP, Moran P, Zheng JL, Mendoza-Ramirez JL, Phillips HS, Winslow JW, Caras IW (1998) Regulation of hippocampal synaptic plasticity by the tyrosine kinase receptor, REK7/EphA5, and its ligand, AL-1/Ephrin-A5. Molecular and cellular neurosciences 11:247-259.
Gaspar P, Lillesaar C (2012) Probing the diversity of serotonin neurons. Philosophical transactions of the Royal Society of London Series B, Biological sciences 367:2382-2394.
Gauthier LR, Robbins SM (2003) Ephrin signaling: One raft to rule them all? One raft to sort them? One raft to spread their call and in signaling bind them? Life sciences 74:207-216.

Geyer MA, Puerto A, Dawsey WJ, Knapp S, Bullard WP, Mandell AJ (1976) Histologic and enzymatic studies of the mesolimbic and mesostriatal serotonergic pathways. Brain research 106:241-256.
Goodrich LV (2008) The plane facts of PCP in the CNS. Neuron 60:9-16.
Goridis C, Rohrer H (2002) Specification of catecholaminergic and serotonergic neurons. Nature reviews Neuroscience 3:531-541.
Grahame-Smith DG (1964) TRYPTOPHAN HYDROXYLATION IN CARCINOID TUMOURS. Biochimica et biophysica acta 86:176-179.
Gras C, Herzog E, Bellenchi GC, Bernard V, Ravassard P, Pohl M, Gasnier B, Giros B, El Mestikawy S (2002) A third vesicular glutamate transporter expressed by cholinergic and serotoninergic neurons. The Journal of neuroscience : the official journal of the Society for Neuroscience 22:5442-5451.
Hale MW, Lowry CA (2011) Functional topography of midbrain and pontine serotonergic systems: implications for synaptic regulation of serotonergic circuits. Psychopharmacology 213:243-264.
Hale MW, Shekhar A, Lowry CA (2011) Development by environment interactions controlling tryptophan hydroxylase expression. Journal of chemical neuroanatomy 41:219-226.
Halliday GM, Li YW, Joh TH, Cotton RG, Howe PR, Geffen LB, Blessing WW (1988) Distribution of substance P-like immunoreactive neurons in the human medulla oblongata: co-localization with monoamine-synthesizing neurons. Synapse (New York, NY) 2:353-370.
Harrison RG (1959) The outgrowth of the nerve fiber as a mode of protoplasmic movement. The Journal of experimental zoology 142:5-73.
Hayashi T, Mendelson B, Phelan KD, Skinner RD, Garcia-Rill E (1997) Developmental changes in serotonergic receptor-mediated modulation of embryonic chick motoneurons in vitro. Brain research Developmental brain research 102:21-33.
Henry JN, Manaker S (1998) Colocalization of substance P or enkephalin in serotonergic neuronal afferents to the hypoglossal nucleus in the rat. The Journal of comparative neurology 391:491-505.
Hermann DM, Luppi PH, Peyron C, Hinckel P, Jouvet M (1997) Afferent projections to the rat nuclei raphe magnus, raphe pallidus and reticularis gigantocellularis pars alpha demonstrated by iontophoretic application of choleratoxin (subunit b). Journal of chemical neuroanatomy 13:1-21.
Herve D, Pickel VM, Joh TH, Beaudet A (1987) Serotonin axon terminals in the ventral tegmental area of the rat: fine structure and synaptic input to dopaminergic neurons. Brain research 435:71-83.
Himanen JP, Yermekbayeva L, Janes PW, Walker JR, Xu K, Atapattu L, Rajashankar KR, Mensinga A, Lackmann M, Nikolov DB, Dhe-Paganon S (2010) Architecture of Eph receptor clusters. Proceedings of the National Academy of Sciences of the United States of America 107:10860-10865.
Hioki H, Nakamura H, Ma YF, Konno M, Hayakawa T, Nakamura KC, Fujiyama F, Kaneko T (2010) Vesicular glutamate transporter 3-expressing nonserotonergic projection neurons constitute a subregion in the rat midbrain raphe nuclei. The Journal of comparative neurology 518:668-686.
Honda T, Semba K (1994) Serotonergic synaptic input to cholinergic neurons in the rat mesopontine tegmentum. Brain research 647:299-306.
Hornberger MR, Dutting D, Ciossek T, Yamada T, Handwerker C, Lang S, Weth F, Huf J, Wessel R, Logan C, Tanaka H, Drescher U (1999) Modulation of EphA receptor function by coexpressed ephrinA ligands on retinal ganglion cell axons. Neuron 22:731-742.
Hornung JP, Fritschy JM (1988) Serotoninergic system in the brainstem of the marmoset: a combined immunocytochemical and three-dimensional reconstruction study. The Journal of comparative neurology 270:471-487.
Hornung JP, Fritschy JM, Tork I (1990) Distribution of two morphologically distinct subsets of serotoninergic axons in the cerebral cortex of the marmoset. The Journal of comparative neurology 297:165-181.
Hruska M, Dalva MB (2012) Ephrin regulation of synapse formation, function and plasticity. Molecular and cellular neurosciences 50:35-44.
Hu H (1999) Chemorepulsion of neuronal migration by Slit2 in the developing mammalian forebrain. Neuron 23:703-711.

Huang TN, Chuang HC, Chou WH, Chen CY, Wang HF, Chou SJ, Hsueh YP (2014) Tbr1 haploinsufficiency impairs amygdalar axonal projections and results in cognitive abnormality. Nature neuroscience 17:240-247.
Imai H, Steindler DA, Kitai ST (1986a) The organization of divergent axonal projections from the midbrain raphe nuclei in the rat. The Journal of comparative neurology 243:363-380.
Imai H, Park MR, Steindler DA, Kitai ST (1986b) The morphology and divergent axonal organization of midbrain raphe projection neurons in the rat. Brain & development 8:343-354.
Ishimura K, Takeuchi Y, Fujiwara K, Tominaga M, Yoshioka H, Sawada T (1988) Quantitative analysis of the distribution of serotonin-immunoreactive cell bodies in the mouse brain. Neuroscience letters 91:265-270.
Iwasato T, Katoh H, Nishimaru H, Ishikawa Y, Inoue H, Saito YM, Ando R, Iwama M, Takahashi R, Negishi M, Itohara S (2007) Rac-GAP alpha-chimerin regulates motor-circuit formation as a key mediator of EphrinB3/EphA4 forward signaling. Cell 130:742-753.
Jacobs BL, Azmitia EC (1992) Structure and function of the brain serotonin system. Physiological reviews 72:165-229.
Jacobs BL, Wise WD, Taylor KM (1974) Differential behavioral and neurochemical effects following lesions of the dorsal or median raphe nuclei in rats. Brain research 79:353-361.
Jacobs BL, Foote SL, Bloom FE (1978) Differential projections of neurons within the dorsal raphe nucleus of the rat: a horseradish peroxidase (HRP) study. Brain research 147:149-153.
Jennings KA, Lesch KP, Sharp T, Cragg SJ (2010) Non-linear relationship between 5-HT transporter gene expression and frequency sensitivity of 5-HT signals. Journal of neurochemistry 115:965-973.
Jennings KA, Loder MK, Sheward WJ, Pei Q, Deacon RM, Benson MA, Olverman HJ, Hastie ND, Harmar AJ, Shen S, Sharp T (2006) Increased expression of the 5-HT transporter confers a low-anxiety phenotype linked to decreased 5-HT transmission. The Journal of neuroscience : the official journal of the Society for Neuroscience 26:8955-8964.
Jensen P, Farago AF, Awatramani RB, Scott MM, Deneris ES, Dymecki SM (2008) Redefining the serotonergic system by genetic lineage. Nature neuroscience 11:417-419.
Johansson F, von Knorring L, Sedvall G, Terenius L (1980) Changes in endorphins and 5-hydroxyindoleacetic acid in cerebrospinal fluid as a result of treatment with a serotonin reuptake inhibitor (zimelidine) in chronic pain patients. Psychiatry research 2:167-172.
Johnson MD, Yee AG (1995) Ultrastructure of electrophysiologically-characterized synapses formed by serotonergic raphe neurons in culture. Neuroscience 67:609-623.
Jolas T, Aghajanian GK (1997) Opioids suppress spontaneous and NMDA-induced inhibitory postsynaptic currents in the dorsal raphe nucleus of the rat in vitro. Brain research 755:229-245.
Jones BE, Cuello AC (1989) Afferents to the basal forebrain cholinergic cell area from pontomesencephalic--catecholamine, serotonin, and acetylcholine--neurons. Neuroscience 31:37-61.
Jorgensen C, Sherman A, Chen GI, Pasculescu A, Poliakov A, Hsiung M, Larsen B, Wilkinson DG, Linding R, Pawson T (2009) Cell-specific information processing in segregating populations of Eph receptor ephrin-expressing cells. Science (New York, NY) 326:1502-1509.
Junghans D, Heidenreich M, Hack I, Taylor V, Frotscher M, Kemler R (2008) Postsynaptic and differential localization to neuronal subtypes of protocadherin beta16 in the mammalian central nervous system. The European journal of neuroscience 27:559-571.
Kellar KJ, Brown PA, Madrid J, Bernstein M, Vernikos-Danellis J, Mehler WR (1977) Origins of serotonin innervation of forebrain structures. Experimental neurology 56:52-62.
Kiyasova V, Gaspar P (2011) Development of raphe serotonin neurons from specification to guidance. The European journal of neuroscience 34:1553-1562.
Kiyasova V, Fernandez SP, Laine J, Stankovski L, Muzerelle A, Doly S, Gaspar P (2011) A genetically defined morphologically and functionally unique subset of 5-HT neurons in the mouse raphe nuclei. The Journal of neuroscience : the official journal of the Society for Neuroscience 31:2756-2768.

Klein R (2004) Eph/ephrin signaling in morphogenesis, neural development and plasticity. Current opinion in cell biology 16:580-589.
Klein R, Kania A (2014) Ephrin signalling in the developing nervous system. Current opinion in neurobiology 27:16-24.
Kohler C, Steinbusch H (1982) Identification of serotonin and non-serotonin-containing neurons of the mid-brain raphe projecting to the entorhinal area and the hippocampal formation. A combined immunohistochemical and fluorescent retrograde tracing study in the rat brain. Neuroscience 7:951-975.
Kohler C, Chan-Palay V, Steinbusch H (1982) The distribution and origin of serotonin-containing fibers in the septal area: a combined immunohistochemical and fluorescent retrograde tracing study in the rat. The Journal of comparative neurology 209:91-111.
Kohler C, Chan-Palay V, Haglund L, Steinbusch H (1980) Immunohistochemical localization of serotonin nerve terminals in the lateral entorhinal cortex of the rat: demonstration of two separate patterns of innervation from the midbrain raphe. Anatomy and embryology 160:121-129.
Kohmura N, Senzaki K, Hamada S, Kai N, Yasuda R, Watanabe M, Ishii H, Yasuda M, Mishina M, Yagi T (1998) Diversity revealed by a novel family of cadherins expressed in neurons at a synaptic complex. Neuron 20:1137-1151.
Kolodkin AL, Tessier-Lavigne M (2011) Mechanisms and molecules of neuronal wiring: a primer. Cold Spring Harbor perspectives in biology 3.
Kosofsky BE, Molliver ME (1987) The serotoninergic innervation of cerebral cortex: different classes of axon terminals arise from dorsal and median raphe nuclei. Synapse (New York, NY) 1:153-168.
Krukoff TL, Vu T, Harris KH, Aippersbach S, Jhamandas JH (1992) Neurons in the rat medulla oblongata containing neuropeptide Y-, angiotensin II-, or galanin-like immunoreactivity project to the parabrachial nucleus. Neuroscience 47:175-184.
Labrador JP, Brambilla R, Klein R (1997) The N-terminal globular domain of Eph receptors is sufficient for ligand binding and receptor signaling. The EMBO journal 16:3889-3897.
Lan NC, Chen CH, Shih JC (1989) Expression of functional human monoamine oxidase A and B cDNAs in mammalian cells. Journal of neurochemistry 52:1652-1654.
Lang S, von Philipsborn AC, Bernard A, Bonhoeffer F, Bastmeyer M (2008) Growth cone response to ephrin gradients produced by microfluidic networks. Analytical and bioanalytical chemistry 390:809-816.
Lauder JM (1990) Ontogeny of the serotonergic system in the rat: serotonin as a developmental signal. Annals of the New York Academy of Sciences 600:297-313; discussion 314.
LeDoux JE (2000) Emotion circuits in the brain. Annual review of neuroscience 23:155-184.
Lee EH, Lin HH, Yin HM (1987) Differential influences of different stressors upon midbrain raphe neurons in rats. Neuroscience letters 80:115-119.
Leger L, Descarries L (1978) Serotonin nerve terminals in the locus coeruleus of adult rat: a radioautographic study. Brain research 145:1-13.
Lemke G, Reber M (2005) Retinotectal mapping: new insights from molecular genetics. Annual review of cell and developmental biology 21:551-580.
Levitt P, Pintar JE, Breakefield XO (1982) Immunocytochemical demonstration of monoamine oxidase B in brain astrocytes and serotonergic neurons. Proceedings of the National Academy of Sciences of the United States of America 79:6385-6389.
Lidov HG, Molliver ME (1982a) An immunohistochemical study of serotonin neuron development in the rat: ascending pathways and terminal fields. Brain research bulletin 8:389-430.
Lidov HG, Molliver ME (1982b) Immunohistochemical study of the development of serotonergic neurons in the rat CNS. Brain research bulletin 9:559-604.
Lillesaar C, Tannhauser B, Stigloher C, Kremmer E, Bally-Cuif L (2007) The serotonergic phenotype is acquired by converging genetic mechanisms within the zebrafish central nervous system. Developmental dynamics : an official publication of the American Association of Anatomists 236:1072-1084.
Line SJ, Barkus C, Rawlings N, Jennings K, McHugh S, Sharp T, Bannerman DM (2014) Reduced sensitivity to both positive and negative reinforcement in mice over-expressing the 5-hydroxytryptamine transporter. The European journal of neuroscience 40:3735-3745.

Lucki I (1998) The spectrum of behaviors influenced by serotonin. Biological psychiatry 44:151-162.
Magoul R, Onteniente B, Oblin A, Calas A (1986) Inter- and intracellular relationship of substance P-containing neurons with serotonin and GABA in the dorsal raphe nucleus: combination of autoradiographic and immunocytochemical techniques. The journal of histochemistry and cytochemistry : official journal of the Histochemistry Society 34:735-742.
Maisonpierre PC, Barrezueta NX, Yancopoulos GD (1993) Ehk-1 and Ehk-2: two novel members of the Eph receptor-like tyrosine kinase family with distinctive structures and neuronal expression. Oncogene 8:3277-3288.
Mamiya PC, Hennesy Z, Zhou R, Wagner GC (2008) Changes in attack behavior and activity in EphA5 knockout mice. Brain research 1205:91-99.
Margolis SS, Salogiannis J, Lipton DM, Mandel-Brehm C, Wills ZP, Mardinly AR, Hu L, Greer PL, Bikoff JB, Ho HY, Soskis MJ, Sahin M, Greenberg ME (2010) EphB-mediated degradation of the RhoA GEF Ephexin5 relieves a developmental brake on excitatory synapse formation. Cell 143:442-455.
Marler KJ, Becker-Barroso E, Martinez A, Llovera M, Wentzel C, Poopalasundaram S, Hindges R, Soriano E, Comella J, Drescher U (2008) A TrkB/EphrinA interaction controls retinal axon branching and synaptogenesis. The Journal of neuroscience : the official journal of the Society for Neuroscience 28:12700-12712.
McHugh SB, Barkus C, Lima J, Glover LR, Sharp T, Bannerman DM (2015) SERT and uncertainty: serotonin transporter expression influences information processing biases for ambiguous aversive cues in mice. Genes, brain, and behavior 14:330-336.
McLaughlin T, O'Leary DD (2005) Molecular gradients and development of retinotopic maps. Annual review of neuroscience 28:327-355.
McQuade R, Sharp T (1997) Functional mapping of dorsal and median raphe 5-hydroxytryptamine pathways in forebrain of the rat using microdialysis. Journal of neurochemistry 69:791-796.
Meima L, Moran P, Matthews W, Caras IW (1997a) Lerk2 (ephrin-B1) is a collapsing factor for a subset of cortical growth cones and acts by a mechanism different from AL-1 (ephrin-A5). Molecular and cellular neurosciences 9:314-328.
Meima L, Kljavin IJ, Moran P, Shih A, Winslow JW, Caras IW (1997b) AL-1-induced growth cone collapse of rat cortical neurons is correlated with REK7 expression and rearrangement of the actin cytoskeleton. The European journal of neuroscience 9:177-188.
Metin C, Godement P (1996) The ganglionic eminence may be an intermediate target for corticofugal and thalamocortical axons. The Journal of neuroscience : the official journal of the Society for Neuroscience 16:3219-3235.
Miao H, Wang B (2012) EphA receptor signaling--complexity and emerging themes. Seminars in cell & developmental biology 23:16-25.
Michelsen KA, Schmitz C, Steinbusch HW (2007) The dorsal raphe nucleus--from silver stainings to a role in depression. Brain research reviews 55:329-342.
Miller JJ, Richardson TL, Fibiger HC, McLennan H (1975) Anatomical and electrophysiological identification of a projection from the mesencephalic raphe to the caudate-putamen in the rat. Brain research 97:133-136.
Millhorn DE, Hokfelt T, Verhofstad AA, Terenius L (1989) Individual cells in the raphe nuclei of the medulla oblongata in rat that contain immunoreactivities for both serotonin and enkephalin project to the spinal cord. Experimental brain research 75:536-542.
Minami M, Kohno Y, Endo T, Nemoto M, Ogawa T, Ihira E, Hamaue N, Hirafuji M (1999) Differential effects of talipexole and bromocriptine on serotonin release from rat intestinal tissues--an in vitro study of the emetic response of antiparkinsonian dopamine agonists. Research communications in molecular pathology and pharmacology 104:3-12.
Mueller BK (1999) Growth cone guidance: first steps towards a deeper understanding. Annual review of neuroscience 22:351-388.
Murai KK, Pasquale EB (2005) New exchanges in eph-dependent growth cone dynamics. Neuron 46:161-163.
Murai KK, Nguyen LN, Irie F, Yamaguchi Y, Pasquale EB (2003) Control of hippocampal dendritic spine morphology through ephrin-A3/EphA4 signaling. Nature neuroscience 6:153-160.

Muzerelle A, Scotto-Lomassese S, Bernard JF, Soiza-Reilly M, Gaspar P (2016) Conditional anterograde tracing reveals distinct targeting of individual serotonin cell groups (B5-B9) to the forebrain and brainstem. Brain structure & function 221:535-561.
Narboux-Neme N, Angenard G, Mosienko V, Klempin F, Pitychoutis PM, Deneris E, Bader M, Giros B, Alenina N, Gaspar P (2013) Postnatal growth defects in mice with constitutive depletion of central serotonin. ACS chemical neuroscience 4:171-181.
Nestor MW, Mok LP, Tulapurkar ME, Thompson SM (2007) Plasticity of neuron-glial interactions mediated by astrocytic EphARs. The Journal of neuroscience : the official journal of the Society for Neuroscience 27:12817-12828.
Nguyen Ba-Charvet KT, Brose K, Marillat V, Kidd T, Goodman CS, Tessier-Lavigne M, Sotelo C, Chedotal A (1999) Slit2-Mediated chemorepulsion and collapse of developing forebrain axons. Neuron 22:463-473.
Nicolas JC, Terouanne B, Balaguer P, Chikhaoui Y, Defacque H, Boussioux AM (1992) [Detection of nucleic acid sequences by bioluminescence. Importance of an internal reference system for qualitative and quantitative analysis]. Annales de biologie clinique 50:713-718.
Nobin A, Bjorklund A (1973) Topography of the monoamine neuron systems in the human brain as revealed in fetuses. Acta physiologica Scandinavica Supplementum 388:1-40.
Noren NK, Pasquale EB (2004) Eph receptor-ephrin bidirectional signals that target Ras and Rho proteins. Cellular signalling 16:655-666.
O'Leary DD, Wilkinson DG (1999) Eph receptors and ephrins in neural development. Current opinion in neurobiology 9:65-73.
Obata S, Sago H, Mori N, Rochelle JM, Seldin MF, Davidson M, St John T, Taketani S, Suzuki ST (1995) Protocadherin Pcdh2 shows properties similar to, but distinct from, those of classical cadherins. Journal of cell science 108 (Pt 12):3765-3773.
Okaty BW, Freret ME, Rood BD, Brust RD, Hennessy ML, deBairos D, Kim JC, Cook MN, Dymecki SM (2015) Multi-Scale Molecular Deconstruction of the Serotonin Neuron System. Neuron 88:774-791.
Parent A (1973) Distribution of monoamine-containing neurons in the brain stem of the frog, Rana temporaria. Journal of morphology 139:67-78.
Parent A, Descarries L, Beaudet A (1981) Organization of ascending serotonin systems in the adult rat brain. A radioautographic study after intraventricular administration of [3H]5-hydroxytryptamine. Neuroscience 6:115-138.
Pasquale EB (2008) Eph-ephrin bidirectional signaling in physiology and disease. Cell 133:38-52.
Pattyn A, Vallstedt A, Dias JM, Samad OA, Krumlauf R, Rijli FM, Brunet JF, Ericson J (2003) Coordinated temporal and spatial control of motor neuron and serotonergic neuron generation from a common pool of CNS progenitors. Genes & development 17:729-737.
Pelletier G, Laflamme G (1977) [Natural antiallergenic factors in bile]. Annales d'immunologie 128:261-263.
Pelletier G, Steinbusch HW, Verhofstad AA (1981) Immunoreactive substance P and serotonin present in the same dense-core vesicles. Nature 293:71-72.
Phillips RJ, Baronowsky EA, Powley TL (2003) Long-term regeneration of abdominal vagus: efferents fail while afferents succeed. The Journal of comparative neurology 455:222-237.
Pierre J, Reperant J, Ward R, Vesselkin NP, Rio JP, Miceli D, Kratskin I (1992) The serotoninergic system of the brain of the lamprey, Lampetra fluviatilis: an evolutionary perspective. Journal of chemical neuroanatomy 5:195-219.
Piper M, Georgas K, Yamada T, Little M (2000) Expression of the vertebrate Slit gene family and their putative receptors, the Robo genes, in the developing murine kidney. Mechanisms of development 94:213-217.
Pitulescu ME, Adams RH (2010) Eph/ephrin molecules--a hub for signaling and endocytosis. Genes & development 24:2480-2492.
Prestoz L, Jaber M, Gaillard A (2012) Dopaminergic axon guidance: which makes what? Frontiers in cellular neuroscience 6:32.
Rapport MM, Green AA, Page IH (1948) Crystalline Serotonin. Science (New York, NY) 108:329-330.

Remedios R, Subramanian L, Tole S (2004) LIM genes parcellate the embryonic amygdala and regulate its development. The Journal of neuroscience : the official journal of the Society for Neuroscience 24:6986-6990.
Richards DA (1979) Electrochemical detection of tryptophan metabolites following high-performance liquid chromatography. Journal of chromatography 175:293-299.
Richardson M (2014) Deep brain stimulation for locomotor recovery following spinal cord injury. Neurosurgery 74:N18-19.
Ringstedt T, Braisted JE, Brose K, Kidd T, Goodman C, Tessier-Lavigne M, O'Leary DD (2000) Slit inhibition of retinal axon growth and its role in retinal axon pathfinding and innervation patterns in the diencephalon. The Journal of neuroscience : the official journal of the Society for Neuroscience 20:4983-4991.
Sahin M, Greer PL, Lin MZ, Poucher H, Eberhart J, Schmidt S, Wright TM, Shamah SM, O'Connell S, Cowan CW, Hu L, Goldberg JL, Debant A, Corfas G, Krull CE, Greenberg ME (2005) Eph-dependent tyrosine phosphorylation of ephexin1 modulates growth cone collapse. Neuron 46:191-204.
Sakano S, Serizawa R, Inada T, Iwama A, Itoh A, Kato C, Shimizu Y, Shinkai F, Shimizu R, Kondo S, Ohno M, Suda T (1996) Characterization of a ligand for receptor protein-tyrosine kinase HTK expressed in immature hematopoietic cells. Oncogene 13:813-822.
Sampath P, Pollard TD (1991) Effects of cytochalasin, phalloidin, and pH on the elongation of actin filaments. Biochemistry 30:1973-1980.
Sato TL, Jequier E, Lovenberg W, Sjoerdsma A (1967) Characterization of a tryptophan hydroxylating enzyme from malignant mouse mast cell. European journal of pharmacology 1:18-25.
Schafer MK, Varoqui H, Defamie N, Weihe E, Erickson JD (2002) Molecular cloning and functional identification of mouse vesicular glutamate transporter 3 and its expression in subsets of novel excitatory neurons. The Journal of biological chemistry 277:50734-50748.
Scott MM, Wylie CJ, Lerch JK, Murphy R, Lobur K, Herlitze S, Jiang W, Conlon RA, Strowbridge BW, Deneris ES (2005) A genetic approach to access serotonin neurons for in vivo and in vitro studies. Proceedings of the National Academy of Sciences of the United States of America 102:16472-16477.
Seiradake E, Harlos K, Sutton G, Aricescu AR, Jones EY (2010) An extracellular steric seeding mechanism for Eph-ephrin signaling platform assembly. Nature structural & molecular biology 17:398-402.
Sharif NA (1989) Quantitative autoradiography of TRH receptors in discrete brain regions of different mammalian species. Annals of the New York Academy of Sciences 553:147-175.
Sheleg M, Yochum CL, Richardson JR, Wagner GC, Zhou R (2015) Ephrin-A5 regulates inter-male aggression in mice. Behavioural brain research 286:300-307.
Shu T, Richards LJ (2001) Cortical axon guidance by the glial wedge during the development of the corpus callosum. The Journal of neuroscience : the official journal of the Society for Neuroscience 21:2749-2758.
Silva BA, Mattucci C, Krzywkowski P, Murana E, Illarionova A, Grinevich V, Canteras NS, Ragozzino D, Gross CT (2013) Independent hypothalamic circuits for social and predator fear. Nature neuroscience 16:1731-1733.
Simons M, Mlodzik M (2008) Planar cell polarity signaling: from fly development to human disease. Annual review of genetics 42:517-540.
Sims KB, de la Chapelle A, Norio R, Sankila EM, Hsu YP, Rinehart WB, Corey TJ, Ozelius L, Powell JF, Bruns G, et al. (1989) Monoamine oxidase deficiency in males with an X chromosome deletion. Neuron 2:1069-1076.
Song HJ, Poo MM (1999) Signal transduction underlying growth cone guidance by diffusible factors. Current opinion in neurobiology 9:355-363.
Sousa VH, Miyoshi G, Hjerling-Leffler J, Karayannis T, Fishell G (2009) Characterization of Nkx6-2-derived neocortical interneuron lineages. Cerebral cortex (New York, NY : 1991) 19 Suppl 1:i1-10.
Steinbusch HW, Nieuwenhuys R (1981) Localization of serotonin-like immunoreactivity in the central nervous system and pituitary of the rat, with special references to the innervation of the hypothalamus. Advances in experimental medicine and biology 133:7-35.

Stoll J, Kozak CA, Goldman D (1990) Characterization and chromosomal mapping of a cDNA encoding tryptophan hydroxylase from a mouse mastocytoma cell line. Genomics 7:88-96.
Stratford TR, Wirtshafter D (1990) Ascending dopaminergic projections from the dorsal raphe nucleus in the rat. Brain research 511:173-176.
Szepietowska B, Zhu W, Czyzyk J, Eid T, Sherwin RS (2013) EphA5-EphrinA5 interactions within the ventromedial hypothalamus influence counterregulatory hormone release and local glutamine/glutamate balance during hypoglycemia. Diabetes 62:1282-1288.
Taber E, Brodal A, Walberg F (1960) The raphe nuclei of the brain stem in the cat. I. Normal topography and cytoarchitecture and general discussion. The Journal of comparative neurology 114:161-187.
Takagi H, Senba E, Shiosaka S, Sakanaka M, Inagaki S, Takatsuki K, Tohyama M (1981) Ascending and cerebellar non-serotonergic projections from the nucleus raphe magnus of the rat. Brain research 206:161-165.
Takamori S, Malherbe P, Broger C, Jahn R (2002) Molecular cloning and functional characterization of human vesicular glutamate transporter 3. EMBO reports 3:798-803.
Tanaka E, Sabry J (1995) Making the connection: cytoskeletal rearrangements during growth cone guidance. Cell 83:171-176.
Tashiro H, Itamoto T, Nakahara H, Ohdan H, Kobayashi T, Asahara T (2003) Resection of hepatocellular carcinoma in a patient with congenital anomaly of the portal system. Digestive surgery 20:163-165.
Teissier A, Chemiakine A, Inbar B, Bagchi S, Ray RS, Palmiter RD, Dymecki SM, Moore H, Ansorge MS (2015) Activity of Raphe Serotonergic Neurons Controls Emotional Behaviors. Cell reports 13:1965-1976.
Tessier-Lavigne M, Goodman CS (1996) The molecular biology of axon guidance. Science (New York, NY) 274:1123-1133.
Tong Q, Ye C, McCrimmon RJ, Dhillon H, Choi B, Kramer MD, Yu J, Yang Z, Christiansen LM, Lee CE, Choi CS, Zigman JM, Shulman GI, Sherwin RS, Elmquist JK, Lowell BB (2007) Synaptic glutamate release by ventromedial hypothalamic neurons is part of the neurocircuitry that prevents hypoglycemia. Cell metabolism 5:383-393.
Tork I (1990) Anatomy of the serotonergic system. Annals of the New York Academy of Sciences 600:9-34; discussion 34-35.
Tremblay ME, Riad M, Bouvier D, Murai KK, Pasquale EB, Descarries L, Doucet G (2007) Localization of EphA4 in axon terminals and dendritic spines of adult rat hippocampus. The Journal of comparative neurology 501:691-702.
Triplett JW, Feldheim DA (2012) Eph and ephrin signaling in the formation of topographic maps. Seminars in cell & developmental biology 23:7-15.
Tuzi NL, Gullick WJ (1994) eph, the largest known family of putative growth factor receptors. British journal of cancer 69:417-421.
Uhl GR, Goodman RR, Snyder SH (1979) Neurotensin-containing cell bodies, fibers and nerve terminals in the brain stem of the rat: immunohistochemical mapping. Brain research 167:77-91.
Ulfhake B, Arvidsson U, Cullheim S, Hokfelt T, Visser TJ (1987) Thyrotropin-releasing hormone (TRH)-immunoreactive boutons and nerve cell bodies in the dorsal horn of the cat L7 spinal cord. Neuroscience letters 73:3-8.
Van Bockstaele EJ, Pickel VM (1993) Ultrastructure of serotonin-immunoreactive terminals in the core and shell of the rat nucleus accumbens: cellular substrates for interactions with catecholamine afferents. The Journal of comparative neurology 334:603-617.
Van Bockstaele EJ, Chan J (1997) Electron microscopic evidence for coexistence of leucine5-enkephalin and gamma-aminobutyric acid in a subpopulation of axon terminals in the rat locus coeruleus region. Brain research 746:171-182.
van der Geer P, Hunter T, Lindberg RA (1994) Receptor protein-tyrosine kinases and their signal transduction pathways. Annual review of cell biology 10:251-337.
van der Kooy D, Hattori T (1980) Bilaterally situated dorsal raphe cell bodies have only unilateral forebrain projections in rat. Brain research 192:550-554.
Vasudeva RK, Lin RC, Simpson KL, Waterhouse BD (2011) Functional organization of the dorsal raphe efferent system with special consideration of nitrergic cell groups. Journal of chemical neuroanatomy 41:281-293.
Vearing CJ, Lackmann M (2005) "Eph receptor signalling; dimerisation just isn't enough". Growth factors (Chur, Switzerland) 23:67-76.

Vertes RP (1991) A PHA-L analysis of ascending projections of the dorsal raphe nucleus in the rat. The Journal of comparative neurology 313:643-668.
Vertes RP, Crane AM (1997) Distribution, quantification, and morphological characteristics of serotonin-immunoreactive cells of the supralemniscal nucleus (B9) and pontomesencephalic reticular formation in the rat. The Journal of comparative neurology 378:411-424.
Vertes RP, Fortin WJ, Crane AM (1999) Projections of the median raphe nucleus in the rat. The Journal of comparative neurology 407:555-582.
Vitalis T, Alvarez C, Chen K, Shih JC, Gaspar P, Cases O (2003) Developmental expression pattern of monoamine oxidases in sensory organs and neural crest derivatives. The Journal of comparative neurology 464:392-403.
Wallace JA, Lauder JM (1983) Development of the serotonergic system in the rat embryo: an immunocytochemical study. Brain research bulletin 10:459-479.
Walther DJ, Bader M (2003) A unique central tryptophan hydroxylase isoform. Biochemical pharmacology 66:1673-1680.
Walther DJ, Peter JU, Winter S, Holtje M, Paulmann N, Grohmann M, Vowinckel J, Alamo-Bethencourt V, Wilhelm CS, Ahnert-Hilger G, Bader M (2003) Serotonylation of small GTPases is a signal transduction pathway that triggers platelet alpha-granule release. Cell 115:851-862.
Wang RY, Aghajanian GK (1977) Inhibiton of neurons in the amygdala by dorsal raphe stimulation: mediation through a direct serotonergic pathway. Brain research 120:85-102.
Wang X, Zhang W, Cheever T, Schwarz V, Opperman K, Hutter H, Koepp D, Chen L (2008) The C. elegans L1CAM homologue LAD-2 functions as a coreceptor in MAB-20/Sema2 mediated axon guidance. The Journal of cell biology 180:233-246.
Wang Y, Nathans J (2007) Tissue/planar cell polarity in vertebrates: new insights and new questions. Development (Cambridge, England) 134:647-658.
Waselus M, Galvez JP, Valentino RJ, Van Bockstaele EJ (2006) Differential projections of dorsal raphe nucleus neurons to the lateral septum and striatum. Journal of chemical neuroanatomy 31:233-242.
Waterhouse BD, Mihailoff GA, Baack JC, Woodward DJ (1986) Topographical distribution of dorsal and median raphe neurons projecting to motor, sensorimotor, and visual cortical areas in the rat. The Journal of comparative neurology 249:460-476, 478-481.
Wegmeyer H, Egea J, Rabe N, Gezelius H, Filosa A, Enjin A, Varoqueaux F, Deininger K, Schnutgen F, Brose N, Klein R, Kullander K, Betz A (2007) EphA4-dependent axon guidance is mediated by the RacGAP alpha2-chimaerin. Neuron 55:756-767.
Weiskrantz L (1956) Behavioral changes associated with ablation of the amygdaloid complex in monkeys. Journal of comparative and physiological psychology 49:381-391.
Whitaker-Azmitia PM, Clarke C, Azmitia EC (1993) Localization of 5-HT1A receptors to astroglial cells in adult rats: implications for neuronal-glial interactions and psychoactive drug mechanism of action. Synapse (New York, NY) 14:201-205.
Wiklund L, Descarries L, Mollgard K (1981) Serotoninergic axon terminals in the rat dorsal accessory olive: normal ultrastructure and light microscopic demonstration of regeneration after 5,6-dihydroxytryptamine lesioning. Journal of neurocytology 10:1009-1027.
Winslow JW, Moran P, Valverde J, Shih A, Yuan JQ, Wong SC, Tsai SP, Goddard A, Henzel WJ, Hefti F, et al. (1995) Cloning of AL-1, a ligand for an Eph-related tyrosine kinase receptor involved in axon bundle formation. Neuron 14:973-981.
Wylie CJ, Hendricks TJ, Zhang B, Wang L, Lu P, Leahy P, Fox S, Maeno H, Deneris ES (2010) Distinct transcriptomes define rostral and caudal serotonin neurons. The Journal of neuroscience : the official journal of the Society for Neuroscience 30:670-684.
Xu NJ, Henkemeyer M (2012) Ephrin reverse signaling in axon guidance and synaptogenesis. Seminars in cell & developmental biology 23:58-64.
Yin Y, Yamashita Y, Noda H, Okafuji T, Go MJ, Tanaka H (2004) EphA receptor tyrosine kinases interact with co-expressed ephrin-A ligands in cis. Neuroscience research 48:285-296.
Yuan W, Zhou L, Chen JH, Wu JY, Rao Y, Ornitz DM (1999) The mouse SLIT family: secreted ligands for ROBO expressed in patterns that suggest a role in morphogenesis and axon guidance. Developmental biology 212:290-306.
Zallen JA (2007) Planar polarity and tissue morphogenesis. Cell 129:1051-1063.

Zhou R (1998) The Eph family receptors and ligands. Pharmacology & therapeutics 77:151-181.
Zhou R, Copeland TD, Kromer LF, Schulz NT (1994) Isolation and characterization of Bsk, a growth factor receptor-like tyrosine kinase associated with the limbic system. Journal of neuroscience research 37:129-143.
Zou Y (2006) Navigating the anterior-posterior axis with Wnts. Neuron 49:787-789.
Zou Y, Lyuksyutova AI (2007) Morphogens as conserved axon guidance cues. Current opinion in neurobiology 17:22-28.